

Modeling and Simulation for UAS in the NAS

*Frederick Wieland, Sricharan Ayyalasomayajula and Rose Mooney
Intelligent Automation, Inc., Rockville, MD*

*Daniel DeLaurentis, Vishnu Vinay, James Goppert and Jason Choi
Purdue University, West Lafayette, IN*

*Gregory Kubat
QinetiQ North America, Cleveland, OH*

NASA STI Program ... in Profile

Since its founding, NASA has been dedicated to the advancement of aeronautics and space science. The NASA scientific and technical information (STI) program plays a key part in helping NASA maintain this important role.

The NASA STI program operates under the auspices of the Agency Chief Information Officer. It collects, organizes, provides for archiving, and disseminates NASA's STI. The NASA STI program provides access to the NASA Aeronautics and Space Database and its public interface, the NASA Technical Reports Server, thus providing one of the largest collections of aeronautical and space science STI in the world. Results are published in both non-NASA channels and by NASA in the NASA STI Report Series, which includes the following report types:

TECHNICAL PUBLICATION. Reports of completed research or a major significant phase of research that present the results of NASA Programs and include extensive data or theoretical analysis. Includes compilations of significant scientific and technical data and information deemed to be of continuing reference value. NASA counterpart of peer-reviewed formal professional papers but has less stringent limitations on manuscript length and extent of graphic presentations.

TECHNICAL MEMORANDUM. Scientific and technical findings that are preliminary or of specialized interest, e.g., quick release reports, working papers, and bibliographies that contain minimal annotation. Does not contain extensive analysis.

CONTRACTOR REPORT. Scientific and technical findings by NASA-sponsored contractors and grantees.

CONFERENCE

PUBLICATION. Collected papers from scientific and technical conferences, symposia, seminars, or other meetings sponsored or co-sponsored by NASA.

SPECIAL PUBLICATION.

Scientific, technical, or historical information from NASA programs, projects, and missions, often concerned with subjects having substantial public interest.

TECHNICAL TRANSLATION.

English-language translations of foreign scientific and technical material pertinent to NASA's mission.

Specialized services also include organizing and publishing research results, distributing specialized research announcements and feeds, providing information desk and personal search support, and enabling data exchange services.

For more information about the NASA STI program, see the following:

Access the NASA STI program home page at <http://www.sti.nasa.gov>

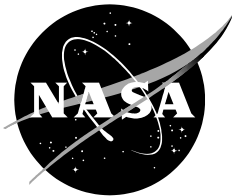
E-mail your question to help@sti.nasa.gov

Fax your question to the NASA STI Information Desk at 443-757-5803

Phone the NASA STI Information Desk at 443-757-5802

Write to:

STI Information Desk
NASA Center for AeroSpace
Information
7115 Standard Drive
Hanover, MD 21076-1320



Modeling and Simulation for UAS in the NAS

*Frederick Wieland, Sricharan Ayyalasomayajula and Rose Mooney
Intelligent Automation, Inc., Rockville, MD*

*Daniel DeLaurentis, Vishnu Vinay, James Goppert and Jason Choi
Purdue University, West Lafayette, IN*

*Gregory Kubat
QinetiQ North America, Cleveland, OH*

National Aeronautics and
Space Administration

*Langley Research Center
Hampton, VA 23681*

September 2012

Acknowledgments

The research represented in this study was funded by the National Aeronautics and Space Administration under contract NND11AQ74C. We would like to thank the Technical Monitor, Maria Consiglio as well as the project COTR, Eric Mueller, for their technical guidance during the project. The authors acknowledge extremely valuable feedback, testing & analysis suggestions from members of the MACS simulation community as well as the NASA UAS program.

Available from:

NASA Center for AeroSpace Information
7115 Standard Drive
Hanover, MD 21076-1320
443-757-5802

Project Summary

The purpose of this project is to create performance data for twelve Unmanned Aerial Systems (UAS) aircraft that can be used by many aviation models. The performance data are presented in two formats: the *Base of Aircraft Data* (BADA) format specified by EUROCONTROL, and the *Multi Aircraft Control System* (MACS) format specified by NASA. During the execution of the project, simulations were conducted using the Kinematic Trajectory Generator (KTG) for the BADA files, and the MACS software for the MACS files. Simulation output from KTG and MACS were examined and validated by the UAS manufacturers. Nine of the twelve UAS aircraft were validated using this process, although some discrepancies were found in the trajectory generators and are documented in this report. Three of the twelve UAS aircraft—two rotorcraft and one hybrid UAS—require different trajectory generators and will need to be validated at some future point.

In addition to the twelve BADA and MACS formatted performance files, the project also conducted simulations using the communication, navigation and surveillance (CNS) capabilities of the UAS aircraft. CNS equipage files provided by the UAS manufacturers were used to configure and conduct the experiments using the Airspace Concept Evaluation System (ACES) with KTG.

Finally, operational requirements and limitations of all twelve UAS aircraft are documented by the project. As UAS aircraft have some unique operating requirements—for example, some aircraft can be launched by a catapult while others cannot fly when the wind speed exceeds thirty knots—documentation of these limitations allows researchers to determine whether the weather conditions and availability of infrastructure limit or prohibit the conduct of UAS missions.

The value to the aviation community of the work generated by this project is enormous. UAS aircraft perform very differently than piloted aircraft. UAS aircraft have vastly different cruise speeds, operating range, altitude ceilings, and departure and approach speeds than equivalent piloted aircraft such that finding a match between piloted aircraft performance and a UAS aircraft is impractical. Because the BADA and MACS files created by the project are specific to UAS aircraft, aviation researchers can use these UAS performance files to correctly experiment with UAS aircraft in the National Airspace System using virtually any standard aviation simulation tool.

Table of Contents

1	Introduction	10
2	Specifications and Basic Attributes of UAS Aircraft.....	11
2.1	Eight Aircraft from AAI	11
2.2	Four Aircraft from General Atomics.....	13
3	Industry Data Presentation	14
4	BADA File Presentation.....	16
5	MACS File Presentation	23
6	Methodology.....	27
7	Modeling Tools	28
7.1	Flight Optimization System (FLOPS).....	28
7.2	DATCOM Aerodynamics Model	29
7.2.1	Propulsion Models	30
7.2.2	Methodology	30
7.2.2.1	Gathering Publically Available Data/ Photographs	31
7.2.2.2	Constructing 3D Models in Blender.....	31
7.2.2.3	Measuring 3D Model to Create DATCOM Input File	32
7.2.2.4	Test Aircraft in Manual Flight Simulation	32
7.2.2.5	JSBSim Trimming and Performance Table Generation.....	33
7.3	Modeling of Electric UAS Aircraft: Orbiter	33
7.4	Rotorcraft Modeling and Analysis: RPAT	34
8	Results: UAS Aircraft Modeling and Development of BADA and MACS Files	37
8.1	Shadow B	38
8.1.1	Summary of BADA Deficiencies and Limitations	39
8.1.2	Summary of MACS Deficiencies and Limitations	39
8.2	Global Hawk	39
8.2.1	Summary of BADA deficiencies and limitations.....	40
8.2.2	MACS	40
8.3	Orbiter.....	40
8.3.1	Summary of BADA deficiencies and limitations.....	42
8.3.2	MACS	42
8.4	Aerosonde	42
8.4.1	Summary of BADA deficiencies and limitations.....	44
8.4.2	MACS	44
8.5	Predator A	44
8.5.1	Summary of BADA deficiencies and limitations.....	45
8.5.2	MACS	45

8.6	Predator B	45
8.6.1	Summary of BADA deficiencies and limitations.....	45
8.6.2	MACS	46
8.7	Gray Eagle.....	46
8.7.1	Summary of BADA deficiencies and limitations.....	46
8.7.2	MACS	46
8.8	Predator C (Avenger).....	47
8.8.1	Summary of BADA deficiencies and limitations.....	47
8.8.2	MACS	47
8.9	Hunter UAS.....	48
8.9.1	Summary of BADA deficiencies and limitations.....	48
8.9.2	MACS	48
8.10	Cargo UAS	48
8.10.1	Summary of BADA deficiencies and limitations.....	49
8.10.2	MACS	49
8.11	Fire Scout	50
8.11.1	Summary of BADA deficiencies and limitations.....	50
8.11.2	MACS	50
8.12	NEO S-300 Mk II VTOL	50
8.12.1	Summary of BADA deficiencies and limitations.....	51
8.12.2	MACS	51
9	BADA File Validation	51
9.1	Simulation of Shadow B (RQ7B) using KTG	51
9.1.1	Issues and Resolution.....	51
9.1.2	Reason for Anomalies.....	52
9.1.3	Simulation results using corrected BADA files.....	52
9.2	Simulation of Global Hawk (RQ4A) using KTG	57
9.3	Simulation of Orbiter (ORBM) using KTG.....	62
9.4	Simulation of Aerosonde (MK47) using KTG.....	63
9.5	Simulation of Predator A (MQ1B) using KTG	65
9.6	Simulation of Predator B (MQ-9) using KTG	67
9.7	Simulation of Gray Eagle (MQ1C) using KTG	69
9.8	Simulation of Predator C (AVEN) using KTG	71
9.9	Simulation of Hunter (MQ5B) using KTG	73
9.10	Simulation of BADA Files for Cargo UAS (CUAS), Fire Scout (MQ8B) and NEO S-300 Mk II VTOL (S350) using KTG.....	75
9.11	Summary of UAS Simulations in KTG	75

10	MACS File Validation.....	76
10.1	Issues and Resolution.....	76
10.1.1	Issue 1: Speed vs. Altitude Constraints in MACS	76
10.1.2	Issue 2: Simulation of Slow Flying UAS Aircraft	77
10.1.3	Issue 3: Simulation of Rotorcraft and Electric Aircraft.....	78
10.2	Simulation of Shadow B (RQ7B) using MACS	78
10.3	Simulation of Global Hawk (RQ4A) using MACS	79
10.4	Simulation of Aerosonde (MK47) using MACS.....	80
10.5	Simulation of Predator A (MQ1B) using MACS	81
10.6	Simulation of Predator B (MQ-9) using MACS	82
10.7	Simulation of Gray Eagle (MQ1C) using MACS	83
10.8	Simulation of Predator C (AVEN) using MACS	84
10.9	Simulation of Hunter (MQ5B) using MACS	85
10.10	Simulation of BADA Files for Orbiter (ORBM), Cargo UAS (CUAS), Fire Scout (MQ8B) and NEO S-300 Mk II VTOL (S350) using MACS.....	86
10.11	Summary of UAS Simulations in MACS	86
11	ACES Simulations for CNS Capabilities	87
11.1	UAS Aircraft/BADA Data Installation and Preparation for CNS Simulations	87
11.1.1	Installation of UAS Aircraft Models into ACES and KTG	87
11.1.2	Develop Flight Data Sets	88
11.1.3	Develop CNS Plugin Configuration Files.....	88
11.2	Simulations: Tabulated Results.....	89
11.3	Test Results.....	92
11.4	Problems Encountered and Precautions for use of CNS models with UAS	92
12	Conclusions.....	92
13	Recommendations for Future Work.....	93
13.1	Recommendations to Modify BADA Format for UAS Simulations	93
13.2	Recommendations to Modify MACS for UAS Simulations	94
13.3	Validation of BADA and MACS Files for Rotorcraft and Hybrid Aircraft	94
13.4	Other Recommendations	94
14	References.....	95
15	Appendix A: Industry Data of UAS Aircraft.....	96
15.1	Shadow B (RQ7B)	96
15.2	Global Hawk (RQ4A)	98
15.3	Orbiter (ORBM).....	100
15.4	Aerosonde (MK47).....	103
15.5	Predator A (MQ1B)	105

15.6	Predator B (MQ-9)	108
15.7	Gray Eagle (MQ1C)	112
15.8	Predator C (AVEN)	115
15.9	Hunter (MQ5B)	117
15.10	Cargo UAS (CUAS)	120
15.11	Fire Scout (MQ8B)	123
15.12	NEO S-300 Mk II VTOL (S350)	125
16	Appendix B: Configuration of ACES and KTG to Simulate UAS Aircraft	127
16.1	Introduction.....	127
16.2	Configuration of KTG Database	127
16.2.1	Configuration of “aircraft_control_gain.csv”.....	128
16.2.2	Configuration of “MPAS_SYNONYM.LST,” “SYNONYM_ALL.LST” and “SYNONYM_ACES_KTG.OLD”	128
16.3	Configuration of ACES Database.....	128

List of Figures

Figure 1. The .APF file for Shadow B (RQ7B). File was compiled by Purdue.	17
Figure 2. The .DCT file for Shadow B (RQ7B). File was compiled by IAI.	18
Figure 3. The .OPF file for Shadow B (RQ7B). File was compiled by Purdue.	19
Figure 4. The .PTF file for Shadow B (RQ7B). File was compiled by Purdue.	20
Figure 5. BADA climb schedules for commercial Jet aircraft	22
Figure 6. BADA standard airline climb increments for commercial Jet aircraft	22
Figure 7. Convention for MACS-BADA mapping	24
Figure 8. Aircraft model data file for Predator B. File produced by Purdue.	25
Figure 9. Airframe drag model data file for Predator B. File produced by Purdue.	26
Figure 10. Snapshot of flight parameters file for Predator B. Speeds are indicated air speeds in knots. File produced by IAI.	27
Figure 11. APM generation and validation flowchart	28
Figure 12. Flowchart representing the BADA generation process using the DATCOM/JSBSim/Flight Sim tool	30
Figure 13. Orthographic projection/picture based modeling	31
Figure 14. Difficulties of non-orthographic projection picture based modeling	31
Figure 15. Blender 3D Modeling of Cargo UAS	32
Figure 16. FlightGear Simulation Testing of Cargo UAS	33
Figure 17. Sample power curve	36
Figure 18. Aircraft model data MACS file for Shadow B	39
Figure 19. Orbiter images used for 3D construction	41
Figure 20. Orbiter DATCOM Input Visualization	42
Figure 21. Aerosonde images used for 3D model construction	43
Figure 22. Aerosonde DATCOM Input Visualization	43
Figure 23. Schematics of Cargo UAS from AAI	49
Figure 24. Cargo UAS DATCOM Input Visualization	49
Figure 25. True airspeed (TAS) vs. altitude for RQ7B for flight from KIAD to KJFK	52
Figure 26. Corrected .APF file for Shadow B (RQ7B). File was compiled by Purdue.	53
Figure 27. Corrected .DCT file for Shadow B (RQ7B). File was compiled by IAI.	53
Figure 28. Corrected .OPF file for Shadow B (RQ7B). File was compiled by Purdue.	54
Figure 29. Corrected .PTF file for Shadow B (RQ7B). File was compiled by Purdue.	55
Figure 30. True airspeed (TAS) vs. altitude for Shadow B flight from KIAD to KJFK using corrected BADA files	56
Figure 31. Plan-view of Shadow B flight path from KIAD to KJFK using corrected BADA files	56
Figure 32. Details of Shadow B flight from KIAD to KJFK using corrected BADA files	57
Figure 33. True airspeed (TAS) vs. altitude for Global Hawk flight from KMSP to KMCO	58
Figure 34. The .PTF file for Global Hawk (RQ4A). File was compiled by Purdue.	59
Figure 35. The .OPF file for Global Hawk (RQ4A). File was compiled by Purdue.	60
Figure 36. Plan-view of Global Hawk flight path from KMSP to KMCO	61
Figure 37. Variation in altitude and airspeed (TAS) with time and distance for Global Hawk flight from KMSP to KMCO	61
Figure 38. True airspeed (TAS) vs. altitude for Orbiter flight from KATL to KBHM	62
Figure 39. Plan-view of Orbiter flight path from KATL to KBHM	62
Figure 40. Variation in altitude and airspeed (TAS) with time and distance for Orbiter flight from KATL to KBHM	63
Figure 41. True airspeed (TAS) vs. altitude for Aerosonde flight from KATL to KBHM	64
Figure 42. Plan-view of Aerosonde flight path from KATL to KBHM	64
Figure 43. Variation in altitude and airspeed (TAS) with time and distance for Aerosonde flight from KATL to KBHM	65

Figure 44. True airspeed (TAS) vs. altitude for Predator A flight from KATL to KJFK	66
Figure 45. Plan-view of Predator A flight path from KATL to KJFK	66
Figure 46. Variation in altitude and airspeed (TAS) with time and distance for Predator A flight from KATL to KJFK	67
Figure 47. True airspeed (TAS) vs. altitude for Predator B flight from KMSP to KMCO	68
Figure 48. Plan-view of Predator B flight path from KMSP to KMCO	68
Figure 49. Variation in altitude and airspeed (TAS) with time and distance for Predator B flight from KMSP to KMCO	69
Figure 50. True airspeed (TAS) vs. altitude for Gray Eagle flight from KATL to KJFK	70
Figure 51. Plan-view of Gray Eagle flight path from KATL to KJFK	70
Figure 52. Variation in altitude and airspeed (TAS) with time and distance for Gray Eagle flight from KATL to KJFK	71
Figure 53. True airspeed (TAS) vs. altitude for Predator C flight from KMSP to KMCO	72
Figure 54. Plan-view of Predator C flight path from KMSP to KMCO	72
Figure 55. Variation in altitude and airspeed (TAS) with time and distance for Predator C flight from KMSP to KMCO	73
Figure 56. True airspeed (TAS) vs. altitude for Hunter flight from KATL to KJFK	74
Figure 57. Plan-view of Hunter flight path from KATL to KJFK	74
Figure 58. Variation in altitude and airspeed (TAS) with time and distance for Hunter flight from KATL to KJFK	75
Figure 59. True airspeed (TAS) vs. altitude for Shadow B flight simulation using MACS from KMSP to KMCO	78
Figure 60. Variation in altitude and airspeed (TAS) with time and distance for Shadow B flight simulation using MACS	79
Figure 61. True airspeed (TAS) vs. altitude for Global Hawk flight simulation using MACS from KMSP to KMCO	79
Figure 62. Variation in altitude and airspeed (TAS) with time and distance for Global Hawk flight simulation using MACS	80
Figure 63. Variation in altitude and airspeed (TAS) with time and distance for Aerosonde flight simulation using MACS	81
Figure 64. Variation in altitude and airspeed (TAS) with time and distance for Predator A flight simulation using MACS	82
Figure 65. Variation in altitude and airspeed (TAS) with time and distance for Predator B flight simulation using MACS	83
Figure 66. Variation in altitude and airspeed (TAS) with time and distance for Gray Eagle flight simulation using MACS	84
Figure 67. Variation in altitude and airspeed (TAS) with time and distance for Predator C flight simulation using MACS	85
Figure 68. Variation in altitude and airspeed (TAS) with time and distance for Hunter flight simulation using MACS	86
Figure 69. Different speeds for Global Hawk (RQ4A) in the BADA file “RQ4A__.PTF”. The file shown here is a section of the complete file.	132
Figure 70. Different stall speeds for Global Hawk (RQ4A) in the BADA file “RQ4A__.OPF”. The file shown here is a section of the complete file.....	133

List of Tables

Table 1. Project Summary.....	10
Table 2. Specifications and basic attributes of Shadow B (RQ7B)	11
Table 3. Specifications and basic attributes of Global Hawk (RQ4A).....	11
Table 4. Specifications and basic attributes of Aerosonde	11
Table 5. Specifications and basic attributes of Orbiter.....	12
Table 6. Specifications and basic attributes of Cargo UAS	12
Table 7. Specifications and basic attributes of NEO S-300 Mk II VTOL.....	12
Table 8. Specifications and basic attributes of Hunter UAS (MQ5B)	12
Table 9. Specifications and basic attributes of Fire Scout	12
Table 10. Specifications and basic attributes of Predator A.....	13
Table 11. Specifications and basic attributes of Predator B.....	13
Table 12. Specifications and basic attributes of Gray Eagle	13
Table 13. Specifications and basic attributes of DHS Avenger/Predator C	14
Table 14. Industry data for Shadow B (RQ7B). Provided by AAI	14
Table 15. Airframe drag model substitutions for UAS aircraft. MACS files for Orbiter, Cargo UAS, Fire Scout and NEO S-300 Mk II VTOL were not simulated.....	24
Table 16. Summary of the actual engines used and the engine decks used in the project to model BADA and MACS for UAS aircraft	37
Table 17. FLOPS sizing results for Shadow B.....	38
Table 18. FLOPS sizing results for Global Hawk.....	40
Table 19. DATCOM-JSBSim sizing results for Orbiter.....	41
Table 20. DATCOM-JSBSim sizing results for Aerosonde	43
Table 21. FLOPS sizing results for Predator A.....	44
Table 22. FLOPS sizing results for Predator B	45
Table 23. FLOPS sizing results for Gray Eagle	46
Table 24. FLOPS sizing results for Predator C.....	47
Table 25. FLOPS sizing results for Hunter UAS	48
Table 26. DATCOM-JSBSim sizing results for Cargo UAS	48
Table 27. RPAT sizing results for Fire Scout.....	50
Table 28. RPAT sizing results for NEO S-300 Mk II VTOL	50
Table 29. Features of Shadow B flight simulation using KTG	51
Table 30. Stall speeds and corresponding altitude constraints employed by KTG. Stall speeds are Calibrated Airspeeds (CAS) in knots	52
Table 31. Features of Shadow B flight using corrected BADA files.....	55
Table 32. Results of Global Hawk flight simulation using KTG	57
Table 33. Features of Orbiter flight simulation using KTG	62
Table 34. Features of Aerosonde flight simulation using KTG	63
Table 35. Features of Predator A flight simulation using KTG	65
Table 36. Features of Predator B flight simulation using KTG	67
Table 37. Features of Gray Eagle flight simulation using KTG	69
Table 38. Features of Predator C flight simulation using KTG	71
Table 39. Features of Hunter flight simulation using KTG	73
Table 40. Summary of nine UAS flights using KTG. Only origin, destination, cruise altitude and cruise speed are included here. Validation of BADA files implies the aircraft reached target cruise altitude in simulation.....	76
Table 41. Features of Shadow B flight simulation using MACS	78
Table 42. Features of Global Hawk flight simulation using MACS	80
Table 43. Features of Aerosonde flight simulation using MACS	80
Table 44. Features of Predator A flight simulation using MACS	81

Table 45. Features of Predator B flight simulation using MACS	82
Table 46. Features of Predator A flight simulation using MACS	83
Table 47. Features of Predator C flight simulation using MACS	84
Table 48. Features of Hunter flight simulation using MACS.....	85
Table 49. Summary of nine UAS flight simulations in MACS. Only origin, destination, cruise altitude and cruise speed are included here.	87
Note 2: Information regarding origin/destination airports, route distances, altitude and speed defined in these FDSs is indicated in the simulation summary chart - Table 50. Summary of results for from ACES simulations to test CNS capabilities of UAS aircraft	88
Table 51. Summary of results for from ACES simulations to test CNS capabilities of UAS aircraft	90
Table 52. Industry data for Shadow B (RQ7B). Provided by AAI.	96
Table 53. Industry data for Global Hawk (RQ4A). Provided by AAI.	98
Table 54. Industry data for Orbiter. Provided by AAI.	100
Table 55. Industry data for Aerosonde. Provided by AAI.	103
Table 56. Industry data for Predator A. Provided by General Atomics.	105
Table 57. Industry data for Predator B. Provided by General Atomics.	108
Table 58. Industry data for Gray Eagle. Provided by General Atomics.	112
Table 59. Industry data for Predator C. Provided by AAI.	115
Table 60. Industry data for Cargo UAS. Provided by AAI.	117
Table 61. Industry data for Cargo UAS. Provided by AAI.	120
Table 62. Industry data for Fire Scout. Provided by AAI.	123
Table 63. Industry data for NEO S-300 Mk II VTOL. Provided by AAI.	125
Table 64. Flight crossing altitudes in TRACON airspace by aircraft weight and engine type ...	130
Table 65. Flight Calibrated Airspeed (CAS) in TRACON airspace by aircraft weight and engine type.....	130
Table 66. Different speed settings of Global Hawk for inclusion in ACES aircraft database. Speeds are Calibrated Airspeed in knots (KCAS).	131

1 Introduction

The purpose of this project was to create performance data for twelve Unmanned Aerial Systems (UAS) aircraft in two formats usable by standard aviation models: the *Base of Aircraft Data* (BADA) that has been specified by EUROCONTROL [1], and the *Multi Aircraft Control System* (MACS) that has been specified by NASA [2]. In addition, simulations were conducted to evaluate the communication, navigation and surveillance (CNS) capabilities of the UAS aircraft using the Airspace Concept Evaluation System (ACES).

This report presents the industry data acquired for twelve UAS aircraft, the BADA and MACS files that were produced for these aircraft and tests to verify the data files. The twelve UAS aircraft are Shadow B, Global Hawk, Orbiter, Aerosonde, Predator A, Predator B, Gray Eagle, Predator C, Hunter, Cargo UAS, Fire Scout and NEO S-300 Mk II VTOL. The tests were able to identify and correct errors in the BADA data. Data for the twelve aircraft analyzed in this project were provided by AAI and General Atomics (GA). A summary of modeling, production and verification of the BADA and MACS files for these aircraft is shown in Table 1. Results from ACES simulations to evaluate CNS capabilities of the aircraft are also presented in this report.

Table 1. Project Summary

UAS Aircraft	Code in BADA and MACS Files	Manufacturer	Industry Data Acquired	BADA Delivered	BADA Verified	MACS Delivered	MACS Verified
Shadow B	RQ7B	AAI	Yes	Yes	Yes*	Yes	Yes
Global Hawk	RQ4A	AAI	Yes	Yes	Yes	Yes	Yes
Orbiter	ORBM	AAI	Yes	Yes	Yes [†]	Yes	No [†]
Aerosonde	MK47	AAI	Yes	Yes	Yes*	Yes	No [†]
Predator A	MQ1B	GA	Yes	Yes	Yes*	Yes	Fail [‡]
Predator B	MQ-9	GA	Yes	Yes	Yes	Yes	Fail [‡]
Gray Eagle	MQ1C	GA	Yes	Yes	Yes*	Yes	Fail [‡]
Predator C	AVEN	GA	Yes	Yes	Yes*	Yes	Fail [‡]
Hunter UAS	MQ5B	AAI	Yes	Yes	Yes	Yes	Fail [‡]
Cargo UAS	CUAS	AAI	Yes	Yes	No [#]	Yes	Fail [‡]
Fire Scout	MQ8B	AAI	Yes	Yes	No [#]	Yes	No ^{##}
NEO S-300 Mk II VTOL	S350	AAI	Yes	Yes	No [#]	Yes	No ^{##}
* Aircraft performance altered by BADA stall speed constraints							
† Aircraft engine profile issues—electric aircraft							
‡ Failed to reach designated cruise altitude							
# Cannot simulate rotorcraft in KTG							
## Cannot simulate rotorcraft in MACS							

2 Specifications and Basic Attributes of UAS Aircraft

2.1 Eight Aircraft from AAI

Manufacturer data for eight aircraft were provided by AAI: Shadow B (RQ7B), Aerosonde, Orbiter, Cargo UAS, NEO S-300 Mk II VTOL, Hunter UAS (MQ-9B), Global Hawk (RQ4A) and Fire Scout. Important specifications and basic attributes of these aircraft are shown in Table 2, Table 3, Table 4, Table 5, Table 6, Table 7, Table 8 and Table 9.

Table 2. Specifications and basic attributes of Shadow B (RQ7B)

Length (ft.)	11.2
Wingspan (ft.)	14.0
Max. gross weight (lb.)	375
Range (nmi.)	685 for air aircraft; 27 for control
Endurance (hr.)	9
Max. altitude (ft.)	15000
Communication capabilities	Primary & secondary datalink, TDMA
Navigation modes	Auto-launch, auto-pilot (altitude, airspeed & heading), fly-to-location, auto-land, flight termination (parachute)
Surveillance	ATC transponder
Example civilian applications	Surveillance: fuel pipelines, power lines, ports & harbors, and law enforcement

Table 3. Specifications and basic attributes of Global Hawk (RQ4A)

Length (ft.)	44.4
Wingspan (ft.)	116.2
Max. gross weight (lb.)	26700
Range (nmi.)	12000
Endurance (hr.)	35
Max. altitude (ft.)	65000
Communication capabilities	Ku SATCOM datalink, CDL line-of-sight, UHF SATCOM/LOS, and ATC voice
Surveillance	Synthetic aperture radar, EO NIIRS 6.0, IR NIIRS 5.0
Example civilian applications	Atmospheric research, forest fire monitoring and support, and natural hazard monitoring

Table 4. Specifications and basic attributes of Aerosonde

Length (ft.)	6.9
Wingspan (ft.)	11.8
Max. gross weight (lb.)	30
Range (nmi.)	608
Endurance (hr.)	10
Max. altitude (ft.)	15000
Communication capabilities	Primary & secondary + independent imagery datalink
Navigation modes	Cloudcap avionics suite
Surveillance	Mode 3 IFF transponder
Example civilian applications	Land survey, ice monitoring, and climate change support

Table 5. Specifications and basic attributes of Orbiter

Length (ft.)	3.2
Wingspan (ft.)	7.2
Max. gross weight (lb.)	14.3
Range (nmi.)	27
Endurance (hr.)	2–3
Max. altitude (ft.)	18000
Communication capabilities	One data uplink and one data downlink channel
Navigation modes	UMAS avionics for flight control, stabilization, mission control, and payload control
Surveillance	
Example civilian applications	SWAT team monitoring, covert law enforcement and monitoring, and agriculture/animal monitoring

Table 6. Specifications and basic attributes of Cargo UAS

Length (ft.)	38.0 (rotor)
Wingspan (ft.)	38.0 (wing) — hybrid
Max. gross weight (lb.)	7250
Range (nmi.)	2800–5500 (based on cargo)
Endurance (hr.)	Up to 20
Max. altitude (ft.)	35000
Navigation modes	Auto-takeoff, auto-land, waypoint, electronic tethering, and auto-tracking
Example civilian applications	Cargo transport

Table 7. Specifications and basic attributes of NEO S-300 Mk II VTOL

Length (ft.)	LxWxH: 9.0 x 3.1 x 2.8; rotor diameter: 9.8
Wingspan (ft.)	N/A (rotorcraft)
Max. gross weight (lb.)	176
Range (nmi.)	87
Endurance (hr.)	2
Max. altitude (ft.)	10000
Communication capabilities	RF Line-of-sight, dedicated datalink for payload
Navigation modes	Auto-takeoff, auto-land, waypoint, electronic tethering, and auto-tracking
Surveillance	EO/IR
Example civilian applications	Law enforcement, and search & rescue

Table 8. Specifications and basic attributes of Hunter UAS (MQ5B)

Length (ft.)	23.0
Wingspan (ft.)	34.25
Max. gross weight (lb.)	1800
Range (nmi.)	144
Endurance (hr.)	21
Max. altitude (ft.)	22000
Communication capabilities	LDS datalink, UAV airborne relay, and voice
Surveillance	EO/IR
Example civilian applications	Surveillance: fuel pipelines, power lines, ports & harbors, and law enforcement

Table 9. Specifications and basic attributes of Fire Scout

Length (ft.)	23.9 (length); 27.5 (rotor); 4.42 (height)
Wingspan (ft.)	N/A (rotorcraft)
Max. gross weight (lb.)	3150

Range (nmi.)	110
Endurance (hr.)	8
Max. altitude (ft.)	20000
Navigation modes	Auto-land
Example civilian applications	Surveillance: persistent maritime or port, and media surveillance

2.2 Four Aircraft from General Atomics

Manufacturer data for four aircraft were provided by General Atomics (GA): Predator A, Predator B, Gray Eagle and DHS Avenger/Predator C. Important aircraft specifications and basic attributes of these aircraft are shown in Table 10, Table 11, Table 12 and Table 13.

Table 10. Specifications and basic attributes of Predator A

Length (ft.)	27.0
Wingspan (ft.)	55.0
Max. gross weight (lb.)	2250
Range (nmi.)	4800
Endurance (hr.)	40
Max. altitude (ft.)	25000
Communication capabilities	C-Band line-of-sight, Ku-Band over-the-horizon SATCOM, UHF/VHF voice, communications relay
Navigation modes	Fully autonomous
Surveillance	MTS-A EO/IR, Lynx Multi-mode radar, SIGINT/ESM system
Example civilian applications	Crop and cattle monitoring, ice passage monitoring, national disaster support, and airborne pollution observation

Table 11. Specifications and basic attributes of Predator B

Length (ft.)	36.0
Wingspan (ft.)	66.0
Max. gross weight (lb.)	10000
Range (nmi.)	5700
Endurance (hr.)	30
Max. altitude (ft.)	50000
Communication capabilities	C-Band line-of-sight data link control, Ku-Band beyond line-of-sight/SATCOM data link control, communications relay
Navigation modes	Fully autonomous
Surveillance	MTS-B EO/IR, Lynx Multi-mode Radar, Multi-mode maritime radar, SIGINT/ESM system
Example civilian applications	Border patrol, search and rescue, maritime surveillance, aerial imaging and mapping, and chemical and petroleum spill monitoring

Table 12. Specifications and basic attributes of Gray Eagle

Length (ft.)	28
Wingspan (ft.)	56
Max. gross weight (lb.)	3600
Range (nmi.)	200
Endurance (hr.)	30
Max. altitude (ft.)	29000
Communication capabilities	TCDL line-of-sight satellite communication, TCDL air data relay communications, over-the-horizon Ku-Band SATCOM
Navigation modes	Auto-takeoff and landing

Surveillance	EO/IR
Example civilian applications	Border patrol, search and rescue, maritime surveillance, aerial imaging and mapping, and chemical and petroleum spill monitoring

Table 13. Specifications and basic attributes of DHS Avenger/Predator C

Length (ft.)	44.0
Wingspan (ft.)	66.0
Max. gross weight (lb.)	15800
Range (nmi.)	
Endurance (hr.)	18
Max. altitude (ft.)	50000
Communication capabilities	Communication relay
Navigation modes	
Surveillance	EO/IR, Lynx Multi-mode Radar, SIGINT/ESM System
Example civilian applications	Environmental monitoring and mapping, in-situ atmospheric research, sea-ice observations, crop monitoring, TV signal transmission, and cell phone signal platform

3 Industry Data Presentation

Industry data for only Shadow B are presented here as a sample and for brevity (Table 14). The data for all twelve UAS aircraft are presented in Appendix A.

Table 14. Industry data for Shadow B (RQ7B). Provided by AAI.

Operations Performance Files (OPF)	
Design Range	685 nmi.
Design Endurance	9 hr.
Basic Geometry	
	
Wing Aspect Ratio	11.1
Wing span	19.8 ft.
Wing taper	0.7
Fuselage length	63.1 in.
Fuselage fineness	0.181
Tail size	
Tail Volume Coefficient	0.65% (horizontal volume coefficient)
Drag Polars	
Equation or Graph	$C_D = 0.0497 + C_L^2 / (\pi * 0.9 * AR) \rightarrow$ Wing drag polar
Mass	
Max. mass of aircraft	333 lb. (Aircraft without fuel. Pop 300 installed)

(Empty Weight)	
Max. mass of aircraft (Gross Weight)	467 lb., max. (TGOW)
Max. payload	60 lb.
Flight envelope	
V _{MO} (in CAS or TAS)	136 KCAS
M _{MO} (Mach Max. Operating)	0.197
H _{max}	18000 ft., MSL
Aerodynamics	
S _{wet}	16.3 ft. ² (Fuselage)
	99.3 ft. ² (Total Surface Area)
S _{ref}	35.36 ft. ² (Wing)
C _{lb,o} (Buffet Onset Lift Coeff.)	1.04
Stall speed (Initial Climb)	54 KIAS
Stall speed (Cruise)	54 KIAS
Stall speed (Take Off)	56 KIAS
Stall speed (Landing)	52 KIAS
Stall speed (Approach)	52 KIAS
Engine Thrust	
Max. thrust at Climb	
Max. thrust at Cruise	
Max. thrust at Descent	
Propulsion	
Engine	UEL 741AR74-1102
Brake engine power	38bhp @ 7800rpm
No. of cylinders	1 rotor (tri-tip)
Baseline engine power	38 bhp
Critical turbocharger altitude	N/A
Fuel consumption	BASFC _{min} = 2.2–2.3 L/hr.
	BSFC _{max} = 13.2–13.4 L/hr.
	BSFC _{cruise} = 0.56 lb./hp-hr.
Max. engine crankshaft speed	8000 rpm
Max. propeller shaft speed	8000 rpm
Engine displacement	208 cc/chamber (6188 cc piston engine equivalent)
Engine compression ratio	9.5:1
Engine envelope	X = 15.5 in.
	Y = 16.5 in.
	Z = 16.5 in.
Propeller type	Fixed pitch
Blade angle	22°
Propeller diameter	29 in.
Activity factor	(Proprietary)
Integrated design lift coefficient (for blade)	0.8
Fuel Consumption	
Thrust Specific Fuel Consumption	Do not currently have for this AV. Mostly used for jet aircraft performance
Brake Specific Fuel	0.54 lb./hp-hr. at 70 KIAS Cruise

Consumption	
Ground Movement	
Landing length	400 ft. (assumes length from touch down point to arresting net)
Takeoff length	AV is launched from ground aircraft
Width of runway	50 ft. (minimum)
Aircraft length	143 in.
Airline Procedures Files (APF)	
Climb Operating Speed	62 KCAS
Cruise Operating Speed	70 KCAS
Descent Operating Speed	65 KCAS

4 BADA File Presentation

Research and development activities in the Air Traffic Management (ATM) and the Air Traffic Control (ATC) systems require accurate information on aircraft performance, expressed via an Aircraft Performance Model (APM). While the primary role of APMs is to provide aircraft performance data to ATM/ATC simulation tools, APMs should also be capable of computing the geometric, kinematic and kinetic aspects of an aircraft in flight. Furthermore, these performance models should also be applicable in all phases of flight and be available for a wide set of aircraft.¹ Currently, APMs do not exist for UAS, and the task of developing them is complicated due to the significant heterogeneity in UAS configuration and operation. In this project, APMs were developed for 12 UAS aircraft and expressed in two formats: the Base of Aircraft Data (BADA) and the Multi-Aircraft Control System (MACS). The resulting UAS APMs, the assumptions used in their generation, and the limitations identified along the way are described in the remainder of this report.

BADA is an APM developed and maintained by EUROCONTROL [1]. BADA provides a set of ASCII files containing performance and operating procedure coefficients for approximately 300 different aircraft in all phases of flight. The coefficients include those used to calculate thrust, drag and fuel flow and those used to specify nominal cruise, climb and descent speeds. BADA is based on a kinetic approach to aircraft performance modeling, which models aircraft forces. The intended use of BADA is trajectory simulation and prediction in ATM research and development and strategic planning in ground ATM operations. Currently, several air traffic modeling and simulation tools such as ACES, FACET etc., use BADA for trajectory simulation.

Four Base of Aircraft Data (BADA) files were generated for each UAS aircraft, consisting of stall speeds during different phases of flight, ascent and descent rates, fuel flow rate, empty and fuel masses, and aircraft speeds at different altitudes during the flight. These four files are:

- Operational Performance File (.OPF): contains performance parameters for a specific aircraft type including drag and thrust coefficients
- Airlines Procedures File (.APF): contains speed procedure parameters for a specific aircraft type
- Performance Table File (.PTF): contains summary performance tables of true airspeed, climb/descent rate and fuel consumption at various flight levels for a specific aircraft type
- Descent file (.DCT): contains descent rate and fuel consumption rate during descent. This file represents data in the .PTF file in a different format.

For each aircraft, the .APF, .OPF and .PTF files were compiled by the Purdue team, whereas the .DCT file was compiled by IAI using the data in the .PTF file. The four BADA files for Shadow B are shown in Figure 1, Figure 2, Figure 3 and Figure 4. It should be noted that only those columns in the .DCT file that are relevant to simulating the flight using the Kinematic Trajectory Generator (KTG) were compiled. KTG is a flight trajectory simulation tool developed at IAI [3], which was used to simulate the UAS flights and validate the BADA files. Therefore, the .DCT file contains less data than the version provided by the EUROCONTROL.

Only the BADA files for Shadow B (Figure 1, Figure 2, Figure 3 and Figure 4), and their corrected versions and the reasons for the corrections later on in this report, are presented here. The files for all the UAS aircraft (including Shadow B) were provided to NASA on a DVD, along with the option to download them from an ftp site: <ftp://ftp.i-a-i.com>. While it is safe to assume that the fuel flow equations and the climb/descent procedures provided in BADA can be used for large UAS, the lightweight aircraft may not perform as intended if modeled using the same formulas. Once the modeling is completed, simulation tools utilize the tables and parameters in the .PTF and .OPF files for each aircraft to describe its trimmed motion or transition at any specified altitudes.

```
CCCCCCCCCCCCCCCCCCCCCCCCCCCCCCCCCCCCCCCCCCCC RQ7B__.APF CCCCCCCCCCCCCCCCCCCCCCCCCCCCCCCCCCCCCCCCCCCCCC/
CC // 
CC          AIRLINES PROCEDURES FILE
CC // 
CC      File_name: RQ7B__.APF
CC // 
CC      Creation_date: Mar 01 2012
CC // 
CC      Modification_date: Mar 01 2012
CC // 
CC // 
CC      LO= --- to --- / AV= --- to --- / HI= --- to ---
CC // 
CC==========
CC  COM CO    Company name -----climb----- --cruise-- -----descent----- --approach- model-
CC          mass lo hi           lo hi           hi lo           (unused)
CC  version engines ma cas cas mc xxxx xx cas cas mc mc cas cas xxxx xx xxx xxx xxx opf_
CC==========
CD *** **  Default Company
CD RQ7B     AR741    LO   62   62 20       70   70   20   20 70   70       0   0   0   RQ7B_/
CD RQ7B     AR741    AV   62   62 20       70   80   20   20 70   70       0   0   0   RQ7B_/
CD RQ7B     AR741    HI   62   62 20       70   70   20   20 70   70       0   0   0   RQ7B_/
CC=====
```

Figure 1. The .APF file for Shadow B (RQ7B). File was compiled by Purdue.

Descent calculation using BADA model															
AIRCRAFT:															
AIRCRAFT_CODE: RQ7B (no ICAO code)															
ENGINE: UAV AR-741															
CALCULATION CONDITIONS:															
CALCULATION TYPE: POINT															
STALL															
CAS below FL100:															
CAS above FL100:															
Mach :															
Atmosphere Model : OLD ISA Model															
RESULTS:															
FL	Mass	CAS	Mach	TAS	ROCD	Gradient	FuelFlow	Temperature	SpeedOfSound	Density	Thrust	Max_Thrust	Drag	AvlPower	ESF
[ft]	[kg]	[kt]		[kt]	[ft/min]	[deg]	[kg/s]	[K]	[m/s]	[kg/m³]	[N]	[N]	[N]	[kW]	
18000	151.0	74.90	.16	99.0	490	0.0	.0033	252.5	318.53	.6982	0.0	0.0	0.0	0.0	0.0
16000	151.0	75.00	.15	96.0	490	0.0	.0033	256.5	321.02	.7460	0.0	0.0	0.0	0.0	0.0
14000	151.0	74.30	.15	92.0	470	0.0	.0033	260.4	323.49	.7963	0.0	0.0	0.0	0.0	0.0
12000	151.0	75.80	.14	91.0	460	0.0	.0033	264.4	325.95	.8492	0.0	0.0	0.0	0.0	0.0
10000	151.0	75.70	.14	88.0	440	0.0	.0033	268.3	328.38	.9047	0.0	0.0	0.0	0.0	0.0
8000	151.0	77.20	.14	87.0	430	0.0	.0033	272.3	330.80	.9629	0.0	0.0	0.0	0.0	0.0
6000	151.0	77.70	.13	85.0	420	0.0	.0033	276.3	333.19	1.0240	0.0	0.0	0.0	0.0	0.0
4000	151.0	77.30	.13	82.0	410	0.0	.0033	280.2	335.57	1.0879	0.0	0.0	0.0	0.0	0.0
3000	151.0	76.50	.12	80.0	400	0.0	.0033	282.2	336.76	1.1211	0.0	0.0	0.0	0.0	0.0
2000	151.0	75.70	.12	78.0	320	0.0	.0033	284.2	337.94	1.1549	0.0	0.0	0.0	0.0	0.0
1500	151.0	73.40	.11	75.0	290	0.0	.0033	285.2	338.53	1.1722	0.0	0.0	0.0	0.0	0.0
1000	151.0	71.00	.11	72.0	270	0.0	.0033	286.2	339.11	1.1896	0.0	0.0	0.0	0.0	0.0
500	151.0	70.50	.11	71.0	230	0.0	.0033	287.2	339.70	1.2072	0.0	0.0	0.0	0.0	0.0
0	151.0	69.00	.10	69.0	200	0.0	.0033	288.2	340.29	1.2251	0.0	0.0	0.0	0.0	0.0

Figure 2. The .DCT file for Shadow B (RQ7B). File was compiled by IAI.

```

CCCCCCCCCCCCCCCCCCCCCCCCCCCCCCCCCCCCCCCC RQ4A__.OPF CCCCCCCCCCCCCC
CC
CC          AIRCRAFT PERFORMANCE OPERATIONAL FILE
CC
CC
CC      File_name: RQ7B__.OPF
CC
CC      Creation_date: Mar 01 2012
CC
CC      Modification_date: Mar 01 2012
CC
CC
CC===== Actype =====/
CD  RQ7B_      1 engines   Piston           L   /
CC  AAI          RQ7B with 1 AR741   engines     wake   /
CC
CC===== Mass (t) =====/
CC  reference    minimum    maximum    max payload  mass grad /
CD  .00193E+02  .00151E+02  .00212E+02  .00027E+02  .00000E+00 /
CC===== Flight envelope =====/
CC  VMO(KCAS)   MMO        Max.Alt     Hmax      temp grad /
CD  .13600E+03  .22500E+00  .18000E+05  .00000E+00  .00000E+00 /
CC===== Aerodynamics =====/
CC Wing Area and Buffet coefficients (SIM)
CCndrst Surf(m2) Clbo(M=0) k CM16
CD 5  .03285E+02  .10400E+01  .00000E+00  .00000E+00 /
CC Configuration characteristics
CC n Phase Name Vstall(KCAS) CD0 CD2 unused
CD 1 CR Clean  .54000E+02  .49700E+01  .31879E-02  .00000E+00 /
CD 2 IC Clean  .54000E+02  .00000E+00  .00000E+00  .00000E+00 /
CD 3 TO Clean  .56000E+02  .00000E+00  .00000E+00  .00000E+00 /
CD 4 AP Clean  .52000E+02  .00000E+00  .00000E+00  .00000E+00 /
CD 5 LD Clean  .52000E+02  .00000E+00  .00000E+00  .00000E+00 /
CC Spoiler
CD 1 RET
CD 2 EXT
CC Gear
CD 1 UP
CD 2 DOWN
CC Brakes
CD 1 OFF
CD 2 ON
CC===== Engine Thrust =====/
CC  Max climb thrust coefficients (SIM)
CD  .62012E+05  .50000E+05  .62006E+05  .00000E+00  .00000E+00 /
CC  Desc(low)  Desc(high) Desc level Desc(app) Desc(ld)
CD  .10000E+00  .10000E+00  .15000E+05  .00000E+00  .00000E+00 /
CC  Desc CAS   Desc Mach  unused  unused  unused
CD  .70000E+02  .22500E+00  .00000E+00  .00000E+00  .00000E+00 /
CC===== Fuel Consumption =====/
CC  Thrust Specific Fuel Consumption Coefficients
CD  .67000E+00  .00000E+00
CC  Descent Fuel Flow Coefficients
CD  .50000E+01  .00000E+00
CC  Cruise Corr.  unused  unused  unused  unused
CD  .10000E+01  .00000E+00  .00000E+00  .00000E+00  .00000E+00 /
CC===== Ground =====/
CC  TOL      LDL      span      length     unused
CD  .25600E+03  .93600E+03  .60350E+01  .34000E+01  .00000E+00 /
CC=====/

```

Figure 3. The .OPF file for Shadow B (RQ7B). File was compiled by Purdue.

BADA PERFORMANCE FILE								Mar 01 2012				
AC/Type: RQ7B_				SOURCE OPF FILE: Mar 01 2012								
				SOURCE APF FILE: Mar 01 2012								
Speeds: CAS (LO/HI) Mach Mass Levels [kg]				Temperature: ISA								
climb -	62/ 70	0.22	low	-	151							
cruise -	70/ 80	0.22	nominal	-	193	Max Alt. [ft]: 18000						
descent -	62/ 70	0.22	high	-	212							
FL	CRUISE			CLIMB			DESCENT					
	TAS	fuel		TAS	ROCD	fuel	TAS	ROCD	fuel			
	[kts]	[kg/min]		[kts]	[fpm]	[kg/min]	[kts]	[fpm]	[kg/min]			
	lo	nom	hi	lo	nom	hi	nom	nom	nom	nom		
0				69	1450	1750	1435	0.1	69	200	0.2	
5				70	1515	1899	1535	0.1	71	230	0.2	
10				72	1743	2371	1713	0.1	72	270	0.2	
15				74	1786	2420	1755	0.1	75	290	0.2	
20				77	1760	2389	1730	0.1	78	320	0.2	
30	72	0.1	0.1	79	1860	2015	1860	0.1	80	400	0.2	
40	74	0.1	0.1	81	2185	2837	2154	0.1	82	410	0.2	
60	77	0.1	0.1	83	894	1263	877	0.1	85	420	0.2	
80	80	0.1	0.1	87	825	1179	809	0.1	87	430	0.2	
100	84	0.1	0.1	89	937	1304	921	0.1	88	440	0.2	
120	89	0.1	0.1	91	854	1200	839	0.1	91	460	0.2	
140	93	0.1	0.1	94	764	1089	750	0.1	92	470	0.2	
160	97	0.1	0.1	97	669	970	656	0.1	96	490	0.2	
180	99	0.1	0.1	99	575	853	563	0.1	99	490	0.2	

Figure 4. The .PTF file for Shadow B (RQ7B). File was compiled by Purdue.

Challenges with BADA File Format for UAS: Deficiencies and Limitations

BADA is primarily used for manned aircraft and its capability to model rotorcrafts, hybrids or electric aircraft is currently unknown. Current BADA format does not have provisions for simulating rotorcraft and electric engines (both frequently used in the UAS family). Performance characteristics and/or aircraft component types that are missing in BADA, but important for understanding the UAS-NAS integration, can be classified as deficiencies in BADA. These deficiencies are of the following types:

- Aircraft type, class and size (e.g., rotorcraft are currently not considered in BADA)
- Propulsion type (e.g., BADA currently handles only jets, turboprops and pistons; electric engines are not considered)

Performance characteristics that are poorly modeled in BADA (fidelity too low to be used in existing simulations) can be classified as limitations of BADA:

- Stall speed buffers that are too limiting
- Climb/descent schedules that are often ill-suited for many UAS

Deficiencies

Aircraft type, class and size: BADA was primarily developed for manned, fixed-wing aircraft, and does not have provisions to include rotorcraft or hybrid aircraft. Additionally, BADA specifies wake categories based on aircraft weight: Small (up to 12,500 lb.), Medium (12,500 to 41,000 lb.), Large (41,000 to 255,000 lb.) and Heavy (more than 255,000 lb.). However, it does not include very-small/light aircraft such as Orbiter or Aerosonde. Consequently, BADA coefficients and procedures are not well-defined for such very-light aircraft. Considering these restrictions, some of the UAS aircraft could not be properly represented in BADA until modifications (revisions to the format) were in place:

- Rotorcraft: NEO S-300 Mk II VTOL and Fire Scout
- Hybrid: Cargo UAS
- Very Light Aircraft: Aerosonde and Orbiter

The following BADA fields, in particular, are difficult, or even impossible, to determine for the three aforementioned aircraft types: a) stall speeds, b) cruise, climb and descent speeds, c) rate of climb/descent coefficients, d) thrust coefficients, and e) ground movements.

Propulsion type: In its current format, BADA can accommodate three engine types: Jet, Turboprop or Piston. This prevents the representation of UAS that use electric motors, such as the Orbiter. Introduction of electric engine format into BADA requires changes to the .APF and .PTF files in BADA, particularly the fuel flow of the aircraft, in addition to the performance coefficients in the .OPF file.

Limitations

Stall Speed Buffer: As described earlier, aircraft speeds in the .PTF file are currently set to accommodate transport aircraft, these buffer values need to be modified for realistic UAS representation. More specifically, current true airspeed values in the .PTF file have to be at least 1.3 times (1.2 in some cases) the stall speeds at different phases of flight. While this is justified in the case of transport aircraft for reasons of passenger comfort, implementing this in UASs alters their performance. The relationship between stall speeds and speeds in the .PTF file are shown in Table 30. Currently these rules are strictly followed while developing the BADA files for the aircraft in our list since most simulation software have a hard constraint on these conditions before flying an aircraft. Discrepancies resulting from this rule directly affect the performance of certain aircraft.

III-suited climb/descent schedules: In BADA, standard airline procedures are defined using speed profiles in different phases of flight. Procedures similar to that need to be defined in order to calculate rate of climb/descent, fuel flow etc., at different flight levels. In the case of commercial jet aircraft, BADA provides methods to calculate speed profiles at different flight levels, as exemplified in Figure 5, where, $C_{V_{min}}$ refers to the stall speed buffer (Table 30) and Vd_{CL} represents standard airline climb speed increments as shown in Figure 6.

The following parameters are defined for each aircraft type to characterise the climb phase:

$V_{cl,1}$ - standard climb CAS (knots) between 1,500 / 6,000 and 10,000 ft

$V_{cl,2}$ - standard climb CAS (knots) between 10,000 ft and Mach transition altitude

M_{cl} - standard climb Mach number above Mach transition altitude

Note that the Mach transition altitude is defined to be the altitude where a CAS value corresponding to $V_{cl,2}$ results in a Mach number of M_{cl} . That is, M_{cl} imposes an upper limit on the Mach number during climb.

- For jet aircraft the following CAS schedule is assumed, based on the parameters mentioned above and the take-off stall speed:

$$\text{from 0 to 1,499 ft} \quad C_{V_{min}} * (V_{stall})_{TO} + Vd_{CL, 1} \quad (4.1-1)$$

$$\text{from 1,500 to 2,999 ft} \quad C_{V_{min}} * (V_{stall})_{TO} + Vd_{CL, 2} \quad (4.1-2)$$

$$\text{from 3,000 to 3,999 ft} \quad C_{V_{min}} * (V_{stall})_{TO} + Vd_{CL, 3} \quad (4.1-3)$$

$$\text{from 4,000 to 4,999 ft} \quad C_{V_{min}} * (V_{stall})_{TO} + Vd_{CL, 4} \quad (4.1-4)$$

$$\text{from 5,000 to 5,999 ft} \quad C_{V_{min}} * (V_{stall})_{TO} + Vd_{CL, 5} \quad (4.1-5)$$

$$\text{from 6,000 to 9,999 ft} \quad \min(V_{cl,1}, 250 \text{ kt})$$

$$\text{from 10,000 ft to transition} \quad V_{cl,2}$$

$$\text{above transition} \quad M_{cl}$$

Figure 5. BADA climb schedules for commercial Jet aircraft

$Vd_{CL, 1}$	Climb speed increment below 1500 ft (jet)	5
$Vd_{CL, 2}$	Climb speed increment below 3000 ft (jet)	10
$Vd_{CL, 3}$	Climb speed increment below 4000 ft (jet)	30
$Vd_{CL, 4}$	Climb speed increment below 5000 ft (jet)	60
$Vd_{CL, 5}$	Climb speed increment below 6000 ft (jet)	80

Figure 6. BADA standard airline climb increments for commercial Jet aircraft

These procedures are also defined in BADA for manned aircraft with turboprops and piston engines (not shown here). Similarly, standard descent procedures are also defined for manned aircraft (not shown here). However, these definitions were not used in the development of BADA files for the UAS aircraft. Climb/descent speeds, rate and fuel flow are directly taken from the output of sizing tools (FLOPS, JSBSim, etc.) with the stall speed buffers being the only added constraint. Also, simulation software such as KTG and FACET do not hard-code these definitions. Considering the vast heterogeneity in design, such standard procedures may be hard to define for UAS aircraft.

5 MACS File Presentation

The Multi Aircraft Control System (MACS) is a comprehensive research platform used in the Airspace Operations Laboratory (AOL) at NASA Ames Research Center [2]. It was developed to increase the overall realism and flexibility of controller- and pilot-in-the loop air traffic simulations [4]. There are three functional classes of aerodynamic models in MACS with varying levels of fidelity, viz. the motion predictor class, the 4-DOF model and the 6-DOF model. These aero models use aircraft performance database files as parameters for the models. Currently, 434 aircraft files exist within the MACS database.

Addition of new aircraft types for simulation in MACS requires adding database entries for those new aircraft. While MACS allows for simple mappings of aircraft and engines to those already in the database, an entirely new database entry was created for each UAS studied. This is due to the vast differences in size, weight, and flight envelope between UAS and aircraft already in the MACS database. The addition of a new aircraft in the MACS database is accomplished by essentially filling out the `aircraft_specific_model_data.dat` file. This master file (Figure 8) contains all top level information regarding an aircraft and has provisions to map the required drag model and engine model of the aircraft.

Three files were produced to simulate UAS flight in the Multi-aircraft Control System (MACS):

- Aircraft model data file: This file contains an aircraft's description and performance parameters such as the engine type and number of engines, limits on the different operational weights and speeds, and drag model.
- Airframe drag model data file: This file specifies the lift and drag coefficients, at different Mach numbers for an aircraft. Further, where applicable, it also specifies changes to these coefficients for other flight parameters such as settings of flaps, landing gear and speed brakes.
- Flight parameters file: This file specifies the flight path in terms of origin and destination airports along with their location and altitudes, the waypoints, different operational speeds (climb, cruise, descent, approach and landing in knots of indicated air speed), cruise altitude, communication and navigational equipage, and flight-specific operational procedures (e.g., self-separation).

The aircraft model data file for each UAS aircraft was produced by Purdue, whereas the flight parameters file was compiled by IAI by utilizing the data from the .OPF and .PTF BADA files. It should be noted that the 'AIRFRAME DRAG MODEL' file and 'ENGINE THRUST MODEL' file in Figure 8 are external files that are called to the motion class while executing a particular aircraft. If a particular UAS aircraft is similar to an existing aircraft in MACS, a simple mapping will accomplish this process (Table 15), but for other aircraft new drag model and thrust model have to be created.

The three MACS files for Predator B are shown in Figure 8, Figure 9 and Figure 10, respectively. The MACS files for the twelve UAS aircraft were provided to NASA on a DVD, along with the option to download them from an ftp site: <ftp://ftp.i-a-i.com>.

Since this project involves representing UAS data in two formats (BADA and MACS), there is a reasonable need for consistency between a MACS file and a BADA file for the same aircraft. Accordingly, a convention was developed such that a majority of the entries in a MACS file were mapped to specific entries in a BADA .OPF or .APF file as shown in Figure 7.

AIRCRAFT NAME:	<Real AC name>
MANUFACTURER:	<Real manuf>
ENGINE NAME:	<Real engine name>
NUMBER OF ENGINES:	<Real number of engines>
+++++ FAA (OR CTAS INTERNAL) ACID: <Look this up>	
GROSS WING AREA (FT^2):	<OPF ndrst Surf>
MAXIMUM TAKEOFF WEIGHT (LB):	<OPF maximum mass>
OPERATING WEIGHT EMPTY (LB):	<OPF minimum mass>
TYPICAL DESCENT WEIGHT (LB):	<OPF reference mass>
AIRFRAME DRAG MODEL:	<Choose existing airframe or create your own>
MAX WEIGHT FLAP DEFLECT SPEEDS:	XXXX
MIN WEIGHT FLAP DEFLECT SPEEDS:	XXXX
APPROACH SPEED SLOPE:	XXXX
MAX APPROACH WEIGHT SPEED:	<APF HI-mass lo-descent speed>
ENGINE THRUST MODEL:	<Select engine that is closest to the real one based on HP>
ENGINE TYPE:	<JET, TURBOPROP, OR PROP>
DESCENT DRAG SCALE FACTOR:	1.0**
EFFECTIVE NUMBER OF ENGINES:	<Ratio of HP of modeled and real engine>
+++++ MAXIMUM MACH NUMBER: <OPF MMO> MAXIMUM CRUISE MACH NUMBER: <OPF MMO> MINIMUM CAS (KT): <OPF Smallest vstall> MAXIMUM CAS (KT): <OPF VMO> MINIMUM CRUISE CAS (KT): <OPF Vstall in CR phase> MAXIMUM CRUISE CAS (KT): <OPF VMO> CAPCASC1: 0.0** CAPCASC2: 0.0** DEFAULT ASCENT CAS: <APF AV-mass Hi-climb> *****	

Figure 7. Convention for MACS-BADA mapping

Table 15. Airframe drag model substitutions for UAS aircraft. MACS files for Orbiter, Cargo UAS, Fire Scout and NEO S-300 Mk II VTOL were not simulated.

UAS Aircraft	Substitution Aircraft
Shadow B	Cessna 172
Global Hawk	No substitution
Aerosonde	No substitution
Orbiter	Not simulated
Predator A	Cessna 172
Predator B	No substitution
Gray Eagle	Cessna 172
Predator C	No substitution
Hunter	Cessna 172
Cargo UAS	Not simulated
Fire Scout	Not simulated
NEO S-300 Mk II VTOL	Not simulated

```
*****  
IRCRAFT NAME: PREDATOR B  
ANUFACTURER: GEN ATOMICS  
NGINE NAME: TP331-10  
NUMBER OF ENGINES: 1  
+++++  
AA (OR CTAS INTERNAL) ACID: MQ-9  
ROSS WING AREA (FT^2): 256  
AXIMUM TAKEOFF WEIGHT (LB): 8341.9  
PERATING WEIGHT EMPTY (LB): 3478.0  
YPICAL DESCENT WEIGHT (LB): 6882.6  
IRFRAME DRAG MODEL: MQ-9  
AX WEIGHT FLAP DEFLECT SPEEDS: { 120.0 90.0 75.0 70.0 60.0 }  
IN WEIGHT FLAP DEFLECT SPEEDS: { 100.0 80.0 60.0 55.0 50.0 }  
PPROACH SPEED SLOPE: 0.52  
AX APPROACH WEIGHT SPEED: 109.0  
NGINE THRUST MODEL: PW118  
NGINE TYPE: TURBOPROP  
ESCENT DRAG SCALE FACTOR: 1.0  
FFECTIVE NUMBER OF ENGINES: 1.0  
+++++  
AXIMUM MACH NUMBER: 0.38  
AXIMUM CRUISE MACH NUMBER: 0.35  
INIMUM CAS (KT): 60.0  
AXIMUM CAS (KT): 127.0  
INIMUM CRUISE CAS (KT): 93.0  
AXIMUM CRUISE CAS (KT): 127.0  
APCASC1: 0.0  
APCASC2: 0.0  
EFAULT DESCENT CAS: 0.0  
EFAULT ASCENT CAS: 122.0  
*****
```

Figure 8. Aircraft model data file for Predator B. File produced by Purdue.

```
*****
MQ-9                      AIRFRAME TYPE NAME
0.0          Max Spoiler Deflection
*****
3      Number of Clean drag polars.           Cd(M,C1)
15     Number of Cl data points for each Mach. Cd(M,C1)
4      Number of Flap drag polars.           Cd(F,C1)
10     Number of Cl data points for each Flap (FLAP). Cd(F,C1)
4      Number of Flap drag polars with gear. Cd(lg,F,C1)
2      Number of Cl data points for each Flap (GEAR). Cd(lg,F,C1)
2      Number of Mach data points for Gear.    Cd(lg,M)
10     Number of Mach data points for Spoiler. Cd(sb,M)

Note that the flap data was manipulated to work with the
current software. This data should be revised in the next
version.

Mach   MinClM   MaxClM       Cd(Mach,C1)
----  -----  -----
0.20   0.35     1.05        0.02227 0.02280 0.02352 0.02443 0.02552 0.02678
          |          |          0.02821 0.02980 0.03158 0.03357 0.03554 0.03752
          |          |          0.03978 0.04218 0.04474

0.30   0.35     1.05        0.02082 0.02135 0.02206 0.02297 0.02406 0.02532
          |          |          0.02675 0.02834 0.03011 0.03211 0.03408 0.03606
          |          |          0.03832 0.04072 0.04327

0.40   0.35     1.05        0.01986 0.02036 0.02107 0.02198 0.02308 0.02435
          |          |          0.02576 0.02734 0.02912 0.03112 0.03309 0.03506
          |          |          0.03732 0.03973 0.04228

Flap   MinClF   MaxClF       Cd(Flap,C1)
----  -----  -----
0       0.0      0.6000     0.0275 0.0280 0.0292 0.0315 0.0350
          |          |          0.0392 0.0455 0.0520 0.0610 0.0720

15      0.0      0.9000     0.0275 0.0280 0.0292 0.0315 0.0350
          |          |          0.0392 0.0455 0.0520 0.0610 0.0720

25      0.0      1.1000     0.0275 0.0280 0.0292 0.0315 0.0350
          |          |          0.0392 0.0455 0.0520 0.0610 0.0720

40      0.0      1.2000     0.0275 0.0280 0.0292 0.0315 0.0350
          |          |          0.0392 0.0455 0.0520 0.0610 0.0720

Flap   MinClG   MaxClG       Cd(Landing Gear,Flap,C1)
----  -----  -----
0       0.0      2.4         0.0159 0.0159
15     0.0      2.4         0.0139 0.0139
25     0.0      2.4         0.0119 0.0119
40     0.0      2.4         0.0090 0.0090

MinMaG  MaxMaG   Landing Gear Multiplier
----  -----  -----
0.00    0.90     1.00      1.00

MinSBM  MaxSBM   Speed Brake Coefficients
----  -----  -----
0.00    0.90     0.000 0.000 0.000 0.000 0.000
          |          |          0.000 0.000 0.000 0.000 0.000
```

Figure 9. Airframe drag model data file for Predator B. File produced by Purdue.

***** MACS Simulation File *****														
callsign	entryTime	entryToD	type	atcType	dest	landingR	u route	filedRout	beacon	depart	departur	climbSpe	cruiseSpe	descentSpe
PredatorB	1	3600	MQ-9	MQ-9	ATL	_NOT_SET	..BNA..ATBNA./..AT	0	BNA	_NOT_SE	115	127	115	

Figure 10. Snapshot of flight parameters file for Predator B. Speeds are indicated air speeds in knots. File produced by IAI.

The various attributes that distinguish UAS from traditional fixed-wing manned aircraft also imply difficulties in populating the aircraft_specific_model_data.dat file since some fields are either not applicable or are not available as a result of the UAS configuration.

Challenges with MACS File Format for UAS

The various attributes that distinguish UAS from traditional fixed-wing manned aircraft also imply difficulties in populating the aircraft_specific_model_data.dat file since some fields are either not applicable or are not available as a result of the UAS configuration.

Lack of Airframe Drag Model

For majority of the twelve UAS aircraft studied in this project, detailed airframe drag data was not available due to the proprietary nature of the information. Efforts were made to substitute or map drag data from similarly sized aircraft to mitigate this problem. However, this was not possible for all twelve UAS aircraft due to vast differences in size between the smaller UAS and existing aircraft in the MACS database. Consequently, these UAS aircraft were not simulated in MACS: Orbiter, Cargo UAS, Fire Scout and NEO S-300 Mk II VTOL.

No Support for Electric Engines and Rotorcraft

In the case of the Orbiter UAS, which is a battery powered fixed-wing aircraft; it was difficult to generate a MACS profile simply because the format only supports jets, turboprops or props. Furthermore, an attempt was made to match a similar engine based on output, but this was unsuccessful since the size of the Orbiter UAS (and its power plant) is much smaller than anything available in the database currently. Similarly, rotorcraft and hybrid engines are also not fully represented in MACS currently. More details regarding the MACS modeling of these aircraft are discussed in later sections.

6 Methodology

The flowchart shown in Figure 11 shows the various steps involved in generating BADA and MACS aircraft performance models (APMs) for a UAS. The process includes validation via test in ATM/ATC simulation software, specifically trajectory generators used in ACES and MACS. The first step in the analysis involves collection of required UAS data to estimate its weights and performance. Data for UAS being studied in this project are collected from their respective manufacturers. Next, an aircraft sizing algorithm (FLOPS, DATCOM-JSBSim, etc.) uses the data to estimate weights, aircraft climb, cruise, descent performance, etc. A MATLAB-based tool was developed to generate BADA and MACS files using outputs from the sizing algorithms. In the last step, the complete APM files are examined via use in ACES/MACS for purposes of validation.

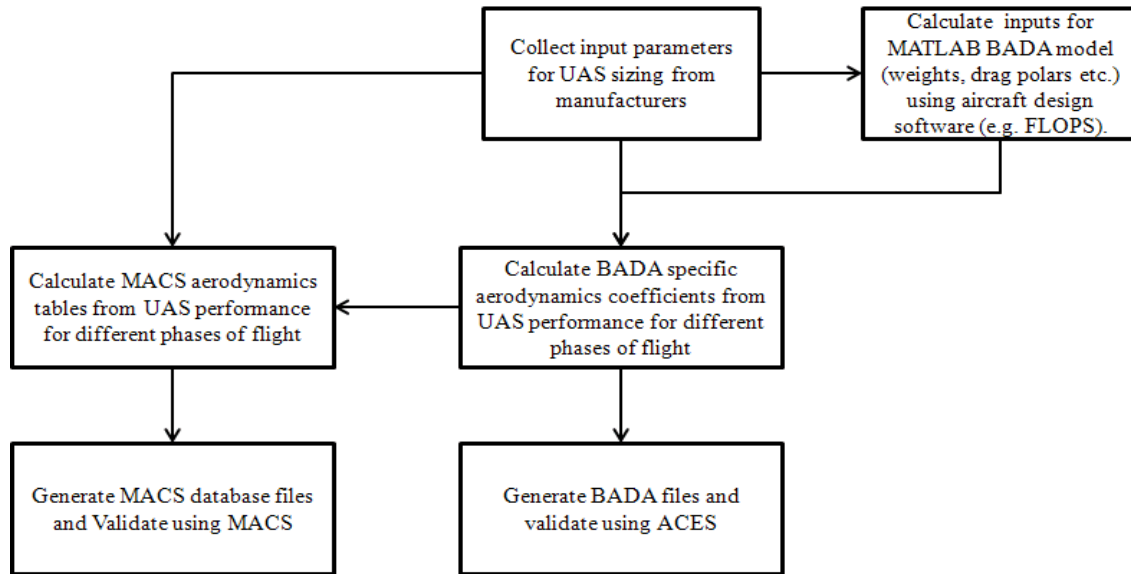


Figure 11. APM generation and validation flowchart

7 Modeling Tools

7.1 Flight Optimization System (FLOPS)

The Flight Optimization System (FLOPS) is a multidisciplinary system of programs for conceptual and preliminary design and evaluation of advanced aircraft concepts. It consists of nine primary modules out of which the first five are used in this project: 1) weights, 2) aerodynamics, 3) engine cycle analysis, 4) propulsion data scaling and interpolation, 5) mission performance, 6) takeoff and landing, 7) noise footprint, 8) cost analysis, and 9) program control.

The weights module uses statistical/empirical and analytical equations to predict the weight of each item in a group weight statement.

The aerodynamics module uses a modified version of the Empirical Drag Estimation Technique (EDET) program to provide drag polars for performance calculations. Modifications include smoothing of the drag polars, more accurate Reynolds number calculations, and the inclusion of other techniques for skin friction calculations. Alternatively, drag polars can also be input, but so far we have been using the FLOPS calculated values until we get it in the same ballpark as the manufacturer provided values.

FLOPS engine cycle analysis module provides the capability to internally generate an engine deck consisting of thrust and fuel flow data at a variety of Mach-altitude conditions. Engine cycle definition decks are provided for turbojets, turboprops, mixed flow turbofans, separate flow turbofans, and turbine bypass engines. Piston engine and propeller performance data can also be generated. Since very detailed engine decks were not available from manufacturers due to security reasons, FLOPS' internal decks were used, while information such as baseline engine thrust, fuel flow, etc. were obtained from the manufacturer.

The propulsion data scaling and interpolation module uses an engine deck that has been input or one that has been generated by the engine cycle analysis module, fills in any missing data, and uses linear or nonlinear scaling laws to scale the engine data to the desired thrust. It

then provides any propulsion data requested by the mission performance module or the takeoff and landing module.

The mission performance module uses the calculated weights, aerodynamics, and propulsion system data to calculate performance. Based on energy considerations, optimum climb profiles may be flown to start of cruise conditions. The cruise segments may be flown at the optimum altitude and/or Mach number for maximum range or endurance or to minimize NOx emissions, at the long range cruise Mach number, or at a constant lift coefficient. Descent may be flown at the optimum lift-drag ratio. FLOPS engine thrust output is validated by comparing the results to the manufacturer-provided thrust data. If the values differ by more than , the FLOPS engine cycle module is re-run by altering coefficients within the module (such as overall pressure ratio, bypass ratio for turbofans, and turbine entry temperature) until the difference is less than .

In this project, the program is used in such a way that an optimal weight of the aircraft is estimated for a given range or endurance, thrust (engine parameters), geometric features etc. FLOPS results are then compared to manufacturer provided data. Cruise, climb and descent phases of flight where scheduled according to the following procedures after consulting with the manufacturers, a) Cruise: fixed Mach number at input maximum altitude or cruise ceiling, b) Climb: minimum fuel-to-distance profile, and c) Descent: descent at optimum lift-drag ratio.

FLOPS can handle only fixed-wing aircraft of the following engine types: Jet, Turboprop and Piston. FLOPS is primarily designed for modeling manned aircraft and hence, it has limitations in modeling very light aircraft such as the Aerosonde and Shadow B. In this project, the following seven aircraft are modeled using FLOPS: Shadow B, Global Hawk, Predator A, Predator B, Gray Eagle, Avenger and Hunter UAS.

Constructing BADA models of UAS from Public Data/ Photos employing 3D Modeling, JSBSim, and DATCOM

In this analysis, publically available data and photographs of UAS are converted into detailed models. These models are used to measure the static performance of the UAS in order to create BADA models. This approach is appropriate for UAS when not enough data is available to characterize the aircraft performance for BADA. The following aircraft in the UAS set are modeled using the JSBSim/DATCOM integrated model: Aerosonde, Orbiter and Cargo UAS.

7.2 DATCOM Aerodynamics Model

In 1976, the McDonnell Douglas Corporation was commissioned to convert the USAF Stability and Control DATCOM to an automated program. Implementation of the Digital DATCOM was completed in 1978. Since that time, it has undergone various updates and is still widely used in industry and academia today [5].

The Digital DATCOM has several limitations. It assumes the fuselage is a body of revolution, so external fuel tanks and other large protrusions from the fuselage cannot be accounted for. There is also no method for a twin vertical tail, so this must be approximated as a single vertical tail. In addition, there is no method to compute the effect of rudder control so this must be estimated.

The underlying methods of the DATCOM are based on charts and equations used in aircraft design. This technique of aerodynamics modeling is faster than a computational fluid dynamics

based approach, but is also less accurate. Previously, our lab has conducted wind tunnel testing of a small UAS in order to validate the Digital DATCOM for application to this domain.

The Digital DATCOM reads a data file describing the aircraft geometry. It then produces tables for the predicted aerodynamics. The lift, drag, and side force coefficients are available in the user manual. The DATCOM output is in the stability frame (rotated from the aircraft body frame by the angle of attack).

7.2.1 Propulsion Models

UAS propulsion systems are modeled using existing methods within the JSBSim library [6]. JSBSim provides models for piston, turbine, and turboprop engines and electric motors. The turbine engine produces its own thrust; however, the turboprop and electric motor must use a propeller to convert the engine power to thrust.

7.2.2 Methodology

The main inputs required for analyzing each aircraft are the mass properties, propulsion characteristics, flight control, and aerodynamic properties. Several programs are used to provide inputs for JSBSim simulation. The aircraft visual model is generated by Blender [7], the aerodynamic properties are generated from DATCOM, and the engine and propeller files are generated from the Aeromatic website [8]. Some other input data includes moments of inertia, which were calculated given the aircraft's configuration data and aerodynamic type, and stability-related characteristics, such as center of gravity and aerodynamic center, which were estimated from the blender model. The interactions between the different elements of this process are shown in Figure 12.

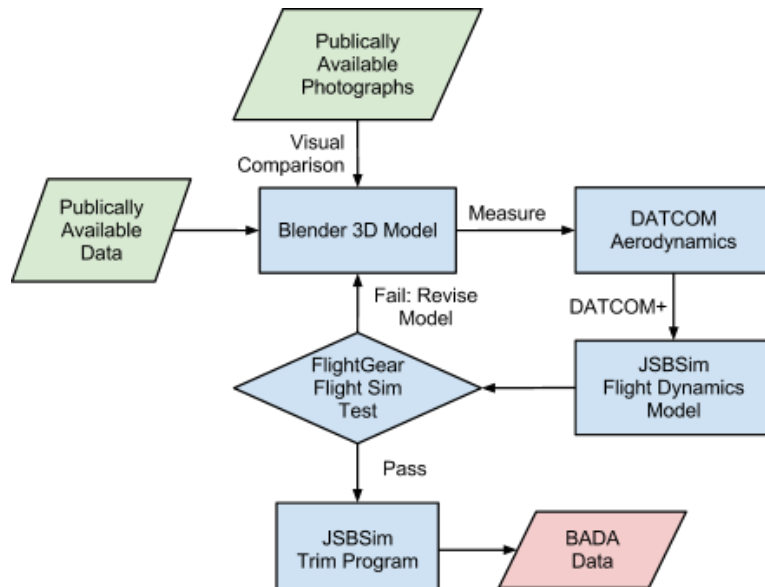


Figure 12. Flowchart representing the BADA generation process using the DATCOM/JSBSim/Flight Sim tool

7.2.2.1 Gathering Publicly Available Data/Photographs

Information on UAV performance specifications, dimensions, propulsion systems, aerodynamics, and mass properties can be found on the internet. Often this information is published as marketing information. Also, various photographs can be obtained on the internet. In addition to the general shape of the aircraft, these photographs provide information on the position of the control surfaces, landing gear, etc. that is typically not published.

7.2.2.2 Constructing 3D Models in Blender

Due to the sensitive nature of UAS dimension information; all of the dimensions of the aircraft required for input into the DATCOM aerodynamics program are not publicly available. To obtain reasonable estimates of this information, 3D models were constructed in the Blender 3D modeling program.

If orthographic drawings are available, these drawings are employed to construct the 3D model as shown in Figure 13. The shape of the aircraft is modified until it agrees with all of the orthographic projection views provided.

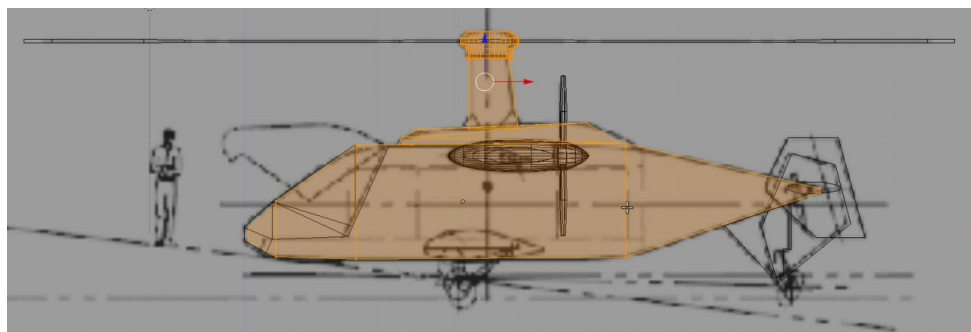


Figure 13. Orthographic projection/picture based modeling

When an orthographic projection drawing is not available, pictures can be utilized. The disadvantage to this method is that it is difficult to correctly account for the perspective distortions. If enough pictures are taken of the same aircraft, it is possible for some algorithms to recover the orthographic projection of the image; however, this approach was not utilized in this analysis. An example of employing a picture to aid in 3D modeling is shown in Figure 14.

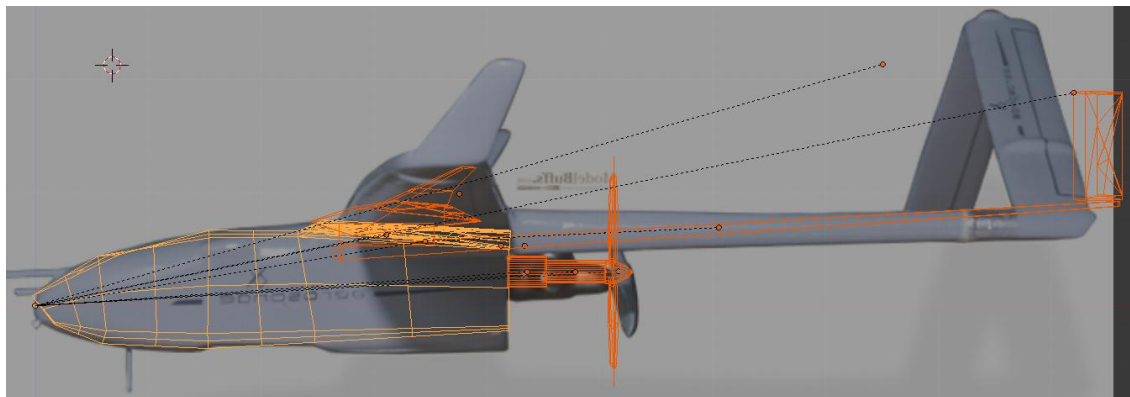


Figure 14. Difficulties of non-orthographic projection picture based modeling

7.2.2.3 Measuring 3D Model to Create DATCOM Input File

Once a 3D model has been created in blender it can be easily used to measure quantities required for the DATCOM aerodynamics input file. For instance, the wing section of the Cargo UAS is being measured (Figure 15).

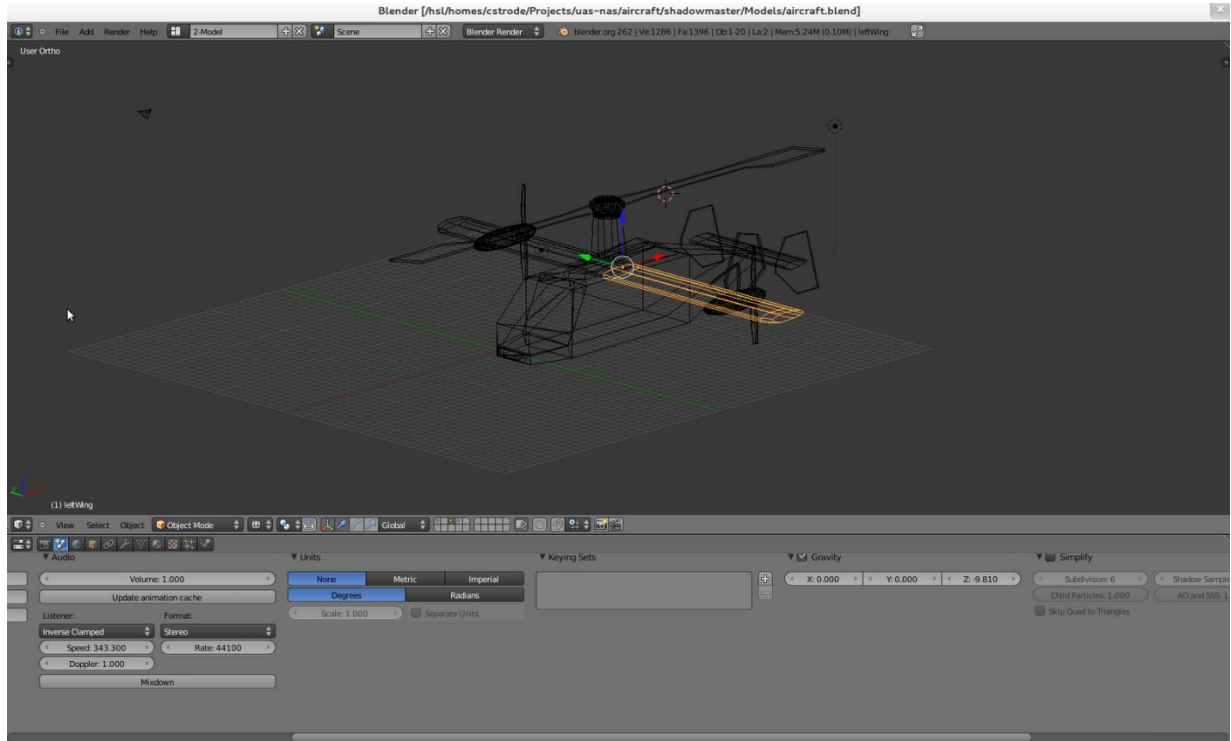


Figure 15. Blender 3D Modeling of Cargo UAS

7.2.2.4 Test Aircraft in Manual Flight Simulation

The FlightGear flight simulator is used to test the accuracy of each aircraft system [9]. FlightGear takes the main JSBSim file for each aircraft as input (Figure 16). The JSBSim file includes file paths for the visual model of each aircraft from the AC extension file from Blender, the aerodynamic flight characteristics from DATCOM, engine and propeller information, flight control details, and ground reaction details. Each path contributes to the entire function of the model in the flight simulator and is then tested for each of the following:

- The aircraft is observed on the runway to test accuracy of ground reactions.
- The simulation is initialized with the aircraft in free fall to test the aircraft glide characteristics. If necessary, stability augmentation systems are added at this stage to make manual flight easier.
- When applicable, the aircraft are tested for smooth and controlled takeoff.
- Control surfaces are checked for proper function.

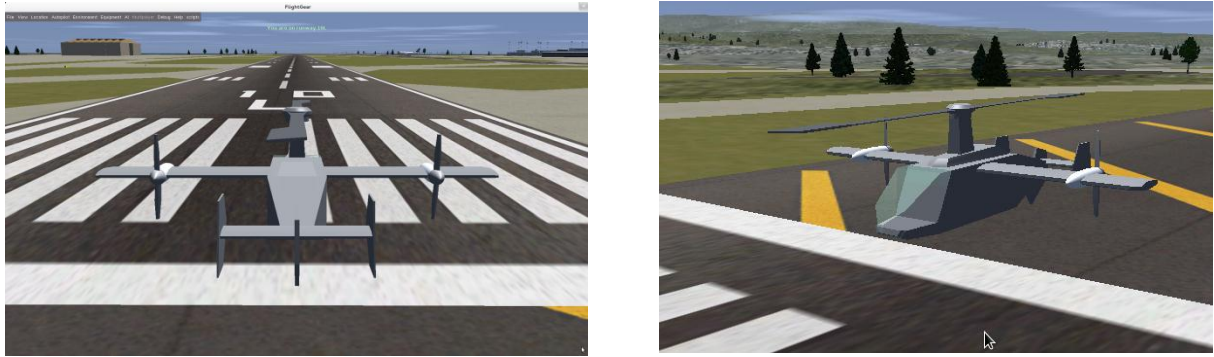


Figure 16. FlightGear Simulation Testing of Cargo UAS

7.2.2.5 JSBSim Trimming and Performance Table Generation

Once the flight testing is completed, the model is trimmed at various conditions using the JSBSim trim program to generate the performance table. For each flight altitude, aircraft's weights are varied by three different fuel levels, low level, nominal level, and hi level. In the original BADA performance table, the corresponding aircraft's true airspeed for each flight level is based on the aircraft's flight procedure. However, such information is not available for most of the UAVs. True airspeed is instead chosen within the operational speed range provided by the manufacturers. Inputs of flight level and true airspeed are then fed into JSBSim as well as aircraft's weight. For cruise flight, flight path angle is set to zero and then JSBSim provides the fuel flow rate. However for climb and descent flights, simulation is conducted with increments of the flight path angle. The maximum flight path angle that ensures the aircraft's trim is then used in the following equation to calculate the rate of climb.

7.3 Modeling of Electric UAS Aircraft: Orbiter

The fundamental idea here is that fuel, fuel consumption, and fuel capacity of any sort can be decomposed into raw energy units (kW-h, BTU, etc.) as a middle ground. Using dimensional analysis, the energy content of an electrical battery is converted into kW-h and that capacity is then normalized by the energy content of a specified fossil fuel. The end result is a volume of fossil fuel (in liters) that contains the same amount of energy as the original electrical battery as shown in Eq. (1), where, B_v is the published battery voltage (in volts), C_v is the published battery capacity (in A-h), and E_q is the energy content of the fossil fuel (in KW-h/L).

$$C_{eq} = \frac{B_v C_v}{E_q 1000} \quad (1)$$

However, this solution is not complete without a way to represent the rate of energy consumption. As with the energy capacity problem, the electric engine power consumption is converted to raw energy units (J/s, BTU/s, etc.), which is often specified by the manufacturer. This energy consumption rate is normalized by the specific energy content of a fossil fuel (J/kg) such that the flow rate is in terms of weight. The result of the conversion is a weight-based fuel flow value (in kg/min) that represents the same amount of energy flow as the electrical systems onboard the aircraft. This is shown in Eq. (2), where P_v is rated electric engine power (in KW), E_q is again the energy content of the fossil fuel (in (KW-h)/L), and ρ is the density of the fossil fuel.

$$f = \frac{60000 P_v \rho}{E_q 3.6 \times 10^6} = \frac{P_v \rho}{60 E_q} \quad (2)$$

This dimensional analysis method, while convenient and simple, is not without its drawbacks. Weight is an important measure in aircraft mission performance analysis and this method does not account for the reality that a battery does not change in weight when it is being charged or drained. As a result, simulations that implement this solution can result in the aircraft losing more weight than possible due to “fuel” consumption.

7.4 Rotorcraft Modeling and Analysis: RPAT

Rotorcraft performance was estimated using Rotorcraft Performance Analysis Tool, RPAT, developed at Cornell. This Microsoft Excel based performance analysis tool is capable of calculating hover performance, maximum gross weight, parasite and profile drag, and forward flight power consumption for given rotorcraft input parameters. At Purdue, the RPAT basic program went through serious modification to output the entire .PTF table for rotorcrafts, which includes the flight speed, fuel flow rates for different phases of flight, climb and descent rates for three different weight settings. The modified RPAT consists of several modules viz. Aircraft Specifications, Hover Performance, Parasite Drag Estimate, Profile Drag Estimate, Forward Flight Power Analysis, Forward Flight Summary and the BADA format .PTF table. As mentioned before, BADA equations are not suitable for rotorcrafts. The calculation follows preliminary design process and performance analysis based on rotorcraft energy equations [10]. Results from the modified version of the RPAT were compared to the existing full scale helicopter performance data for verification. The flight profile assumes that the rotorcrafts climb at the best rate of climb and cruise at the best range speed. The descent profile is adjusted to match the performance characteristics given by the manufacturer.

In the Aircraft Specifications module, the basic sizes of components and performance parameters are estimated using statistical/empirical equations based on 7 initial inputs: aircraft gross weight, range, maximum forward flight speed, number of blades in rotors, number of engines and specific fuel consumption [11]. The estimated values are only used when specific data are not available.

In the Hover Performance module, with complete aircraft specifications from aircraft specifications, ‘out of ground effect’ rotorcraft hover performance is calculated. In the modified RPAT, rotorcrafts are assumed to be ‘out of ground’. The essence of hover performance calculation is to analyze distribution of required power to main rotor and tail rotor using iterations. For hover performance, power available at varying altitude is also calculated.

From Parasite Drag Estimation and Profile Drag Estimation, power required correspond the drag components for varying altitude and varying forward flight speed are estimated.

Parasite drag is estimated using Eq. 3, where D_p is the parasite drag, f is equivalent flat plate area, V is forward velocity and q is dynamic pressure. The flat plate area of the aircraft can be obtained by drag build up; however, since data was available, given flat plate area were used in both aircraft calculations.

$$D_p = f * q = f \frac{\rho}{2} V^2 \quad (3)$$

Using parasite drag, atmospheric condition and flight velocity, parasite power can be calculated for the forward flight as given in Eq. 4, where hp_p is the parasite power in Horse Power units.

$$hp_p = \frac{D_p * V}{550} = \frac{f\rho V^3}{1100} \quad (4)$$

Profile power caused by both main rotor and tail rotor is given by Eq. 5, where hp_{pro} is the profile power in Horse Power units, $C_d C_d$ is profile drag coefficient, Ω is angular velocity of rotor blades, A_b is area of rotor blades, R is rotor radius and μ is rotor tip speed ratio.

$$h.p.pro = \frac{\rho A_b (\Omega R)^3 C_d}{550} \frac{C_d}{8} (1 + 3\mu^2) \quad (5)$$

Rotor disk angle of attack (α) is also calculated using the parasite drag as given in Eq. 6, where GW is gross weight of the aircraft.

$$\alpha = \sin^{-1} \left(\frac{GW}{D_p} \right) \quad (6)$$

Rotor disk angle of attack calculation assumes that angle of attack is positive for forward flight. The estimated rotor disk angle of attack is then used in forward flight for induced velocity calculation.

In the Forward Flight Power Analysis module, previously calculated power components are added to the induced power estimated. With the assumption that rotors are ideal, induced drag is calculated using the same equation used for a fixed wing aircraft (Eq. 7), where T is thrust, A is disk area and ρ is the density of fossil fuel or air.

$$D_{ind} = T\alpha_{ind} = \frac{Tv_1}{V} = \frac{T^2}{2\rho AV^2} \quad (7)$$

Using induced drag calculations, induced power is estimated using Eq. 8, where hp_{ind} is induced power in Horse Power units.

$$h.p.ind = \frac{D_{ind}V}{550} = \frac{T^2}{1,100\rho AV} \quad (8)$$

By combining estimated power components, power required for forward flight is calculated using Eq. 9, where hp_{access} is the access power. Access power was assumed to be zero for aircraft used in this project.

$$h.p.required = h.p.p + h.p.ind + h.p.pro + h.p.access \quad (9)$$

Power required is a function of forward flight velocity and thus can be represented in a graph known as the power curve, shown in Figure 17.

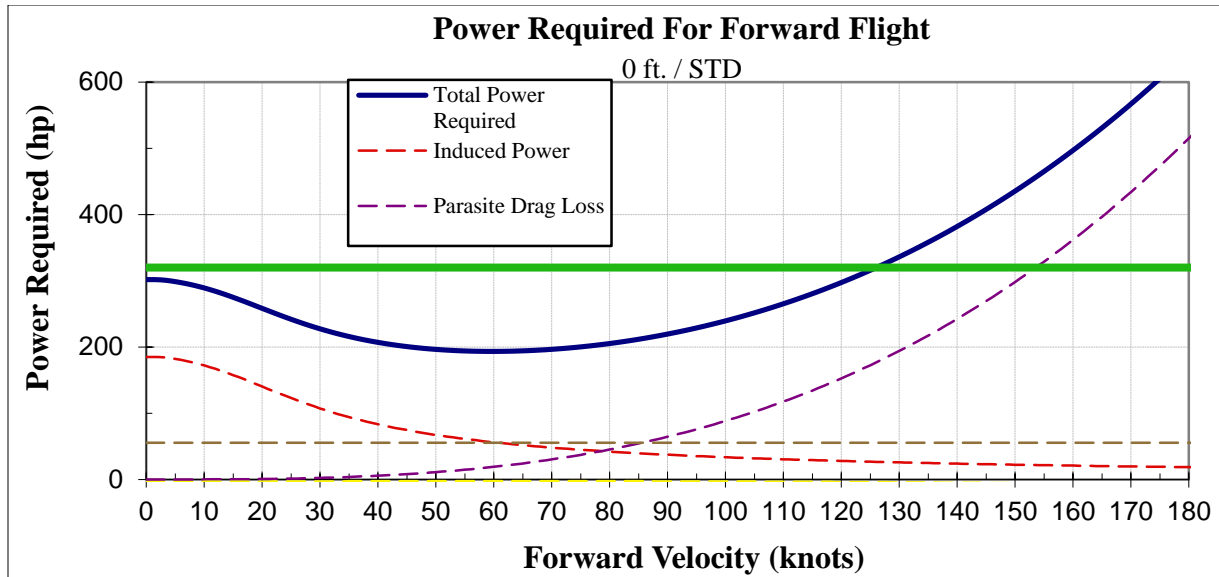


Figure 17. Sample power curve

The power required and available power data are produced for entire range of flight altitudes and for three different weight settings. Using the power required and power available data, cruise, climb and descent performance data are calculated for .PTF. When generating a .PTF table, the rotorcrafts are assumed to be flying at the most efficient flight profile: best rate of climb, maximum range speed at cruise and maximum glide range speed at descent. This results in a flight profile very similar to fixed wing aircrafts, where the rotorcraft does not perform any vertical flight, which is highly unlikely.

First, the cruise performances are calculated using best range forward velocity setting. Best range forward velocity will maximize the UAS mission range. Speed is calculated assuming there are no head or tail wind and the engine models are turbine engines. The maximum range speed for cruise is determined at the speed where a line through origin is tangent to the power curve.

For climb performance analysis, Eq. 10 is used to calculate the extra power required to climb. When the difference between the power available and power required from the power curve is maximum, the flight profile during climb corresponds to the best rate of climb.

$$\Delta h. p_{climb} = \frac{(R/C)(G.W.)}{33,000} \quad (10)$$

Unlike fixed wing aircraft, forward flight speed during best rate of climb is much different from that of cruise or descent for rotorcraft. Furthermore, the differences between the rate of climb for low, nominal and high mass configurations are large, because rotors are the source of both lift and thrust for rotorcrafts.

Descent velocity is found at speeds for maximum glide range speed. This velocity is found by determining a point on the power curve where through the origin is tangent to the required power curve, similar to cruise speed. Fuel flow rates during descent are estimated by adjusting the throttle to match the manufacturer determined rate of descent. Using partial power of level flight setting, Eq. 10 is used to calculate the negative climb. In this project, the following aircraft are modeled using RPAT: Fire Scout and NEO S-300 Mk II VTOL.

8 Results: UAS Aircraft Modeling and Development of BADA and MACS Files

This section documents the sizing of the aircraft chosen for analyses, comparison of the sizing results with data provided by aircraft manufacturers, analysis of BADA and MACS files and the deficiencies or limitations associated with BADA and MACS in representing the aircraft. A summary of the manufacturer prescribed engines and the engine decks actually used in this project is provided in Table 16. High resolution data for the actual engines were not available due to security reasons and therefore, either an alternative deck was used to mirror the actual engine or an engine type within the modeling tool is used to duplicate the original. Mismatches between engines lead to several discrepancies, which are described in detail in the following subsections. If an internal engine cycle is used, FLOPS uses linear or non-linear scaling laws to scale the engine data to the desired thrust. If the maximum thrust at cruise for a particular vehicle is provided by its manufacturer, for example, this value is input to FLOPS before the execution of the program. The desired thrust values are sometimes not achieved due to conflicts in the FLOPS optimization regimes. Since priority is given to sizing the vehicle to the exact weights and configurations, the engine thrust values are sometimes compromised. An exact match between thrust values from data and FLOPS can lead to discrepancies in weights, configurations etc., and vice versa. Mismatches between engine thrust values for a number of aircraft are listed in the subsequent sections. In some cases the transport weight equation coefficients within FLOPS were altered by trial and error until the weights, configuration and engine thrust match the manufacturer data to provide a reasonable vehicle performance output. If a desired thrust value is not provided by the manufacturer, FLOPS chooses a default starting point for sizing, based on the type of the engine in use. Similar procedures were followed in the other sizing tools as well.

Table 16. Summary of the actual engines used and the engine decks used in the project to model BADA and MACS for UAS aircraft

Aircraft (Engine Type)	Engine Name	BADA Model	MACS Model	Comments
Shadow B (Piston)	UEL 741AR74-1102	FLOPS internal piston engine	O-320-H2AD	Engine data from manufacturers were used to change parameters in FLOPS. No changes made to the MACS model
Global Hawk (Jet)	Rolls-Royce F137-AD-100	AE3007	PW_JT8D-07	AE3007 mimicked the RR F137 parameters provided by manufacturers
Predator A (Piston)	Not given	FLOPS internal piston engine	O-320-H2AD	Lack of higher granularity engine data resulted in faulty climb rates and fuel flow rates
Predator B (Turboprop)	Honeywell TPE331-10YGD	Flops internal turboprop	PW118	Better thrust model provided by manufacturers used to alter the FLOPS model. Awaiting validation
Gray Eagle (Piston)	Thielert Centurion 2.0L HFE	Flops internal piston engine	PW_PT6A-34	Indicative measures given by manufacturers used to alter FLOPS piston deck. Awaiting validation
Avenger (Jet)	Pratt & Whitney 545B	AE3007	PW_JT8D-07	Lack of higher granularity engine data resulted in faulty climb rates and fuel flow rates. AE3007 is not suitable
Hunter UAS (Piston)	APL HFE	Flops internal piston engine	O-320-H2AD	Indicative measures given by manufacturers used to alter

				FLOPS piston deck
Aerosonde (Piston)	75 HFDI	DATCOM-JSBSim piston engine model	HFDI75	New MACS engine model developed using manufacturer data and the DATCOM-JSBSim model
Orbiter (Electric)	Not given	DATCOM-JSBSim electric engine model.	None	For BADA, converted current into equivalent gas consumption. MACS engine model yet to be developed as the current MACS format does not support electric engines.
Cargo UAS (Turboshaft)	GE T700-701C	DATCOM-JSBSim turboshaft model	None	MACS does not support hybrid engine models
Fire Scout (Turboshaft)	Rolls-Royce 250-C20W	RPAT	None	MACS does not support rotorcraft
NEO S-300 Mk II VTOL (Jet)	JetA1	RPAT	None	MACS does not support rotorcraft

8.1 Shadow B

Shadow B is a small-scale, fixed wing aircraft equipped with a piston engine. Data for Shadow B were provided by its manufacturer, AAI. FLOPS was used to model the Shadow B as closely as possible. FLOPS generated the drag polars, fuel flow rates and climb rates for different phases of flight based on primary input data for Shadow B. The MATLAB-based BADA tool developed at Purdue was used to translate FLOPS output to the required BADA files in the format mandated by EUROCONTROL.

The current FLOPS model predicts a maximum take-off gross weight of 593 lb., which is higher than the actual Shadow B gross weight of 467 lb., a difference of approximately 20%. Additionally, FLOPS specifies a cruise Mach number of 0.225 while the actual value is 0.197. Table 17 provides a summary of FLOPS sizing results compared to industry (AAI) data. This model, therefore, is not a perfect representation of Shadow B. However, by using FLOPS' General Aviation module and with the help of correlation factors, it is possible to model an aircraft in the same weight category as that of Shadow B. While matching the exact performance values requires further refinement, the present model appears to be a reasonable basis for this refinement. The .PTF file for Shadow B was shown in Figure 4.

Table 17. FLOPS sizing results for Shadow B

Shadow-B	Industry data from AAI Data	FLOPS
Operating Empty Weight	333 lb.	412 lb.
Payload Weight	60 lb.	60 lb.
Gross Weight	467 lb.	593 lb.
Max. Operating Mach No.	0.197	0.225
Max. Cruise Speed	136 KTAS	100 KTAS
Cruise Altitude	8000 ft.	8000 ft.
Reference Wing Area	35.41 ft. ²	39.22 ft. ²
Max. Thrust at Cruise	Unknown	287.2 lb.

Shadow B is equipped with a UEL 741AR74-1102 piston engine. Since all or most of the engine performance details were provided, the .PTF file predicted reasonable values for speed, climb/descent rates and fuel flow.

8.1.1 Summary of BADA Deficiencies and Limitations

BADA deficiencies: None

BADA limitations: None. Though the BADA climb/descent schedules were not expected to suite an aircraft as small as the Shadow B, the cruise, climb and descent speeds, fuel flow and climb rates matched manufacturer provided data with reasonable accuracy.

8.1.2 Summary of MACS Deficiencies and Limitations

MACS files were generated directly from the BADA outputs. In addition to filling out the aircraft_specific_model_data.dat file, existing drag models and engine thrust models were mapped. The MACS drag model and engine thrust model used for Shadow B are C172 and O-320-H2AD, respectively. The completed aircraft_specific_model_data.dat file for Shadow B is shown in Figure 18.

```
*****
AIRCRAFT NAME: SHADOW
MANUFACTURER: AAI CORP
ENGINE NAME: AR741
NUMBER OF ENGINES: 1
+++++
FAA (OR CTAS INTERNAL) ACID: RQ7
GROSS WING AREA (FT^2): 35.4
MAXIMUM TAKEOFF WEIGHT (LB): 467.0
OPERATING WEIGHT EMPTY (LB): 333.0
TYPICAL DESCENT WEIGHT (LB): 425.5
AIRFRAME DRAG MODEL: C172
MAX WEIGHT FLAP DEFLECT SPEEDS: { 100.0 80.0 70.0 65.0 60.0 }
MIN WEIGHT FLAP DEFLECT SPEEDS: { 80.0 75.0 65.0 60.0 55.0 }
APPROACH SPEED SLOPE: 1.0
MAX APPROACH WEIGHT SPEED: 70.0
ENGINE THRUST MODEL: O-320-H2AD
ENGINE TYPE: PROP
DESCENT DRAG SCALE FACTOR: 1.0
EFFECTIVE NUMBER OF ENGINES: 0.26
+++++
MAXIMUM MACH NUMBER: 0.22
MAXIMUM CRUISE MACH NUMBER: 0.22
MINIMUM CAS (KT): 52.0
MAXIMUM CAS (KT): 100.0
MINIMUM CRUISE CAS (KT): 54.0
MAXIMUM CRUISE CAS (KT): 100.0
CAPCASC1: 0.0
CAPCASC2: 0.0
DEFAULT DESCENT CAS: 0.0
DEFAULT ASCENT CAS: 70.0
*****
```

Figure 18. Aircraft model data MACS file for Shadow B

8.2 Global Hawk

Global Hawk is a medium scale, fixed-wing aircraft equipped with a Rolls-Royce turbofan engine. The aircraft cruises at 31000 ft., with a maximum altitude of 65000 ft., and weighs approximately 26700 lb. The BADA model of Global Hawk was developed using data provided by AAI (collected from Northrop Grumman). The FLOPS model of the Global Hawk is generated by using the built-in Transport Aircraft weight equations, engine deck, and aerodynamic data of FLOPS. The size and propulsion system (e.g. jet) of the Global Hawk aircraft make FLOPS a

reasonable choice as a sizing tool. A comparison of sizing results from FLOPS and manufacturer provided data is shown in Table 18.

For reasonable estimations of the weights and performance of this aircraft using FLOPS, modifications to the FLOPS built-in weight equations were made as would be appropriate for modeling an unmanned aircraft; weight multipliers for furnishings, passenger compartment, and other amenities were set to zero. Avionics and electrical systems weights were increased to reflect the likelihood of the additional instrumentation carried by the Global Hawk to perform its surveillance mission and to be remotely piloted. Additionally, structural weight equation multipliers were calibrated so as to result in an empty weight that closely matches the published Global Hawk empty weight.

Table 18. FLOPS sizing results for Global Hawk

Global Hawk	Industry Data from AAI	FLOPS
Operating Empty Weight	9200 lb.	9500 lb.
Payload Weight	2000 lb.	2000 lb.
Gross Weight	26700 lb.	27200 lb.
Max. Operating Mach No.	Unknown	0.65
Max. Cruise Speed	400 KTAS (estimated)	343 KTAS
Cruise Altitude	31000 ft.	31000 ft.
Reference Wing Area	551.3 ft. ²	570.3 ft ²
Max. Thrust at Cruise	7059 lb.	7600 lb.

FLOPS generated the drag polars, fuel flow rates and climb rates for different phases of flight based on primary input data for Global Hawk. These values are used in the BADA model to generate BADA specific coefficients, which are then used to generate performance characteristics found in the .PTF.

Due to their resemblance in design to traditional manned aircraft, generating BADA files for Shadow B and Global Hawk is not complicated. Again, most of the performance characteristics available in the .PTF file matches with the manufacturer provided data with reasonable accuracy.

8.2.1 Summary of BADA deficiencies and limitations

BADA deficiencies: None

BADA limitations: None

8.2.2 MACS

MACS master files were developed by mapping the BADA files. A new drag model was created for Global Hawk and was mapped as an external file. The following MACS engine thrust model was used for Global Hawk: PW_JT8D-07.

8.3 Orbiter

The Orbiter is a small UAS only capable of launch by a slingshot system. Notable features of the aircraft include an aft fuselage propeller electric engine, large swept wings with winglets, and no tail. The engine is an HB2815-2000 electric engine with a two-blade propeller. The

empty weight of the aircraft is 12 lb. and the gross weight is 16 lb. The fuselage is 42 in. in length and the wingspan is 86.6 in. A comparison of sizing results from FLOPS and manufacturer provided data is shown in Table 19. The images used in constructing 3D models of Orbiter, and the model generated therefrom, are shown in Figure 19 and Figure 20, respectively. The DATCOM-JSBSim flight modeling tool was used to model Orbiter, from which the BADA files are developed.

Table 19. DATCOM-JSBSim sizing results for Orbiter

Orbiter	Industry data from AAI	DATCOM-JSBSim
Operating Empty Weight	12.13 lb.	12.13 lb.
Payload Weight	2.9 lb.	2.9 lb.
Gross Weight	16.5 lb.	16.5 lb.
Max. Operating Mach No.	Unknown	0.11
Max. Cruise Speed	70 KTAS	45 KTAS
Cruise Altitude	8000 ft.	8000 ft.
Reference Wing Area	8.8 ft. ²	8.8 ft. ²

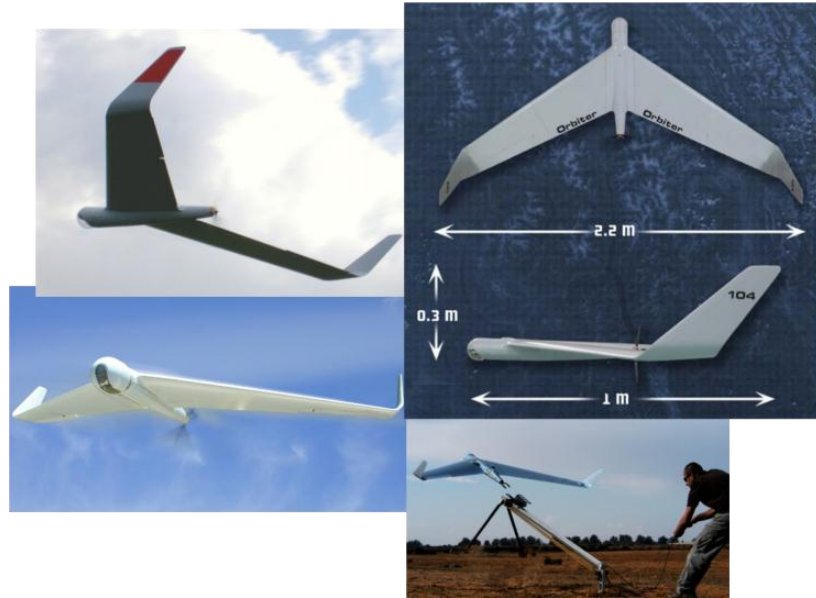


Figure 19. Orbiter images used for 3D construction

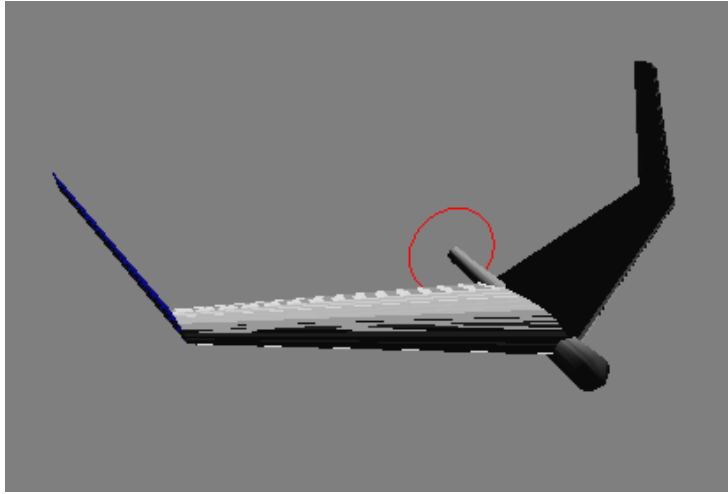


Figure 20. Orbiter DATCOM Input Visualization

Orbiter is equipped with an electric engine which posed challenges in accurately calculating fuel flow rates. JSBSim cannot produce fuel flow rate of an electric engine in terms of kilogram per minute. In fact, an electric engine uses batteries as a power source and therefore weight does not change over time. To resolve this matter, fuel flow rate was considered as the current usage rate. Since JSBSim provides throttle usage for each trim state, it was converted into current usage rate in terms of ampere per min. These current usage rates were then converted into equivalent fuel usage in order to represent the aircraft in BADA.

8.3.1 Summary of BADA deficiencies and limitations

BADA deficiencies: Engine type missing. Orbiter is an electric engine and therefore, no fuel flow rates could be provided as mandated by BADA. This calls for a provision for electric engines in the BADA format.

BADA limitations: BADA model is currently not defined for electric engines and therefore, the Orbiter BADA files were generated directly from the modeling software, ignoring BADA equations.

8.3.2 MACS

The Orbiter MACS model is not completely developed as MACS is not equipped to handle electric air aircraft. Converting the Orbiter current usage rates to fuel usage rates is not sufficient to complete a MACS engine thrust model. A MACS engine thrust model requires the engine pressure ratio, corrected fuel flow rates etc., to represent a gas engine in its entirety. This calls for a provision to add electric engine capabilities into the motion predictor class of MACS. In addition to the engine thrust file, the drag model of the aircraft is also not available to the level of detail that MACS mandates. Therefore, these fields are left empty in the MACS master file. All fields that are not related to the engine model or drag model are completed using available data from the manufacturers and BADA output files.

8.4 Aerosonde

The Aerosonde is a small UAV designed for collecting weather data. It is powered by a small piston engine. Notable features of the aircraft include an inverted V-tail at the end of a twin boom. It is also a pusher prop with the engine located behind the wing. The aircraft has an empty weight of 48.9 lb. It has a wingspan of 11 ft. A comparison of sizing results from FLOPS

and manufacturer provided data is shown in Table 20. The images used in constructing 3D models of Aerosonde, and the model generated therefrom, are shown in Figure 21 and Figure 22, respectively. The DATCOM-JSBSim flight modeling tool was used to model Aerosonde, from which the BADA files are developed.

Table 20. DATCOM-JSBSim sizing results for Aerosonde

Aerosonde	Industry data from AAI	DATCOM-JSBSim
Operating Empty Weight	48.9 lb.	48.9 lb.
Payload Weight	13.3 lb.	13.3 lb.
Gross Weight	75 lb.	75 lb.
Max. Operating Mach No.	Unknown	0.12
Max. Cruise Speed	65 KTAS	61 KTAS
Cruise Altitude	15000 ft.	15000 ft.
Reference Wing Area	9.67 ft. ²	9.67 ft. ²
Max. Thrust at Cruise	4.9 lb. (estimate)	12.4 lb.

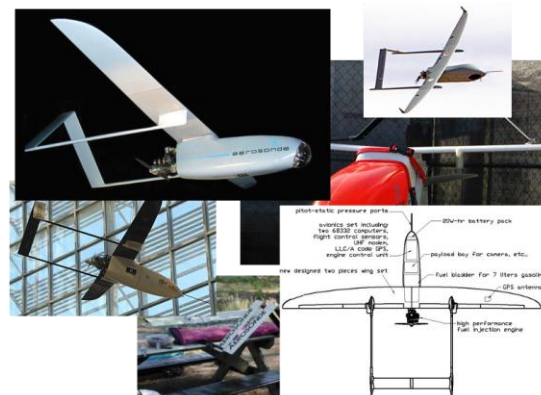


Figure 21. Aerosonde images used for 3D model construction

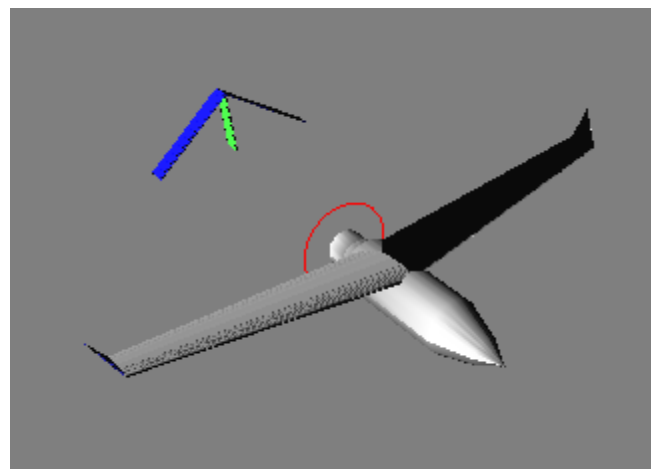


Figure 22. Aerosonde DATCOM Input Visualization

While running JSBSim, the trim condition was not achieved with the engine model provided by the manufacturer. This may be caused by the lack of propulsion or aerodynamic data. To achieve trim, more powerful engine was used in DATCOM and JSBSim. The excessive thrust input resulted in larger maximum flight path angles and eventually larger rates of climb. More

accurate propulsion and aerodynamic information will be able to improve the rate of climb accuracy.

8.4.1 Summary of BADA deficiencies and limitations

BADA deficiencies: None

BADA limitations: Ill-suited climb/descent schedules overshoot the speed limits of the aircraft in climb and descent, suggesting modifications that may have to be made in BADA to account for procedures pre-defined by the aircraft manufacturers.

8.4.2 MACS

MACS performance files were generated by mapping the BADA files. MACS drag model and engine thrust model were custom made for Aerosonde as the MACS database does not have drag models or thrust models capable of representing an aircraft as light as the Aerosonde.

8.5 Predator A

Predator A is a small-scale, fixed-wing aircraft equipped with a Rotax914 four cylinder piston engine. The aircraft cruises at an altitude of 16000 ft., with maximum altitude at 31000 ft. and weighs approximately 2250 lb. The BADA model of Predator A was developed using data provided by General Atomics (GA). FLOPS piston engine deck was generated using engine data provided by the manufacturer. A comparison of sizing results from FLOPS and manufacturer provided data is shown in Table 21.

Table 21. FLOPS sizing results for Predator A

Predator A	Industry data from GA	FLOPS
Operating Empty Weight	1665 lb.	1745 lb.
Payload Weight	450 lb.	450 lb.
Gross Weight	2250 lb.	2770 lb.
Max. Operating Mach No.	Unknown	0.24
Max. Cruise Speed	120 KTAS	111 KTAS
Cruise Altitude	16000 ft.	16000 ft.
Reference Wing Area	132 ft. ²	143 ft. ²
Max. Thrust at Cruise	140 lb.	330 lb.

FLOPS generated values for the drag polar, speed schedules, and climb rates and fuel flow were used in the MATLAB-based BADA model to generate BADA specific coefficients. These coefficients are further used to generate the .PTF file for Predator A.

The BADA .PTF file generated for Predator A was found to have several discrepancies in comparison to the manufacturer provided data. The cruise, climb and descent TAS were overpredicted by at least 20% in the .PTF, while the fuel flow rates and climb rates were overpredicted by more than 200% in certain cases. A combination of several problems can be attributed to these discrepancies, such as lack of higher granularity engine thrust data, incompatibilities of BADA climb equations with the aircraft, etc. Additionally, pre-defined procedures set by the manufacturer may alter the performance of the aircraft which may perform differently in different flight profiles. For example, Predator A always descends at a CAS of 75 kts while the FLOPS-BADA combination assumes descent at optimum lift-drag ratio. Modifications along these lines and further investigation into the problem are being conducted at Purdue in order to produce better results.

8.5.1 Summary of BADA deficiencies and limitations

BADA deficiencies: None

BADA limitations: Ill-suited climb/descent schedules overshoot the speed limits of the aircraft in climb and descent, suggesting modifications that may have to be made in BADA to account for procedures pre-defined by the aircraft manufacturers

8.5.2 MACS

MACS performance files were generated by mapping the BADA files. The following MACS drag model and engine thrust model were used respectively for Predator A: C172 and O-320-H2AD.

8.6 Predator B

Predator B is a medium-scale, fixed-wing aircraft equipped with a Honeywell TPE331-10YGD turboprop engine. The aircraft cruises at an altitude of 31000 ft., with maximum altitude also at 31000 ft. and weighs approximately 10500 lb. The BADA model of Predator B was developed using data provided by GA. FLOPS model of the Predator B is generated by using the built-in Transport Aircraft weight equations, engine deck, and aerodynamic data of FLOPS. A comparison of sizing results from FLOPS and manufacturer provided data is shown in Table 22.

Table 22. FLOPS sizing results for Predator B

Predator B	Industry data from GA	FLOPS
Operating Empty Weight	4900 lb.	4823 lb.
Payload Weight	4800 lb.	4800 lb.
Gross Weight	10500 lb.	10462 lb.
Max. Operating Mach No.	0.38	0.38
Max. Cruise Speed	160 KTAS	209 KTAS
Cruise Altitude	31000 ft.	31000 ft.
Reference Wing Area	256 ft. ²	251 ft. ²
Max. Thrust at Cruise	Unknown	1680 lb.

FLOPS generated values for the drag polar, speed schedules, climb rates and fuel flow are used in the MATLAB-based BADA model to generate BADA specific coefficients. These coefficients are further used to generate the .PTF file for Predator B.

During BADA production it was identified that the cruise, climb and descent TAS of Predator B were over-predicted by the BADA model due to the stall speed buffer condition employed in BADA. Simulation tools compatible with BADA also apply this limit, making it a hard constraint on the aircraft. Additional discrepancies, if any, are currently being investigated by the manufacturers.

8.6.1 Summary of BADA deficiencies and limitations

BADA deficiencies: None

BADA limitations: Stall speed buffer constraints in BADA overshoot the speed of Predator B in cruise, climb and descent. Manufacturer reported cruise speed at 31000 ft. is 160 kts while BADA constraint sets the speed at 209 kts. Further limitations can be identified only after complete validation of the aircraft.

8.6.2 MACS

MACS performance files were generated by mapping the BADA files. The following MACS drag model and engine thrust model were used respectively for Predator B: MQ-9 (created externally and added into the database) and PW118.

8.7 Gray Eagle

Gray Eagle is a small-scale, fixed-wing aircraft equipped with a Thielert Centurion 2.0L heavy fuel engine. The aircraft cruises at an altitude of 32000 ft., with maximum altitude also at 32000 ft. and weighs approximately 3600 lb. The BADA model of Gray Eagle was developed using data provided by GA. FLOPS piston engine deck was generated using engine data provided by the manufacturer. A comparison of sizing results from FLOPS and manufacturer provided data is shown in Table 23.

Table 23. FLOPS sizing results for Gray Eagle

Gray Eagle	Industry data from GA	FLOPS
Operating Empty Weight	2600 lb.	2791 lb.
Payload Weight	1500 lb.	820 lb.
Gross Weight	3600 lb.	3813 lb.
Max. Operating Mach No.	Unknown	0.27
Max. Cruise Speed	180 KTAS	203 KTAS
Cruise Altitude	32000 ft.	32000 ft.
Reference Wing Area	150 ft. ²	161 ft. ²
Max. Thrust at Cruise	Unknown	340 lb.

FLOPS generated values for the drag polar, speed schedules, climb rates and fuel flow are used in the MATLAB-based BADA model to generate BADA specific coefficients. These coefficients are further used to generate the .PTF file for Gray Eagle.

During BADA production it was identified that the cruise, climb and descent TAS of Gray Eagle were over-predicted by the BADA model due to the stall speed buffer condition employed in BADA. Simulation tools compatible with BADA also apply this limit, making it a hard constraint on the aircraft. Additional discrepancies, if any, are currently being investigated by the manufacturers.

8.7.1 Summary of BADA deficiencies and limitations

BADA deficiencies: None

BADA limitations: Stall speed buffer constraints in BADA overshoot the speed of Predator B in cruise, climb and descent. Manufacturer reported cruise speed at 24000 ft. is 140 kts while BADA constraint sets the speed at 177 kts. Further limitations can be identified only after complete validation of the aircraft

8.7.2 MACS

MACS performance files were generated by mapping the BADA files. The following MACS drag model and engine thrust model were used respectively for Gray Eagle: C172 and PW_PT6A-34.

8.8 Predator C (Avenger)

Avenger is a medium-scale, fixed-wing aircraft equipped with a Pratt and Whitney 545B, high bypass ratio, turbofan engine. The aircraft cruises at an altitude of 40000 ft., with maximum altitude also at 40000 ft. and weighs approximately 15800 lb. The BADA model of Avenger was developed using data provided by GA. FLOPS model of the Avenger is generated by using the built-in Transport Aircraft weight equations, engine deck, and aerodynamic data of FLOPS. A comparison of sizing results from FLOPS and manufacturer provided data is shown in Table 24.

Table 24. FLOPS sizing results for Predator C

Predator C	Industry data from GA	FLOPS
Operating Empty Weight	8650 lb.	8545 lb.
Payload Weight	6500 lb.	6000 lb.
Gross Weight	15800 lb.	14920 lb.
Max. Operating Mach No.	0.62	0.62
Max. Cruise Speed	400 KTAS	331 KTAS
Cruise Altitude	40000 ft.	40000 ft.
Reference Wing Area	267 ft. ²	243 ft. ²
Max. Thrust at Cruise	1000 lb.	1220 lb.

FLOPS generated values for the drag polar, speed schedules, climb rates and fuel flow are used in the MATLAB-based BADA model to generate BADA specific coefficients. These coefficients are further used to generate the .PTF file for Avenger.

The BADA .PTF file generated for Avenger was found to have several discrepancies in comparison to the manufacturer provided data. The cruise, climb and descent TAS were overpredicted by at least 13% in the .PTF, while the fuel flow rates and climb rates were overpredicted by more than 200% in certain cases. GA reports decreasing fuel flow rates with altitude whereas the BADA model predicts the opposite trend. A combination of several problems can be attributed to these discrepancies, such as, lack of higher granularity engine thrust data, incompatibility of BADA equations with the aircraft etc. Additionally, pre-defined procedures set by the manufacturer may alter the performance of the aircraft which may perform differently in different flight profiles. For example, Avenger always descends at a CAS of 150 kts, while the FLOPS-BADA combination assumes descent at optimum lift-drag ratio. Modifications along these lines and further investigation into the problem are being conducted at Purdue in order to produce better results.

8.8.1 Summary of BADA deficiencies and limitations

BADA deficiencies: None

BADA limitations: Ill-suited climb/descent schedules overshoot the speed limits of the aircraft in climb and descent, suggesting modifications that may have to be made in BADA to account for procedures pre-defined by the aircraft manufacturers.

8.8.2 MACS

MACS performance files were generated by mapping the BADA files. The following MACS drag model and engine thrust model were used respectively for Avenger: AVEN(created externally and added into the database) and PW_JT8D-07.

8.9 Hunter UAS

Hunter UAS is a small-scale, fixed-wing aircraft equipped with two APL heavy fuel engines. The aircraft cruises at an altitude of 18000 ft., with maximum altitude also at 18000 ft. and weighs approximately 1950 lb. The BADA model of Hunter UAS was developed using data provided by AAI. FLOPS piston engine deck was generated using engine data provided by the manufacturer. A comparison of sizing results from FLOPS and manufacturer provided data is shown in Table 25.

Table 25. FLOPS sizing results for Hunter UAS

Hunter UAS	Industry data from AAI	FLOPS
Operating Empty Weight	1450 lb.	1510 lb.
Payload Weight	630 lb.	650 lb.
Gross Weight	1950 lb.	2090 lb.
Max. Operating Mach No.	Unknown	0.2
Max. Cruise Speed	120 KTAS	119 KTAS
Cruise Altitude	18000 ft.	18000 ft.
Reference Wing Area	106 ft. ²	111 ft. ²
Max. Thrust at Cruise	Unknown	300 lb.

FLOPS generated values for the drag polar, speed schedule, climb rates and fuel flow are used in the MATLAB-based BADA model to generate BADA specific coefficients. These coefficients are further used to generate the .PTF file for Gray Eagle.

8.9.1 Summary of BADA deficiencies and limitations

BADA deficiencies: None

BADA limitations: None

8.9.2 MACS

MACS performance files were generated by mapping the BADA files. The following MACS drag model and engine thrust model were used respectively for Hunter UAS: C172 and O-320-H2AD.

8.10 Cargo UAS

The Cargo UAS aircraft is a medium sized hybrid UAS with a single piston engine at the rear of the fuselage, a rectangular wing planform, and a unique triangular bent tail design. The engine is a UEL 741AR74-1102 piston engine. The empty weight of Cargo UAS is 333 lb. and the gross weight is 467 lb. The fuselage length is 63.1 inches and the wing span is 19.8 feet. A comparison of sizing results from FLOPS and manufacturer provided data is shown in Table 26. The images used in constructing 3D models of Cargo UAS, and the model generated therefrom, are shown in Figure 23 and Figure 24, respectively. The DATCOM-JSBSim flight modeling tool was used to model Cargo UAS, from which the BADA files are developed.

Table 26. DATCOM-JSBSim sizing results for Cargo UAS

Cargo UAS	Industry data from AAI	DATCOM-JSBSim
Operating Empty Weight	12050 lb.	12050 lb.
Payload Weight	8000 lb.	8000 lb.
Gross Weight	22750 lb.	22750 lb.
Max. Operating Mach No.	Unknown	0.40
Max. Cruise Speed	250 KTAS	270 KTAS

Cruise Altitude	30000 ft.	30000 ft.
Reference Wing Area	200 ft. ²	200 ft. ²
Max. Thrust at Cruise	11350 lb.	12450 lb.

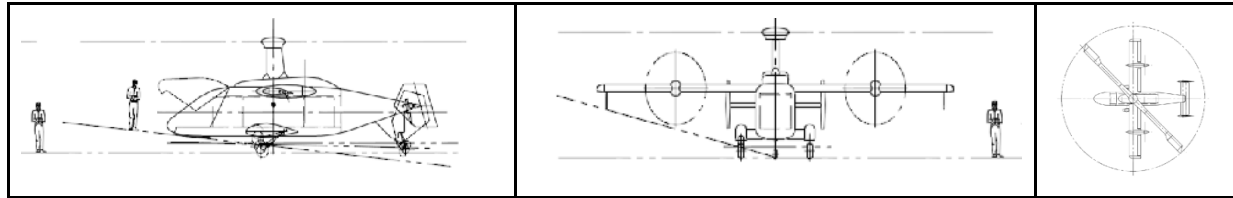


Figure 23. Schematics of Cargo UAS from AAI

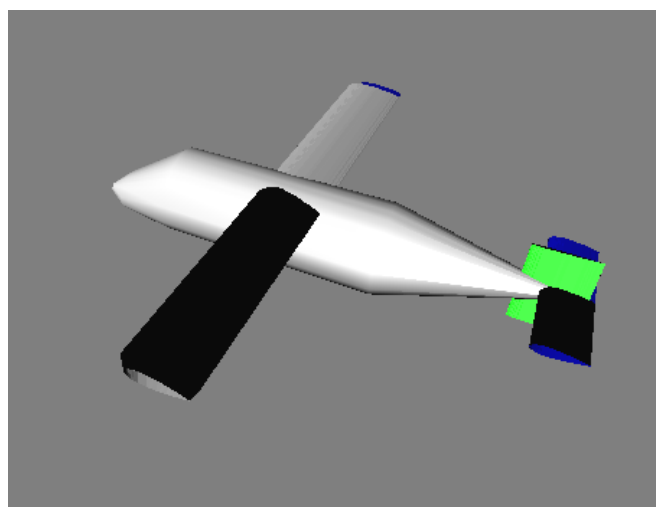


Figure 24. Cargo UAS DATCOM Input Visualization

Cargo UAS is a hybrid aircraft that uses its rotor for vertical takeoff and landing while it switches to propeller for climb, cruise, and descent segment. It was assumed that only propeller was used for .PTF generation, even for climb and descent close to sea level. Any lift or drag developed by the rotor blades and shaft were neglected in the model and simulation.

8.10.1 Summary of BADA deficiencies and limitations

BADA deficiencies: Aircraft type missing. Cargo UAS is a hybrid air aircraft and therefore, no stall speeds exist during take-off or landing. Additional modes, such as hover, may have to be introduced.

BADA limitations: BADA model is currently defined only for fixed-wing aircraft. The Cargo UAS BADA files were generated directly using the modeling software, ignoring equations provided by BADA.

8.10.2 MACS

The Cargo UAS MACS model is not completely developed as MACS is not equipped to handle hybrid air aircraft. Engine thrust file and the drag model of this hybrid air aircraft is not available to the detail that MACS mandates. Therefore, these fields are left empty in the MACS master file. All fields that are not related to the engine model or drag model are completed using available data from the manufacturers and BADA output files.

8.11 Fire Scout

Fire Scout is a small-scale rotorcraft with a Rolls-Royce 250 C20W turboshaft engine. The empty weight of Fire Scout is 1457 lb. and the gross weight is 3150 lb. The fuselage length is 23.95 feet and the main rotor diameter is 27.5 feet. A comparison of sizing results from FLOPS and manufacturer provided data is shown in Table 27.

Table 27. RPAT sizing results for Fire Scout

Fire Scout	Industry data from AAI	RPAT
Operating Empty Weight	1457 lb.	1510 lb.
Payload Weight	600 lb.	600 lb.
Gross Weight	3150 lb.	3234 lb.
Max. Operating Mach No.	Unknown	0.22
Max. Cruise Speed	125 KTAS	128 KTAS
Cruise Altitude	20000 ft.	20000 ft.
Fuselage Wet Surface Area	286 ft. ²	291 ft. ²

The .PTF of Fire Scout closely matches the maximum altitude, cruise speed, and rates of climb/descent provided by the manufacturer. Amongst the two rotorcrafts—Fire Scout and NEO S-300 Mk II VTOL (S350)—Fire Scout is perhaps analyzed better by RPAT, mainly due to the larger size of the aircraft and also due to the availability of adequate aircraft specifications from the manufacturer.

8.11.1 Summary of BADA deficiencies and limitations

BADA deficiencies: Aircraft type missing. Since rotorcrafts neither have stall speeds nor drag polars as in the same context as fixed wing aircrafts, some of the blocks in the OPF are not completed. Also, main characteristics of rotorcrafts such as vertical takeoff, land, and hover capabilities cannot be encapsulated in the BADA format.

BADA limitations: BADA model is currently not defined for rotorcrafts and therefore, the Fire Scout BADA files were generated directly from the modeling software, ignoring BADA equations.

8.11.2 MACS

The Fire Scout MACS model is not completely developed as MACS is not equipped to handle rotorcrafts. Engine thrust file is not available to the detail that MACS mandates and a drag model cannot be conceived in the same manner as that of aircraft. Therefore, these fields are left empty in the MACS master file. All fields that are not related to the engine model or drag model are completed using available data from the manufacturers and BADA output files.

8.12 NEO S-300 Mk II VTOL

NEO S-300 Mk II VTOL (S350) is a small-scale rotorcraft with a JETA1 powered single turbine engine. The empty weight of S350 is 187.4 lb. and the gross weight is 330.7 lb. The fuselage length is 10.33 feet and the main rotor diameter is 11.5 feet. A comparison of sizing results from FLOPS and manufacturer provided data is shown in Table 28.

Table 28. RPAT sizing results for NEO S-300 Mk II VTOL

NEO S-300 Mk II VTOL	Industry data from AAI	RPAT
Operating Empty Weight	187.4 lb.	222.6 lb.
Payload Weight	99.2 lb.	99.2 lb.
Gross Weight	330.7 lb.	387.8 lb.

Max. Operating Mach No.	Unknown	0.14
Max. Cruise Speed	116 KTAS	77 KTAS
Cruise Altitude	8000 ft.	8000 ft.
Fuselage Wet Surface Area	44.8 ft. ²	47.3 ft. ²

The .PTF file of S350 has several mismatches in comparison with the maximum altitude, cruise speed, and rates of climb/descent provided by the manufacturer. The RPAT estimates of fuel flow values for S350 resulted in similar values across different altitudes. This is because the size of S350 is at the lower end of the rotorcraft spectrum.

8.12.1 Summary of BADA deficiencies and limitations

BADA deficiencies: Vehicle type missing. Since rotorcrafts neither have stall speeds nor drag polars as in the same context as fixed wing aircrafts, some of the blocks in the OPF are not completed. Also, main characteristics of rotorcrafts such as vertical takeoff, land, and hover capabilities cannot be encapsulated in the BADA format.

BADA limitations: BADA model is currently not defined for rotorcrafts and therefore, the BADA files for S350 were generated directly from the modeling software, ignoring BADA equations.

8.12.2 MACS

The S350 MACS model is not completely developed as MACS is not equipped to handle rotorcrafts. Engine thrust file is not available to the detail that MACS mandates and a drag model cannot be conceived in the same manner as that of aircraft. Therefore, these fields are left empty in the MACS master file. All fields that are not related to the engine model or drag model are completed using available data from the manufacturers and BADA output files.

9 BADA File Validation

As mentioned earlier, UAS aircraft were simulated using KTG with the BADA files providing the necessary input. The purpose of these simulations was twofold:

- Understand the flight characteristics of the UAS aircraft and identify any anomalies
- Submit simulation results to the manufacturers of the UAS and thereby validate the BADA files

9.1 Simulation of Shadow B (RQ7B) using KTG

9.1.1 Issues and Resolution

Important features of Shadow B's flight simulation using KTG are shown in Table 29.

Table 29. Features of Shadow B flight simulation using KTG

Origin	KIAD
Destination	KJFK
Cruise speed	93 KTAS
Cruise altitude	8000 ft.
Total flight time	138 min.
Total flight distance	201 nmi.

Anomalies were observed in the simulation results. For example, the graphs in Figure 25 depict variations in the true airspeed (TAS) of Shadow B with altitude, divided into two phases of

the flight: from takeoff at KIAD to cruise altitude, and from cruise altitude to landing at KJFK. TAS increased from 56 kts to about 67 kts during takeoff within a very short altitude, and later to about 71 kts during the climb (identified by the long red-oval). Also, TAS decreased from about 79 kts to 76 kts for a very small change in altitude during descent (identified by the short red-oval).

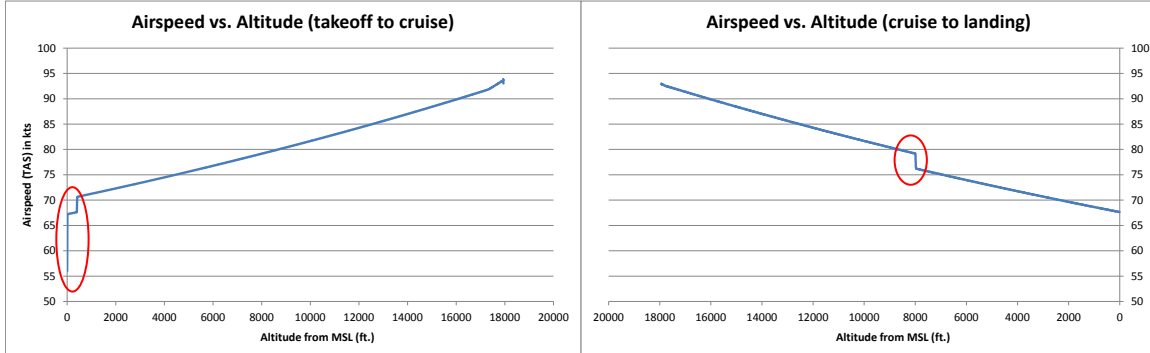


Figure 25. True airspeed (TAS) vs. altitude for RQ7B for flight from KIAD to KJFK

9.1.2 Reason for Anomalies

The anomalies in Figure 25 were found to be caused by errors in compiling BADA files by the Purdue team. BADA user manual dictates that the flight speed at a given altitude described in the .PTF file should be higher than the stall speeds indicated in the .OPF file by a factor of 1.2 for takeoff and 1.3 for all other segments of the flight—these factors were probably established by airlines to augment safety at flight speeds approaching the stall limits. The different types of stall speeds specified in the .OPF file and the altitudes when they are taken into consideration by KTG are shown in Table 30. The BADA files used in compiling the results in Figure 25 did not correctly take this into consideration and the resulting speed–altitude data in the .PTF file were in conflict with the factors of safety described earlier. The Purdue team was notified of this violation and the BADA files were corrected. The BADA files in Figure 1, Figure 2, Figure 3 and

Figure 4 are the corrected versions. However, these criteria affected the way some of the UAS aircraft were modeled, which will be mentioned in later sections of this report.

Table 30. Stall speeds and corresponding altitude constraints employed by KTG. Stall speeds are Calibrated Airspeeds (CAS) in knots

Flight phase	Altitude constraint	Stall speed in .OPF file	Buffer factor
Climb	< 400 ft.	TO	1.2
	400 ft. to 2000 ft.	IC	1.3
	> 2000 ft.	CR	1.3
Top of climb	Not applicable	CR	1.3
Cruise	Not applicable	CR	1.3
Descent	≥ 8000 ft.	CR	1.3
	3000 ft. to 8000 ft.	AP	1.3
	< 3000 ft.	LD	1.3
Landing	Not applicable	LD	1.3

9.1.3 Simulation results using corrected BADA files

Shadow B was simulated using the corrected BADA files (Figure 26, Figure 27, Figure 28 and Figure 29), with the main features of the flight shown in Table 31. The cruise TAS increased to 99 kts (as compared to that in Table 29), which the Purdue team explained as being a result of the factors of safety imposing a higher effective stall speed and causing the aircraft to fly

faster. Airspeed vs. altitude graphs compiled from simulation results with corrected BADA files are shown in Figure 30. Plan-view of the flight path is shown in Figure 31. Graphs describing other aspects of the flight are shown in Figure 32. It should be noted that Shadow B's cruise altitude and ceiling were assumed to be equal (18000 ft. MSL) in developing the BADA files. However, commercial aircraft usually cruise at a lower altitude than their ceiling.

Figure 26. Corrected .APF file for Shadow B (RQ7B). File was compiled by Purdue.

```

Descent calculation using BADA model
AIRCRAFT:
  AIRCRAFT_CODE: RQ7B (no ICAO code)
  ENGINE:        UAV AR-741

CALCULATION CONDITIONS:
  CALCULATION TYPE: POINT
    STALL
  CAS below FL100:
  CAS above FL100:
  Mach
  Atmosphere Model: OLD ISA Model

RESULTS:

```

FL [ft]	Mass [kg]	CAS [kt]	Mach	TAS [kt]	ROCD [ft/min]	Gradient [deg]	FuelFlow [kg/s]	Temperature [K]	SpeedOfSound [m/s]	Density [kg/m³]	Thrust [N]	Max_Thrust [N]	Drag [N]	AvlPower [kW]	ESF
18000	151.0	00.00	.00	99.0	490	0.0	0.0033	000.0	000.00	0.0000	0.0	0.0	0.0	0.0	0.0
16000	151.0	00.00	.00	96.0	490	0.0	0.0033	000.0	000.00	0.0000	0.0	0.0	0.0	0.0	0.0
14000	151.0	00.00	.00	92.0	470	0.0	0.0033	000.0	000.00	0.0000	0.0	0.0	0.0	0.0	0.0
12000	151.0	00.00	.00	91.0	460	0.0	0.0033	000.0	000.00	0.0000	0.0	0.0	0.0	0.0	0.0
10000	151.0	00.00	.00	88.0	440	0.0	0.0033	000.0	000.00	0.0000	0.0	0.0	0.0	0.0	0.0
8000	151.0	00.00	.00	87.0	430	0.0	0.0033	000.0	000.00	0.0000	0.0	0.0	0.0	0.0	0.0
6000	151.0	00.00	.00	85.0	420	0.0	0.0033	000.0	000.00	0.0000	0.0	0.0	0.0	0.0	0.0
4000	151.0	00.00	.00	82.0	410	0.0	0.0033	000.0	000.00	0.0000	0.0	0.0	0.0	0.0	0.0
3000	151.0	00.00	.00	80.0	400	0.0	0.0033	000.0	000.00	0.0000	0.0	0.0	0.0	0.0	0.0
2000	151.0	00.00	.00	78.0	320	0.0	0.0033	000.0	000.00	0.0000	0.0	0.0	0.0	0.0	0.0
1500	151.0	00.00	.00	75.0	290	0.0	0.0033	000.0	000.00	0.0000	0.0	0.0	0.0	0.0	0.0
1000	151.0	00.00	.00	72.0	270	0.0	0.0033	000.0	000.00	0.0000	0.0	0.0	0.0	0.0	0.0
500	151.0	00.00	.00	71.0	230	0.0	0.0033	000.0	000.00	0.0000	0.0	0.0	0.0	0.0	0.0
0	151.0	00.00	.00	69.0	200	0.0	0.0033	000.0	000.00	0.0000	0.0	0.0	0.0	0.0	0.0

Figure 27. Corrected .DCT file for Shadow B (RQ7B). File was compiled by IAI.

```

CCCCCCCCCCCCCCCCCCCCCCCCCCCCCCCCCCCC RQ4A__.OPF CCCCCCCCCCCCCC
CC
CC          AIRCRAFT PERFORMANCE OPERATIONAL FILE
CC
CC
CC      File_name: RQ7B__.OPF
CC
CC      Creation_date: Mar 01 2012
CC
CC      Modification_date: Mar 01 2012
CC
CC
CC===== Actype =====
CD  RQ7B__      1 engines    Piston           L
CC  AAI          RQ7B with 1 AR741   engines     wake
CC
CC===== Mass (t) =====
CC  reference      minimum      maximum      max payload  mass grad
CD  .00193E+02   .00151E+02   .00212E+02   .00027E+02   .00000E+00
CC===== Flight envelope =====
CC  VMO(KCAS)    MMO        Max.Alt       Hmax      temp grad
CD  .13600E+03   .22500E+00   .18000E+05   .00000E+00   .00000E+00
CC===== Aerodynamics =====
CC Wing Area and Buffet coefficients (SIM)
CCndrst Surf(m2)  Clbo(M=0)   k      CM16
CD 5   .03285E+02   .10400E+01   .00000E+00   .00000E+00
CC Configuration characteristics
CC n Phase Name  Vstall(KCAS)  CD0      CD2      unused
CD 1 CR  Clean    .54000E+02   .49700E+01   .31879E-02   .00000E+00
CD 2 IC  Clean    .54000E+02   .00000E+00   .00000E+00   .00000E+00
CD 3 TO  Clean    .56000E+02   .00000E+00   .00000E+00   .00000E+00
CD 4 AP  Clean    .52000E+02   .00000E+00   .00000E+00   .00000E+00
CD 5 LD  Clean    .52000E+02   .00000E+00   .00000E+00   .00000E+00
CC Spoiler
CD 1   RET
CD 2   EXT      .00000E+00   .00000E+00
CC Gear
CD 1   UP
CD 2   DOWN     .00000E+00   .00000E+00   .00000E+00
CC Brakes
CD 1   OFF
CD 2   ON       .00000E+00   .00000E+00
CC===== Engine Thrust =====
CC  Max climb thrust coefficients (SIM)
CD  .62012E+05   .50000E+05   .62006E+05   .00000E+00   .00000E+00
CC  Desc(low)    Desc(high)   Desc level  Desc(app)  Desc(lid)
CD  .10000E+00   .10000E+00   .15000E+05   .00000E+00   .00000E+00
CC  Desc CAS     Desc Mach   unused      unused      unused
CD  .70000E+02   .22500E+00   .00000E+00   .00000E+00   .00000E+00
CC===== Fuel Consumption =====
CC  Thrust Specific Fuel Consumption Coefficients
CD  .67000E+00   .00000E+00
CC  Descent Fuel Flow Coefficients
CD  .50000E+01   .00000E+00
CC  Cruise Corr.  unused      unused      unused      unused
CD  .10000E+01   .00000E+00   .00000E+00   .00000E+00   .00000E+00
CC===== Ground =====
CC      TOL      LDL      span      length      unused
CD  .25600E+03   .93600E+03   .60350E+01   .34000E+01   .00000E+00
CC

```

Figure 28. Corrected .OPF file for Shadow B (RQ7B). File was compiled by Purdue.

BADA PERFORMANCE FILE										Mar 01 2012					
AC/Type: RQ7B_								SOURCE OPF FILE:	Mar 01 2012						
								SOURCE APF FILE:	Mar 01 2012						
Speeds: CAS(LO/HI) Mach Mass Levels [kg]								Temperature: ISA							
climb -	62/ 70	0.22	low	- 151											
cruise -	70/ 80	0.22	nominal	- 193								Max Alt. [ft]: 18000			
descent -	62/ 70	0.22	high	- 212											
FL	CRUISE				CLIMB				DESCENT						
	TAS	fuel		TAS	ROCD	fuel		TAS	ROCD	fuel					
	[kts]	[kg/min]		[kts]	[fpm]	[kg/min]		[kts]	[fpm]	[kg/min]					
		lo	nom	hi		lo	nom	hi	nom		nom	nom			
0						69	1450	1750	1435	0.1	69	200	0.2		
5						70	1515	1899	1535	0.1	71	230	0.2		
10						72	1743	2371	1713	0.1	72	270	0.2		
15						74	1786	2420	1755	0.1	75	290	0.2		
20						77	1760	2389	1730	0.1	78	320	0.2		
30	72	0.1	0.1	0.1		79	1860	2015	1860	0.1	80	400	0.2		
40	74	0.1	0.1	0.1		81	2185	2837	2154	0.1	82	410	0.2		
60	77	0.1	0.1	0.1		83	894	1263	877	0.1	85	420	0.2		
80	80	0.1	0.1	0.1		87	825	1179	809	0.1	87	430	0.2		
100	84	0.1	0.1	0.1		89	937	1304	921	0.1	88	440	0.2		
120	89	0.1	0.1	0.1		91	854	1200	839	0.1	91	460	0.2		
140	93	0.1	0.1	0.1		94	764	1089	750	0.1	92	470	0.2		
160	97	0.1	0.1	0.1		97	669	970	656	0.1	96	490	0.2		
180	99	0.1	0.1	0.1		99	575	853	563	0.1	99	490	0.2		

Figure 29. Corrected .PTF file for Shadow B (RQ7B). File was compiled by Purdue.

Table 31. Features of Shadow B flight using corrected BADA files

Origin	KIAD
Destination	KJFK
Flight time	179.7 min.
Flight distance	239.5 nmi.
Cruise speed	80 KTAS
Cruise altitude	8000 ft.
Takeoff mass	212 kg
Landing mass	191.8 kg
Duration of climb	5.9 min.
Duration of cruise	151.4 min.
Duration of descent	18 min.
Duration of landing	4.3 min.

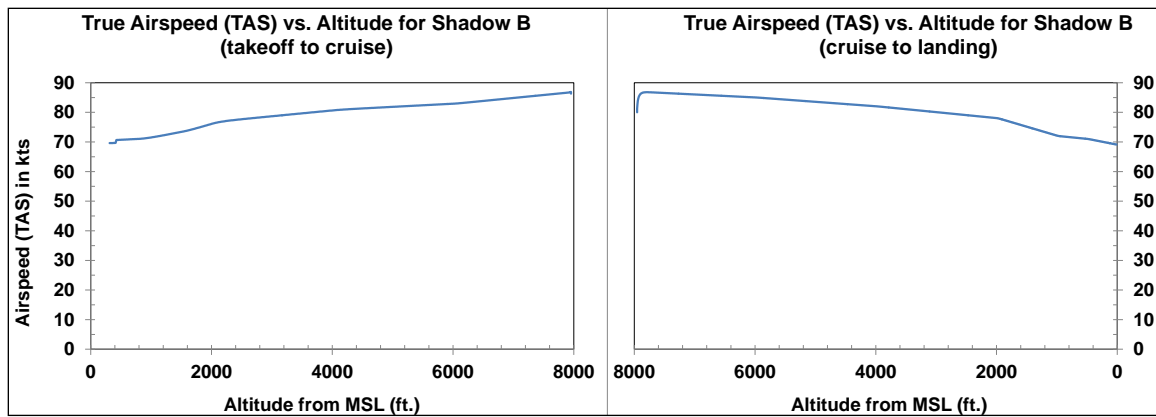


Figure 30. True airspeed (TAS) vs. altitude for Shadow B flight from KIAD to KJFK using corrected BADA files



Figure 31. Plan-view of Shadow B flight path from KIAD to KJFK using corrected BADA files

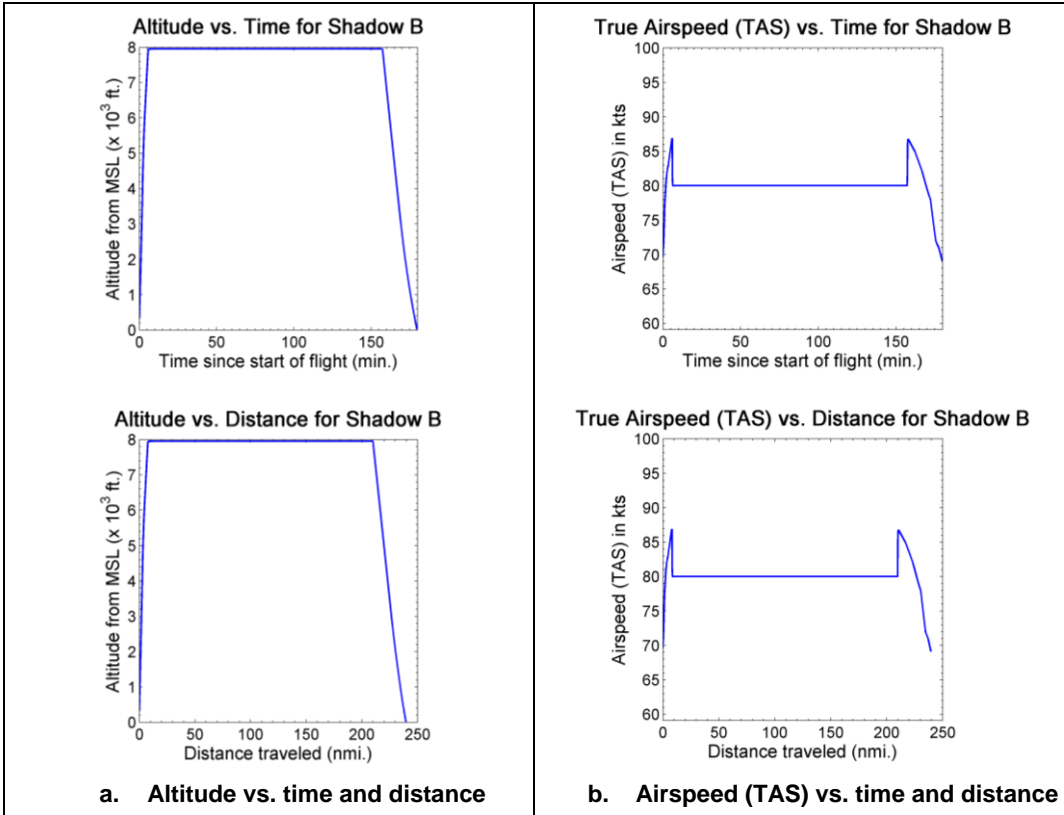


Figure 32. Details of Shadow B flight from KIAD to KJFK using corrected BADA files

9.2 Simulation of Global Hawk (RQ4A) using KTG

Important simulation features of Global Hawk's flight are shown in Table 32. The variation of TAS with altitude is shown in Figure 33. The sharp increase in TAS during climb (red oval in Figure 33) was due to the fact that the airspeed at the corresponding altitude was in conflict with the factor of safety described earlier. For example, the .PTF file for Global Hawk indicates TAS as 124 kts at 2000 ft. (Figure 34), which was less than 1.3 times the cruise stall speed of 107.82 kts from the .OPF file (Table 30 and Figure 35). Since KTG attempts to follow the speed profiles described in the BADA files, TAS increased rapidly in a very short period of time and during a small change in altitude at the beginning of the climb phase. Plan-view of the flight path is shown in Figure 36 and plots describing other aspects of the flight are shown in Figure 37.

Table 32. Results of Global Hawk flight simulation using KTG

Origin	KMSP
Destination	KMCO
Flight time	217.9 min.
Flight distance	1167.7 nmi.
Cruise speed	343 KTAS
Cruise altitude	31000 ft.
Takeoff mass	14203 kg
Landing mass	10774.93 kg
Duration of climb	13.9 min.
Duration of cruise	179.8 min.
Duration of descent	23.7 min.
Duration of landing	0.5 min.

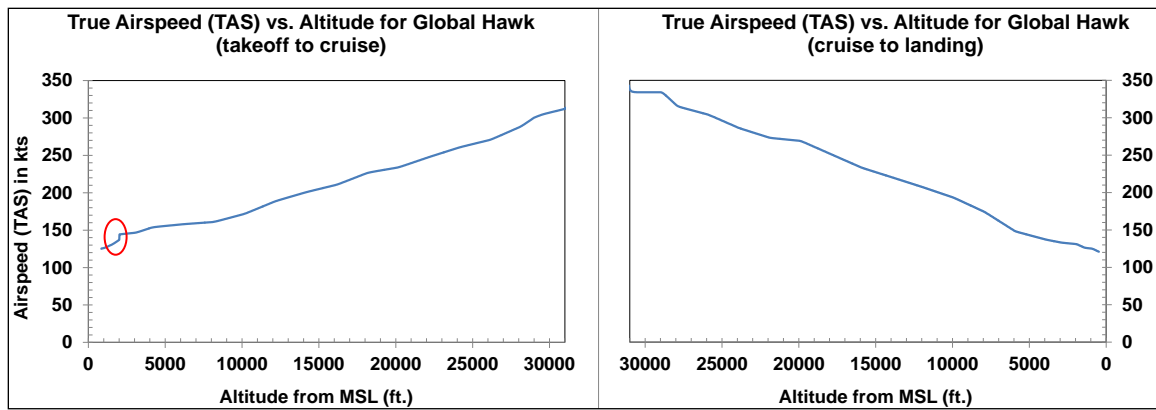


Figure 33. True airspeed (TAS) vs. altitude for Global Hawk flight from KMSP to KMCO

BADA PERFORMANCE FILE										Mar 07 2012		
AC/Type: RQ4A										SOURCE OPF FILE:	Mar 07 2012	
										SOURCE APF FILE:	Mar 07 2012	
Speeds: CAS(LO/HI) Mach Mass Levels [kg]										Temperature:	ISA	
climb - 210/230 0.40 low - 6280										Max Alt. [ft]:	65000	
cruise - 220/240 0.40 nominal - 11512												
descent - 230/230 0.40 high - 14203												
FL		CRUISE				CLIMB				DESCENT		
	TAS	fuel			TAS	ROCD	fuel		TAS	ROCD	fuel	
	[kts]	[kg/min]			[kts]	[fpm]	[kg/min]		[kts]	[fpm]	[kg/min]	
		lo	nom	hi		lo	nom	hi		nom	nom	nom
0					115	1826	2452	1795	19.3	115	1140	2.5
5					119	1766	2399	1735	19.1	117	1140	2.5
10					121	1743	2371	1713	18.4	120	1225	2.5
15					123	1786	2420	1755	18.1	126	1214	2.5
20					124	1760	2389	1730	18.1	131	1079	2.5
30	135	7.4	7.9	8.1	127	2047	2669	2017	17.6	133	1100	2.5
40	140	8.4	8.9	9.1	131	2185	2837	2154	19.1	137	1080	2.5
60	151	9.4	9.9	10.2	142	2271	2881	2173	18.2	148	1080	2.4
80	176	10.1	10.6	10.8	161	2364	2917	2195	18.1	174	1080	2.4
100	196	11.0	11.6	11.8	172	2392	2987	2264	17.6	193	1080	2.4
120	211	11.9	12.5	12.8	189	2409	3032	2297	17.5	207	1020	2.4
140	222	12.9	13.5	13.8	201	2485	3101	2348	14.5	220	1280	2.3
160	239	13.8	14.4	14.7	211	2533	3180	2389	14.1	233	1300	2.3
180	258	14.3	14.9	15.2	227	2511	3143	2319	11.3	251	1380	2.3
200	271	15.3	16.9	15.9	234	2504	3104	2300	12.3	269	1470	2.3
220	278	16.3	16.9	16.2	248	2432	3080	2276	12.2	273	1520	2.2
240	291	17.3	17.2	16.7	261	2396	3043	2212	10.1	286	1520	2.2
260	309	17.8	17.2	16.9	271	2301	3011	2183	9.0	304	1460	2.2
280	323	18.3	17.7	17.3	289	2217	2982	2100	9.5	315	1420	2.2
290	343	19.3	17.9	17.7	303	2143	2777	2079	12.8	334	1490	2.2
310	343	18.6	17.9	17.2	313	2084	2645	2032	11.4	334	1530	2.1
330	329	18.3	17.4	16.8	318	2028	2558	1982	8.2	332	1590	2.1
350	321	17.8	17.2	16.9	323	1986	2481	1913	7.3	325	1650	2.1
370	305	17.1	16.7	16.1	331	1970	2388	1877	8.6	319	1690	2.1
390	292	16.4	16.6	16.1	312	1910	2314	1801	8.9	311	1790	2.0
410	288	15.3	16.2	15.9	306	1859	2276	1730	8.3	304	1800	2.0
430	276	14.8	15.7	15.3	301	1803	2219	1654	7.6	299	1830	2.0
450	270	13.9	15.0	14.9	297	1561	2191	1497	6.9	293	1860	2.0
470	259	13.1	14.4	14.1	290	1511	2102	1322	6.2	288	1880	1.9
490	259	11.8	13.5	13.2	287	1398	1958	1230	5.4	273	2276	1.9
510	259	10.9	11.9	11.6	281	1200	1893	1109	5.1	271	2300	1.9
530	259	9.8	10.8	10.2	277	1108	1620	1095	4.8	269	2370	1.9
550	259	9.4	10.2	9.6	263	1058	1474	918	4.2	269	2410	1.8
570	259	9.0	9.9	9.2	251	994	1263	877	3.9	261	2450	1.8
590	259	8.2	9.3	8.8	242	825	1179	809	3.7	261	2010	1.8
610	259	7.7	9.0	8.5	242	764	1089	750	3.9	261	1960	1.8
630	259	7.4	8.7	8.1	242	669	970	656	3.2	261	1890	1.8
650	259	6.8	8.1	7.7	242	575	853	563	3.2	261	1870	1.8

Figure 34. The .PTF file for Global Hawk (RQ4A). File was compiled by Purdue.

```

CCCCCCCCCCCCCCCCCCCCCCCCCCCCCCCCCCCCCCCC RQ4A__.OPF CCCCCCCCCCCCCC/
CC
CC          AIRCRAFT PERFORMANCE OPERATIONAL FILE
CC
CC
CC      File_name: RQ4A__.OPF
CC
CC      Creation_date: Mar 07 2012
CC
CC      Modification_date: Mar 07 2012
CC
CC
CC===== Actype =====
CD  RQ4A__      1 engines    Jet           M      /
CC  Northrop Grumman RQ4A with 1 F137AD100 engines     wake   /
CC
CC===== Mass (t) =====
CC  reference      minimum      maximum      max payload  mass grad /
CD  .11512E+02    .52337E+01    .14203E+02    .00000E+00    .12868E+00 /
CC===== Flight envelope =====
CC  VMO(KCAS)      MMO        Max.Alt     Hmax      temp grad /
CD  .24100E+03    .66600E+00    .65000E+05    .28927E+05    .00000E+00 /
CC===== Aerodynamics =====
CC Wing Area and Buffet coefficients (SIM)
CCndrst Surf(m2)  Clbo(M=0)      k       CM16
CD 5  .50168E+02    .27236E+01    .00000E+00    .00000E+00 /
CC Configuration characteristics
CC n Phase Name  Vstall(KCAS)  CDO      CD2      unused
CD 1 CR  Clean    .10782E+03    .21180E-01    .77917E-02    .00000E+00 /
CD 2 IC  Clean    .95406E+02    .21180E-01    .17508E-01    .00000E+00 /
CD 3 TO  Clean    .82990E+02    .21180E-01    .14705E-01    .00000E+00 /
CD 4 AP  Clean    .79831E+02    .21180E-01    .11454E-01    .00000E+00 /
CD 5 LD  Clean    .76672E+02    .21180E-01    .77308E-02    .00000E+00 /
CC Spoiler
CD 1  RET
CD 2  EXT      .00000E+00    .00000E+00 /
CC Gear
CD 1  UP
CD 2  DOWN      XXX      .00000E+00    .00000E+00 /
CC Brakes
CD 1  OFF
CD 2  ON      .00000E+00    .00000E+00 /
CC===== Engine Thrust =====
CC  Max climb thrust coefficients (SIM)
CD  .25517E+05    .31494E+05    .45707E-10    .00000E+00    .00000E+00 /
CC  Desc(low)  Desc(high)  Desc level  Desc(app)  Desc(Id)
CD  .13901E+00    .13570E+00    .15000E+05    .13890E+00    .13650E+00 /
CC  Desc CAS    Desc Mach    unused      unused      unused
CD  .00000E+00    .00000E+00    .00000E+00    .00000E+00    .00000E+00 /
CC===== Fuel Consumption =====
CC  Thrust Specific Fuel Consumption Coefficients
CD  .56725E+00    .37146E+03
CC  Descent Fuel Flow Coefficients
CD  .24975E+01    .21197E+06
CC  Cruise Corr.  unused      unused      unused      unused
CD  .10000E+01    .00000E+00    .00000E+00    .00000E+00    .00000E+00 /
CC===== Ground =====
CC  TOL      LDL      span      length      unused
CD  .10660E+04    .24380E+04    .35418E+02    .13588E+02    .00000E+00 /
CC

```

Figure 35. The .OPF file for Global Hawk (RQ4A). File was compiled by Purdue.

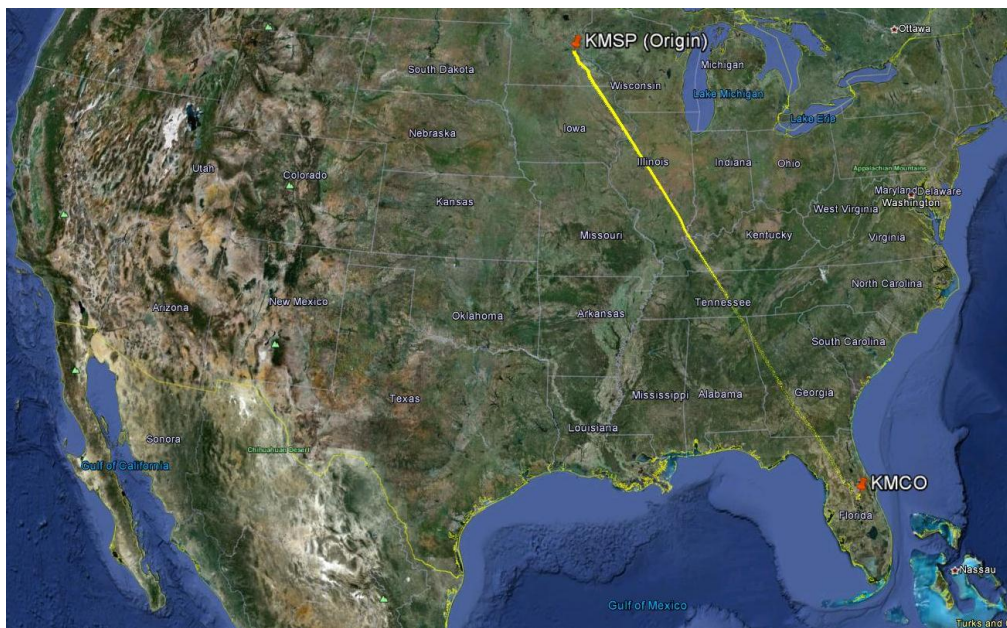


Figure 36. Plan-view of Global Hawk flight path from KMSP to KMCO

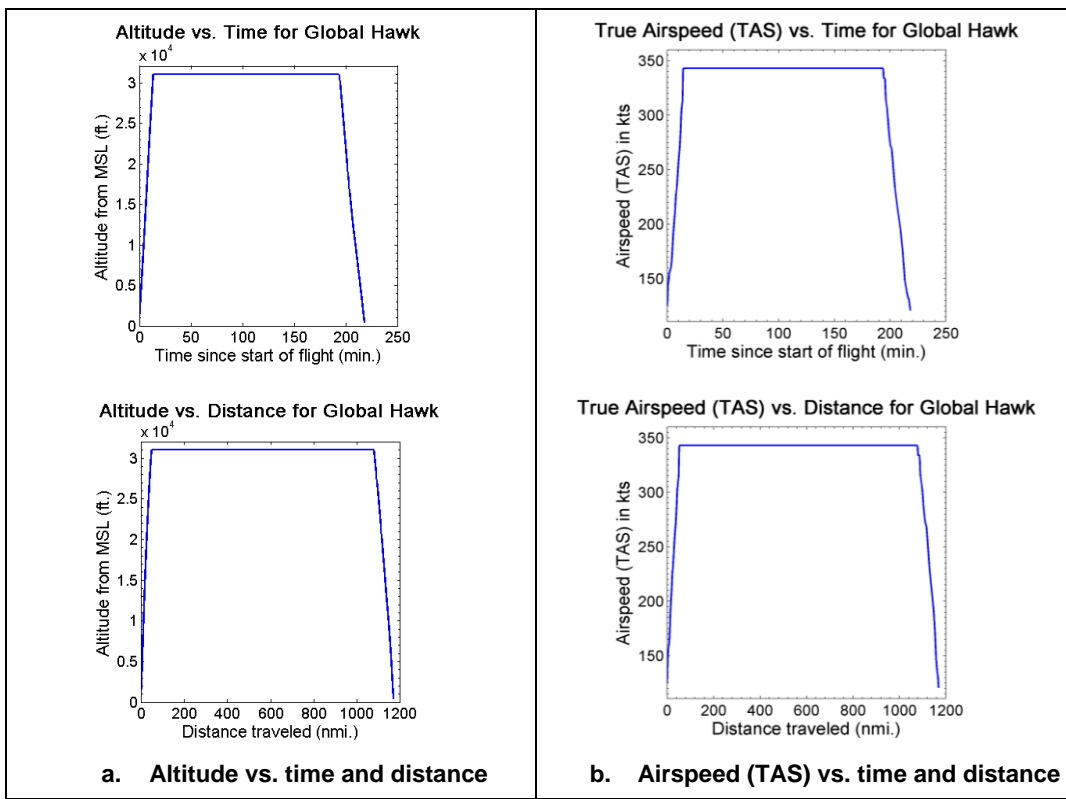


Figure 37. Variation in altitude and airspeed (TAS) with time and distance for Global Hawk flight from KMSP to KMCO

9.3 Simulation of Orbiter (ORBM) using KTG

Important features of Orbiter's flight simulation are shown in Table 33. Anomalies and unexpected flight profile were not observed in the simulation results. Simulation results are shown in Figure 38, Figure 39 and Figure 40.

Table 33. Features of Orbiter flight simulation using KTG

Origin	KATL
Destination	KBHM
Flight time	177.6 min.
Flight distance	117.4 nmi.
Cruise speed	39 KTAS
Cruise altitude	8000 ft.
Takeoff mass	7.5 kg
Landing mass	7.496 kg
Duration of climb	8.3 min.
Duration of cruise	149.9 min.
Duration of descent	15.8 min.
Duration of landing	3.6 min.

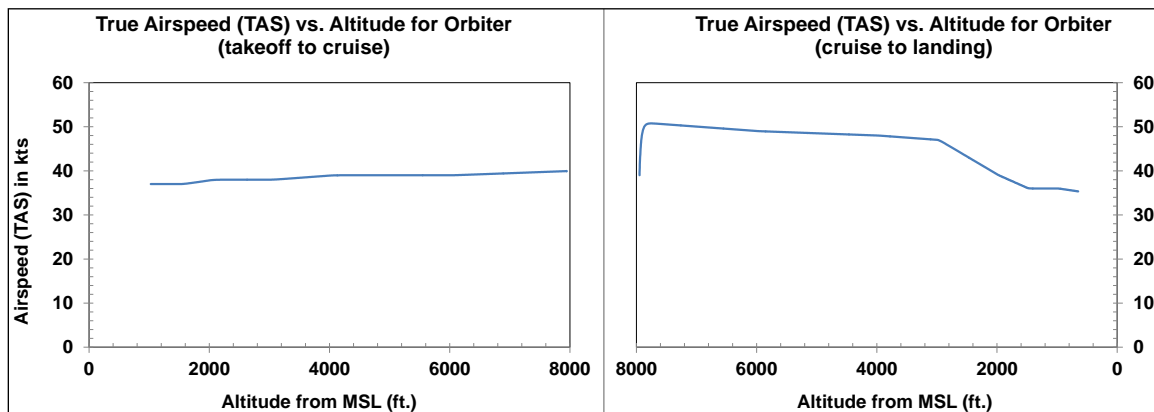


Figure 38. True airspeed (TAS) vs. altitude for Orbiter flight from KATL to KBHM

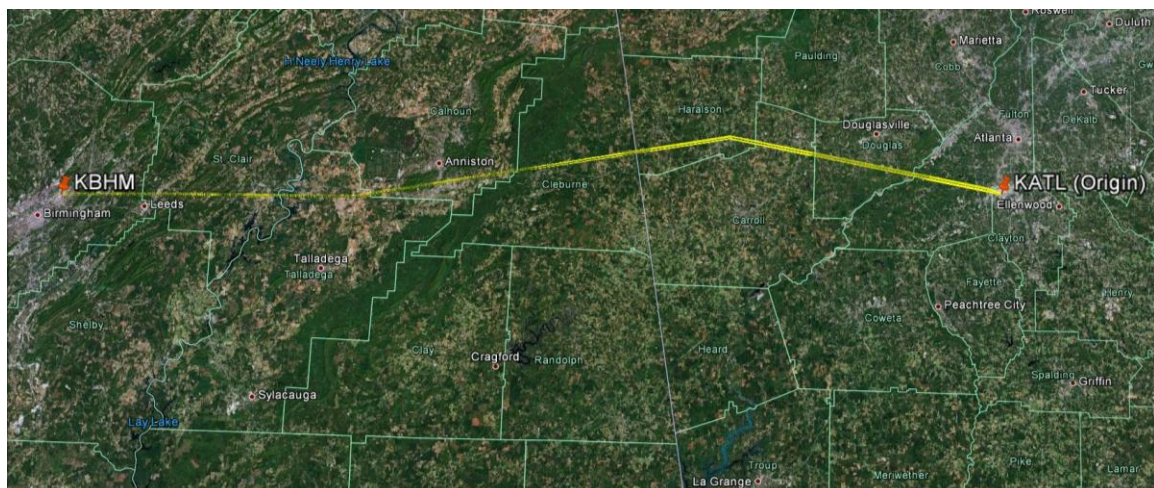


Figure 39. Plan-view of Orbiter flight path from KATL to KBHM

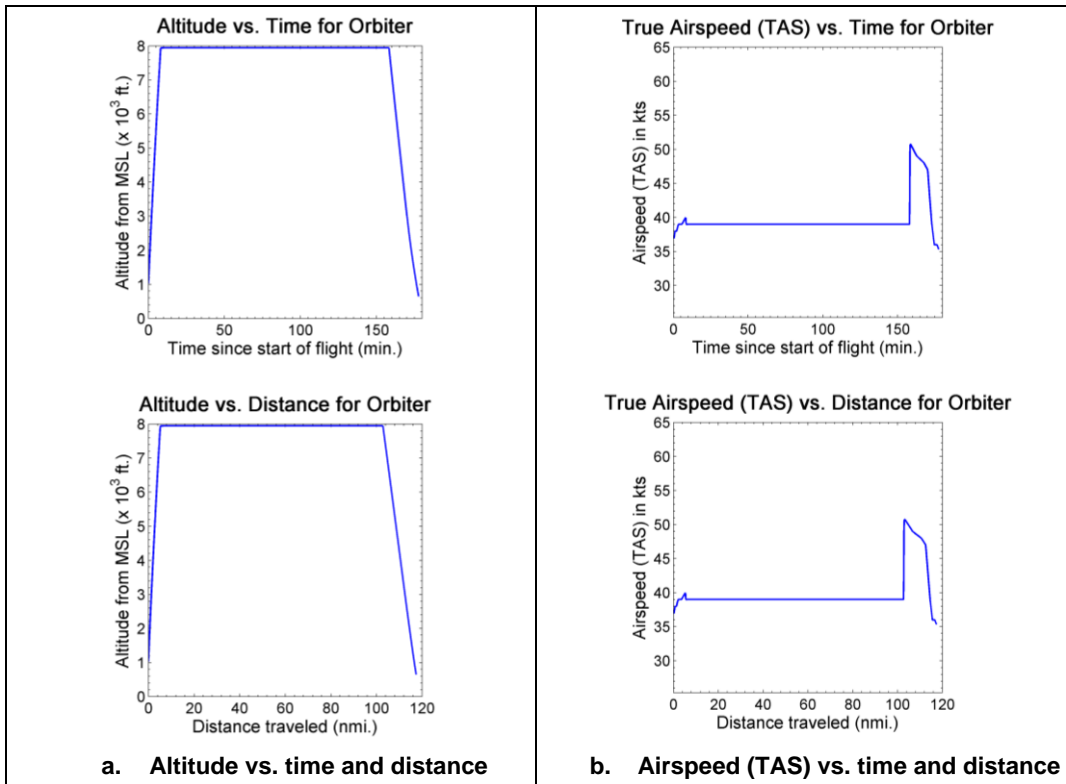


Figure 40. Variation in altitude and airspeed (TAS) with time and distance for Orbiter flight from KATL to KBHM

9.4 Simulation of Aerosonde (MK47) using KTG

Important features of Aerosonde's flight simulation are shown in Table 34. Anomalies and unexpected flight profile were not observed in the simulation results. Simulation results are shown in Figure 44, Figure 45 and Figure 43.

Table 34. Features of Aerosonde flight simulation using KTG

Origin	KATL
Destination	KBHM
Flight time	143 min.
Flight distance	117.6 nmi.
Cruise speed	49 KTAS
Cruise altitude	8000 ft.
Takeoff mass	34.01 kg
Landing mass	31.37 kg
Duration of climb	3.7 min.
Duration of cruise	124.8 min.
Duration of descent	12.5 min.
Duration of landing	1.9 min.

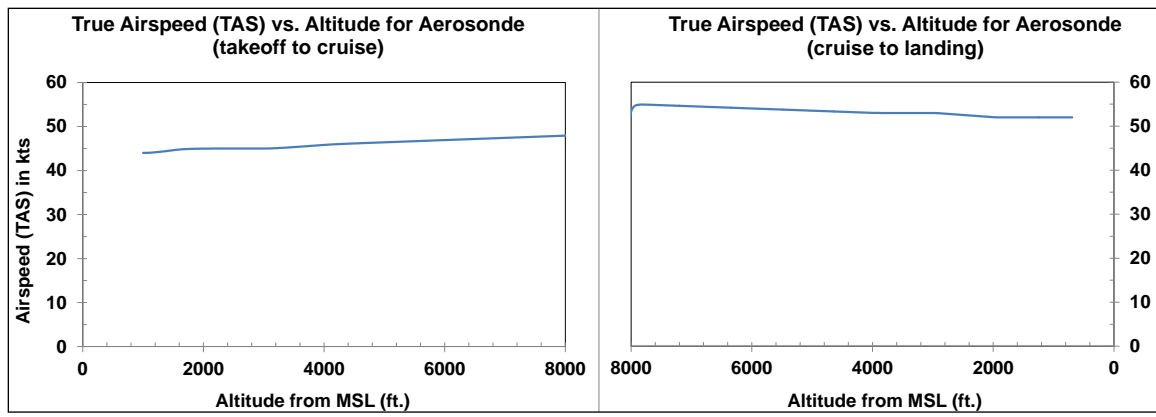


Figure 41. True airspeed (TAS) vs. altitude for Aerosonde flight from KATL to KBHM

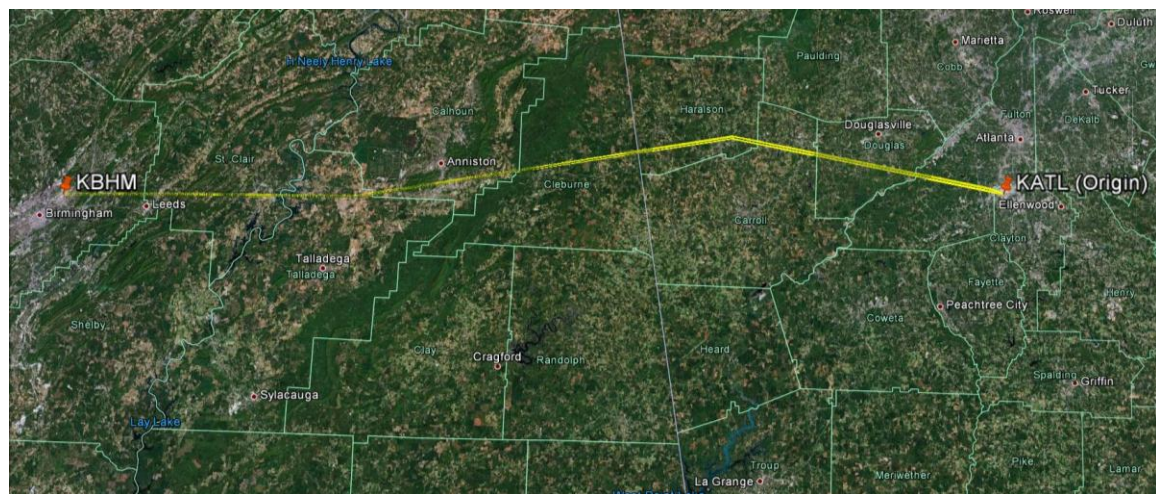


Figure 42. Plan-view of Aerosonde flight path from KATL to KBHM

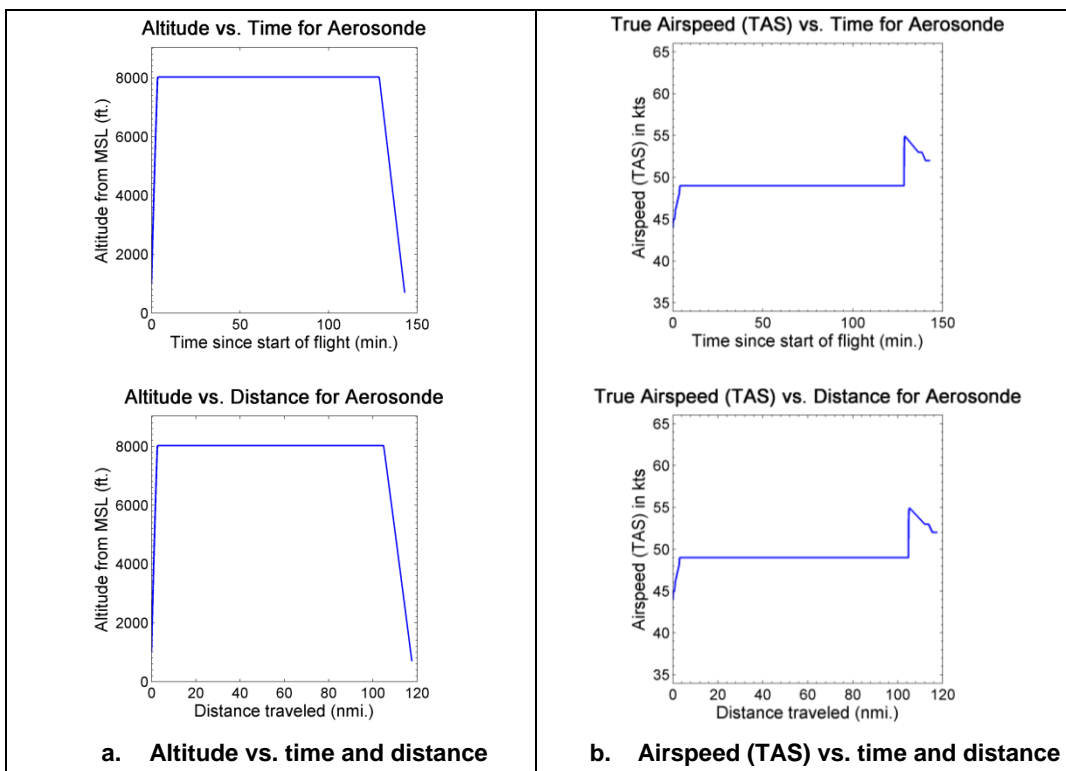


Figure 43. Variation in altitude and airspeed (TAS) with time and distance for Aerosonde flight from KATL to KBHM

9.5 Simulation of Predator A (MQ1B) using KTG

Important features of Predator A's flight simulation are shown in Table 35. No anomalies were observed in the flight profile. The simulation results are shown in Figure 44, Figure 45 and Figure 46. It should be noted that, similar to Global Hawk, the cruise altitude of Predator A (16000 ft. MSL) is lower than its ceiling (24000 ft. MSL).

Table 35. Features of Predator A flight simulation using KTG

Origin	KATL
Destination	KJFK
Flight time	395 min.
Flight distance	715.3 nmi.
Cruise speed	111 KTAS
Cruise altitude	16000 ft.
Takeoff weight	1020.5 kg
Landing weight	870.7 kg
Duration of climb	12.9 min.
Duration of cruise	354 min.
Duration of descent	26.3 min.
Duration of landing	1.7 min.

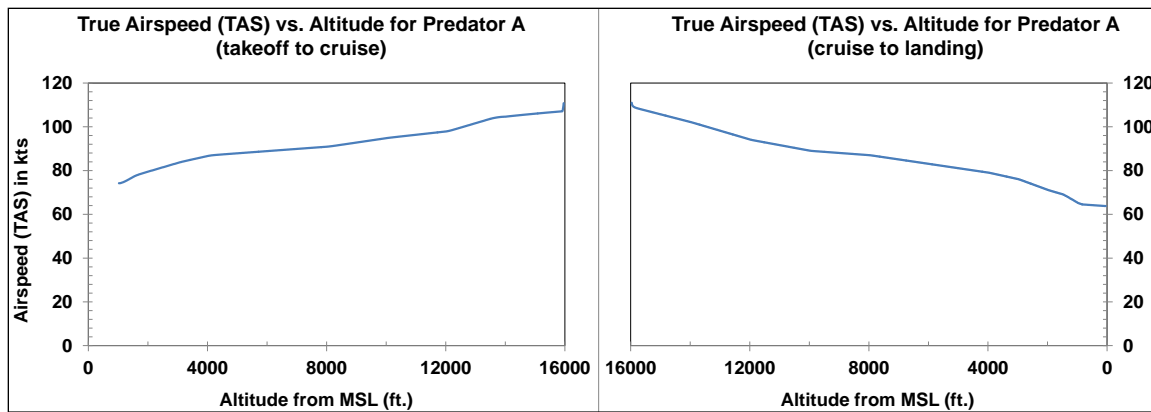


Figure 44. True airspeed (TAS) vs. altitude for Predator A flight from KATL to KJFK

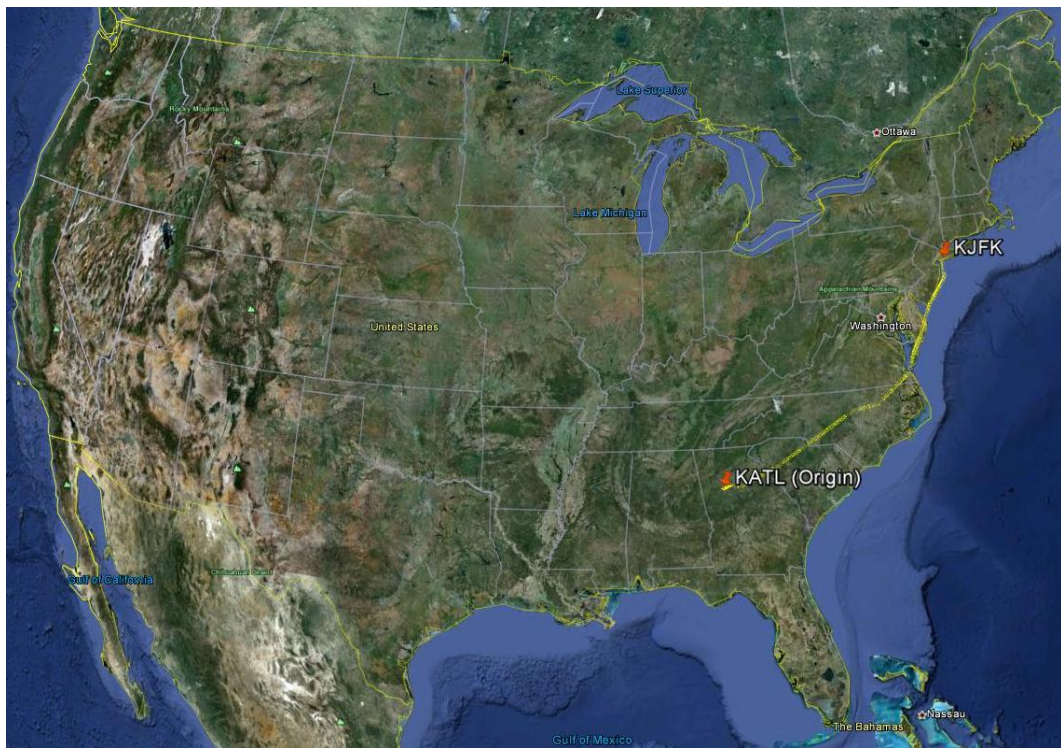


Figure 45. Plan-view of Predator A flight path from KATL to KJFK

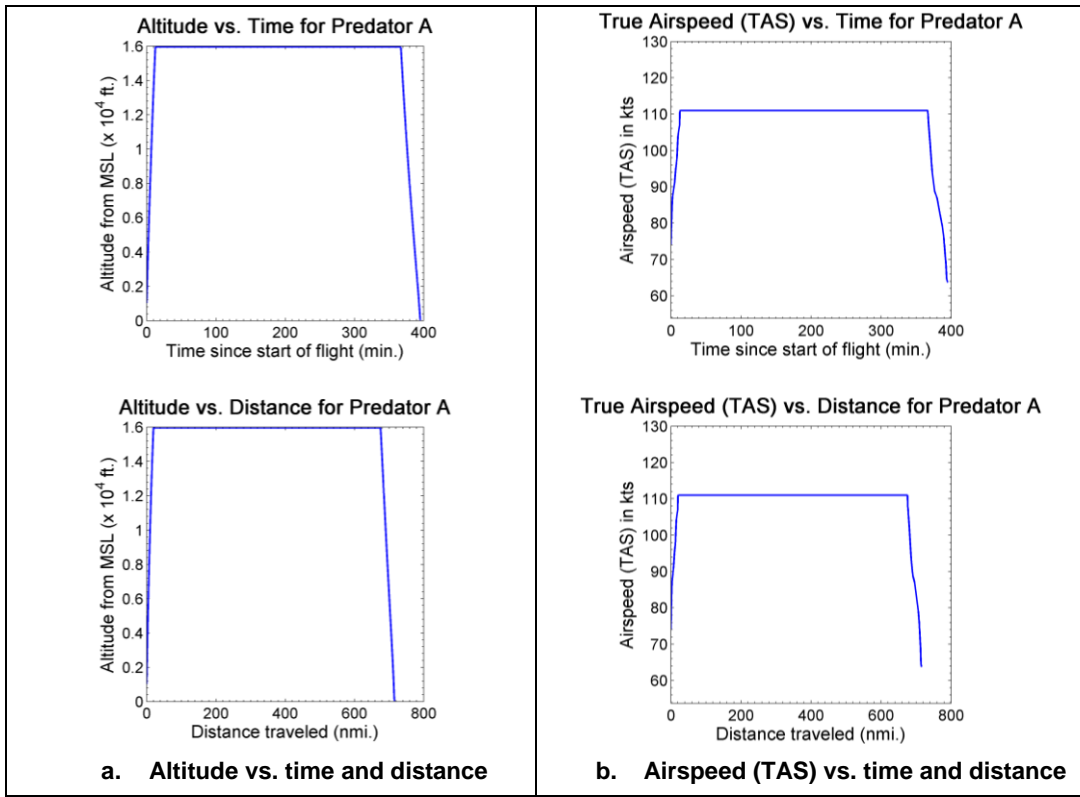


Figure 46. Variation in altitude and airspeed (TAS) with time and distance for Predator A flight from KATL to KJFK

9.6 Simulation of Predator B (MQ-9) using KTG

Important features of Predator B's flight simulation are shown in Table 36. No anomalies were observed in the flight profile. The simulation results are shown in Figure 44, Figure 45 and Figure 46.

Table 36. Features of Predator B flight simulation using KTG

Origin	KMSP
Destination	KMCO
Flight time	350.4 min
Flight distance	1167.6 nmi
Cruise speed	209 KTAS
Cruise altitude	31000 ft.
Takeoff weight	3734.6 kg
Landing weight	3072.28 kg
Duration of climb	23.8 min.
Duration of cruise	292 min.
Duration of descent	31.7 min.
Duration of landing	2.9 min.

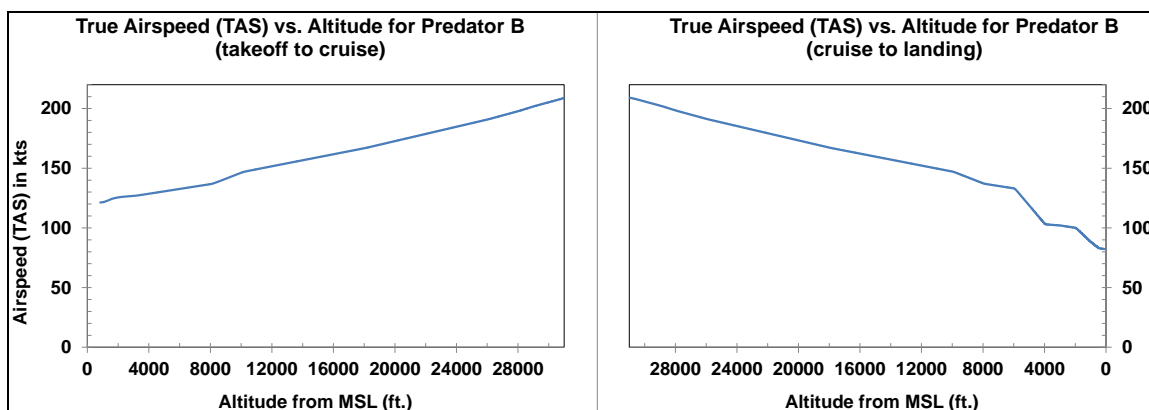


Figure 47. True airspeed (TAS) vs. altitude for Predator B flight from KMSP to KMCO

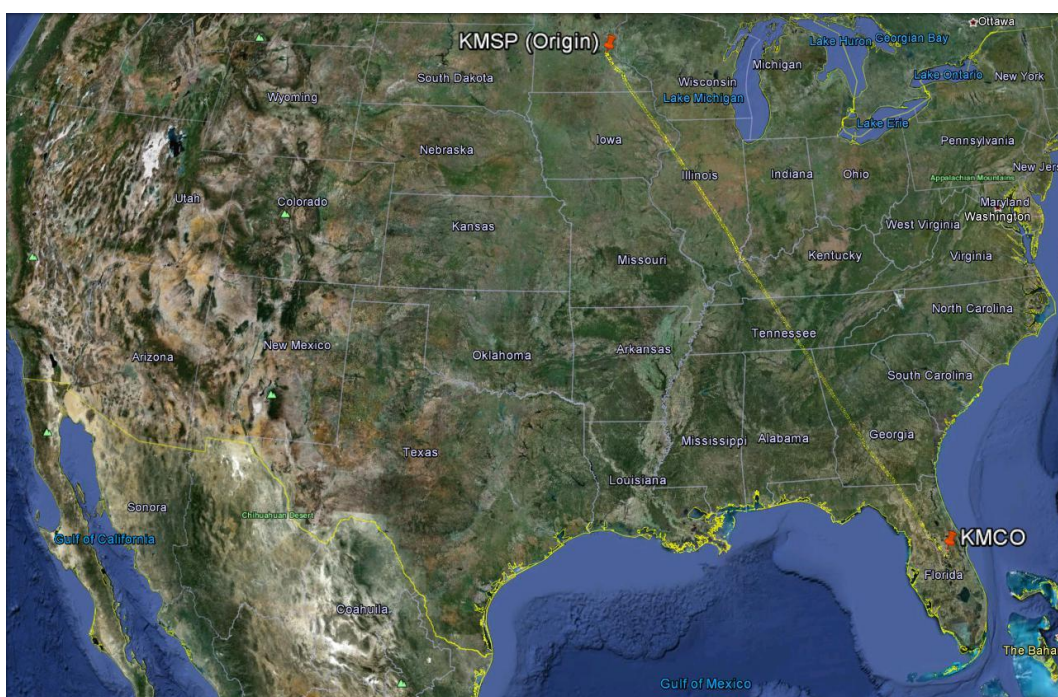


Figure 48. Plan-view of Predator B flight path from KMSP to KMCO

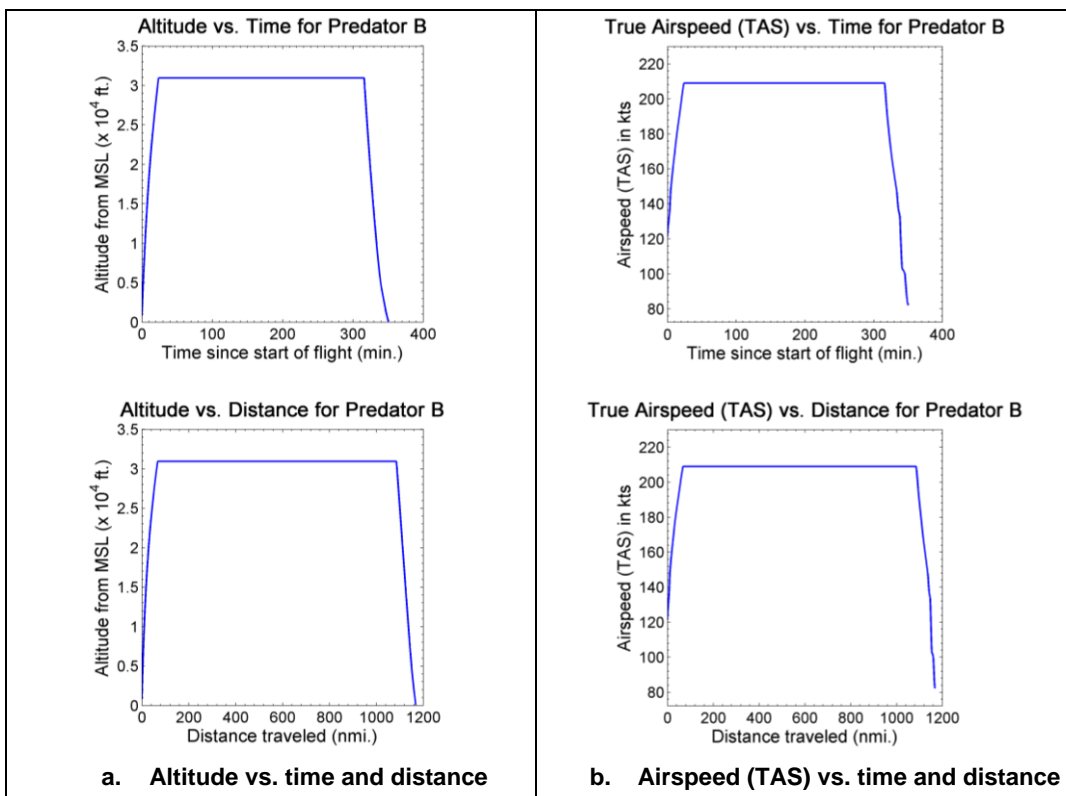


Figure 49. Variation in altitude and airspeed (TAS) with time and distance for Predator B flight from KMSP to KMCO

9.7 Simulation of Gray Eagle (MQ1C) using KTG

Important features of Gray Eagle's flight simulation are shown in Table 37. No anomalies were observed in the flight profile. The simulation results are shown in Figure 50, Figure 51 and Figure 52.

Table 37. Features of Gray Eagle flight simulation using KTG

Origin	KATL
Destination	KJFK
Flight time	234.4 min.
Flight distance	714.9 nmi.
Cruise speed	203 KTAS
Cruise altitude	32000 ft.
Takeoff weight	1620.2 kg
Landing weight	1542 kg
Duration of climb	45 min.
Duration of cruise	136 min.
Duration of descent	53.8 min.
Duration of landing	1.5 min.

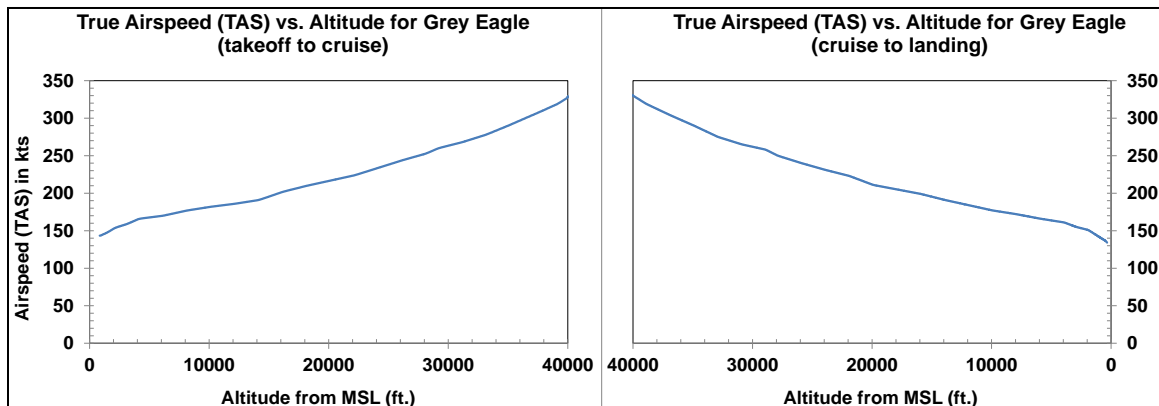


Figure 50. True airspeed (TAS) vs. altitude for Gray Eagle flight from KATL to KJFK

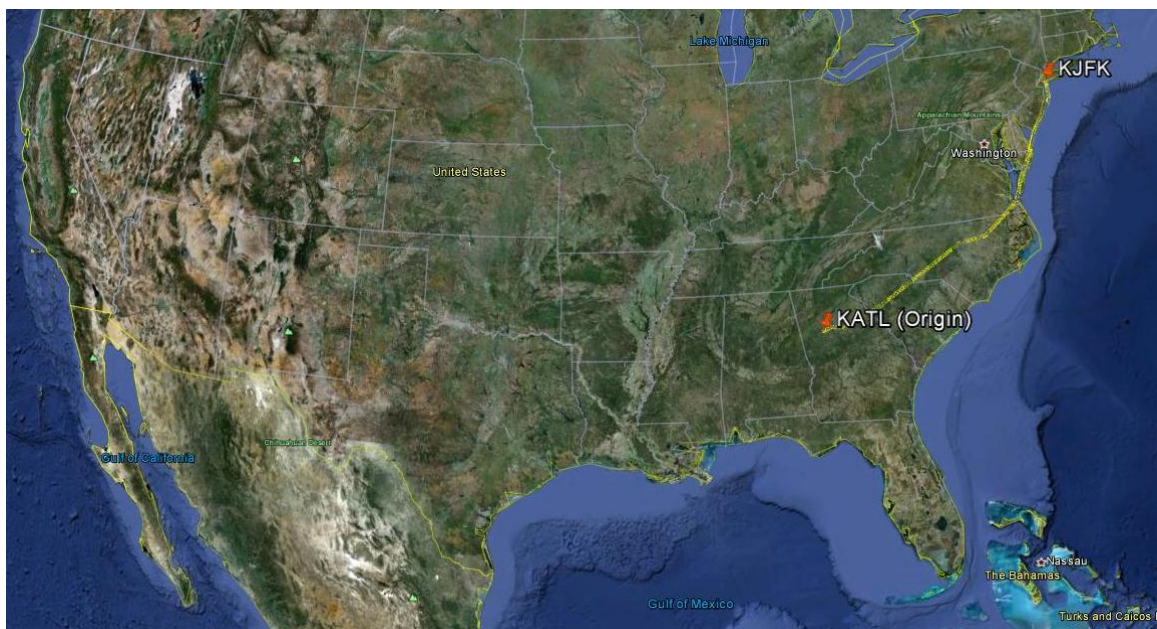


Figure 51. Plan-view of Gray Eagle flight path from KATL to KJFK

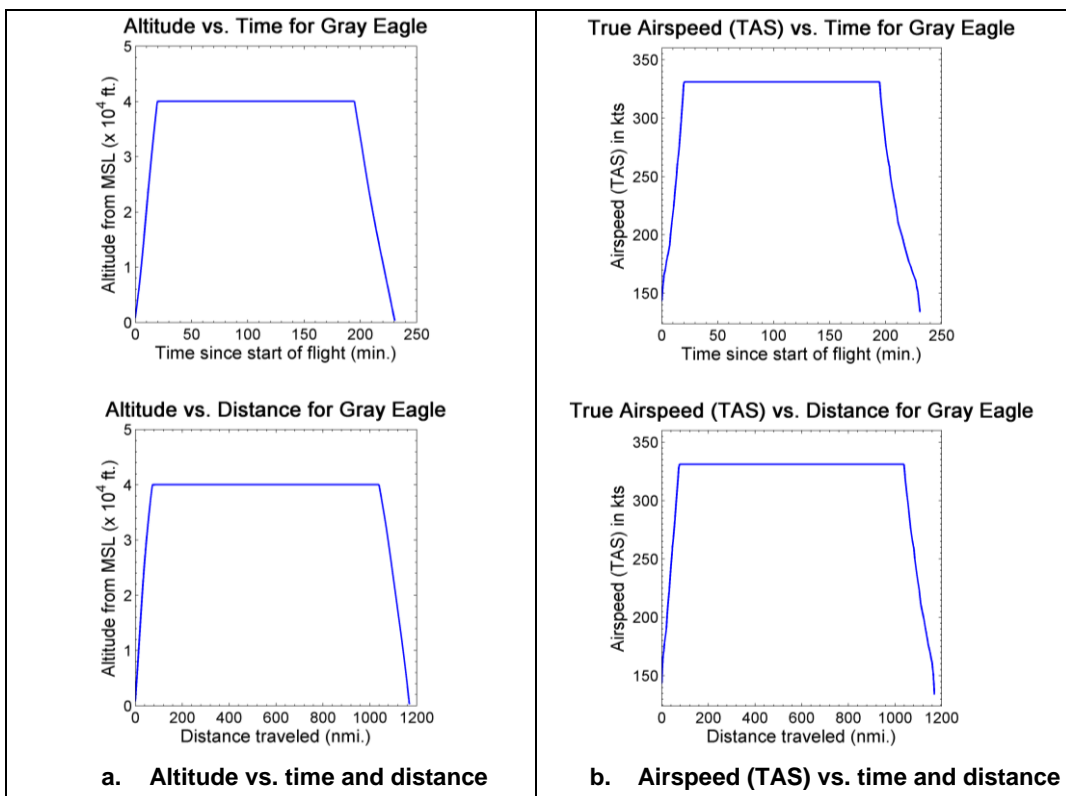


Figure 52. Variation in altitude and airspeed (TAS) with time and distance for Gray Eagle flight from KATL to KJFK

9.8 Simulation of Predator C (AVEN) using KTG

Important features of Predator C's flight simulation are shown in Table 38. No anomalies were observed in the flight profile. The simulation results are shown in Figure 53, Figure 54 and Figure 55.

Table 38. Features of Predator C flight simulation using KTG

Origin	KMSP
Destination	KMCO
Flight time	230.5 min.
Flight distance	1168.6 nmi.
Cruise speed	331 KTAS
Cruise altitude	40000 ft.
Takeoff weight	7166.7 kb
Landing weight	4951 kg
Duration of climb	19.8 min.
Duration of cruise	174.8 min.
Duration of descent	35.1 min.
Duration of landing	0.8 min.

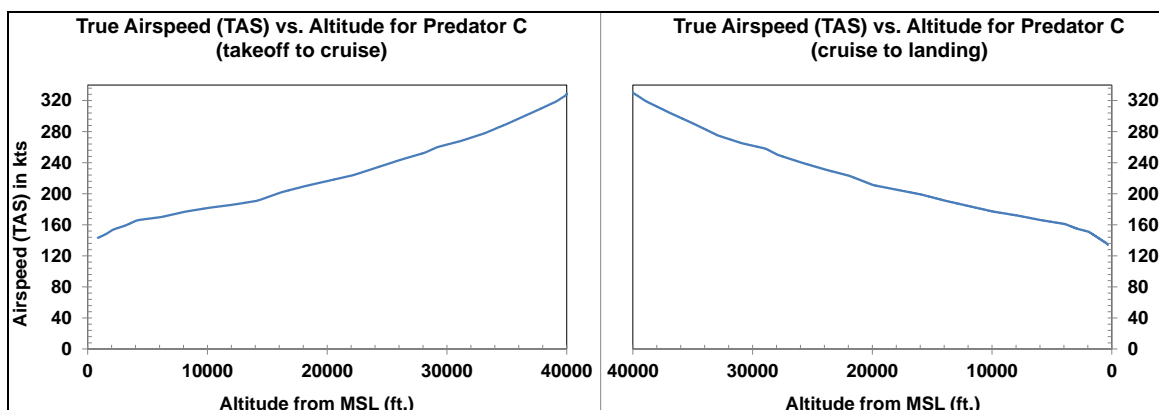


Figure 53. True airspeed (TAS) vs. altitude for Predator C flight from KMSP to KMCO

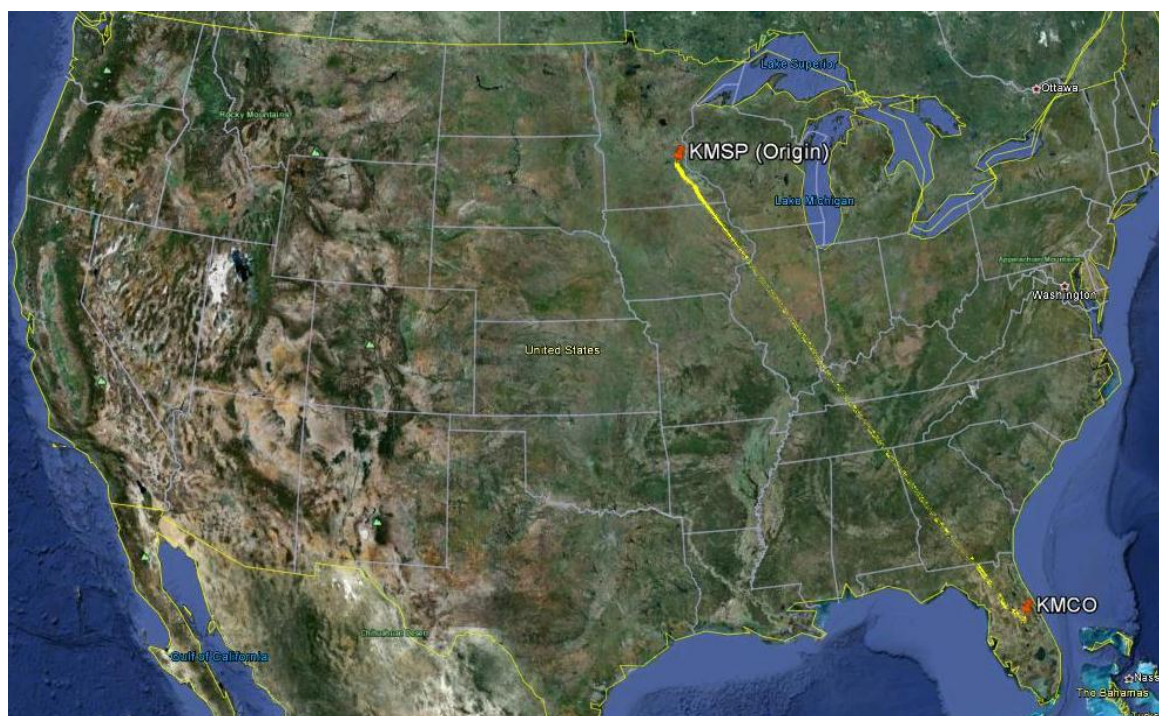


Figure 54. Plan-view of Predator C flight path from KMSP to KMCO

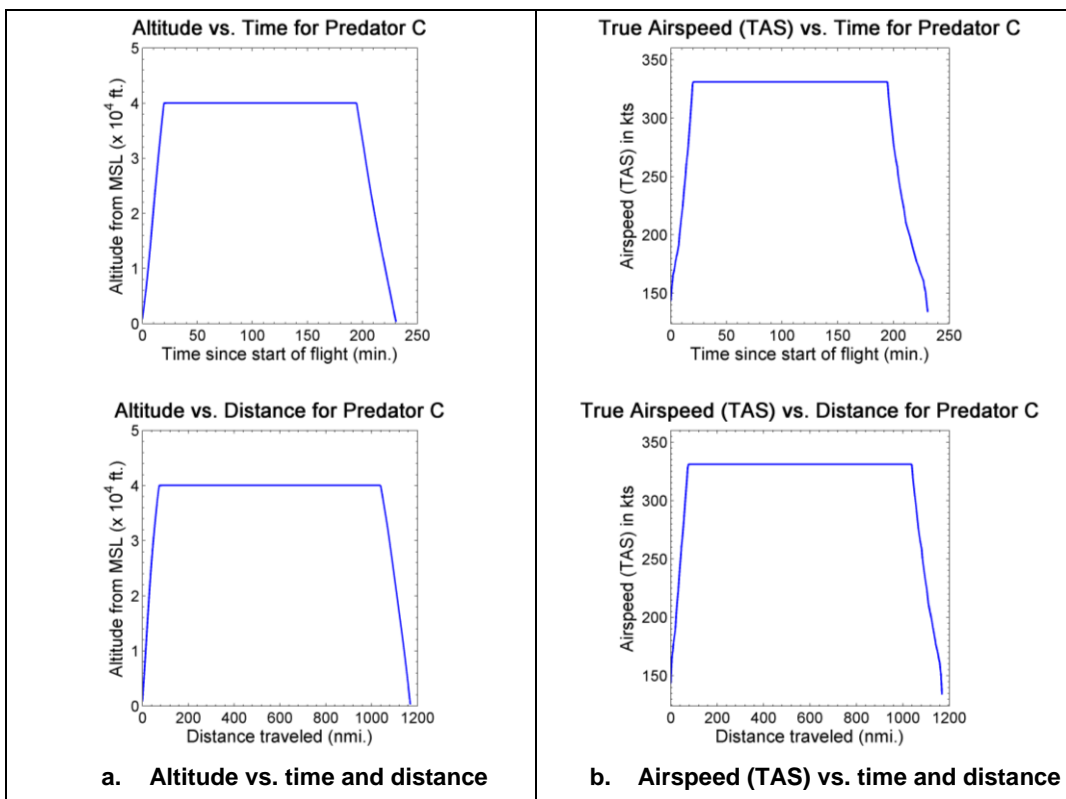


Figure 55. Variation in altitude and airspeed (TAS) with time and distance for Predator C flight from KMSP to KMCO

9.9 Simulation of Hunter (MQ5B) using KTG

Important features of Hunter's flight simulation are shown in Table 39. No anomalies were observed in the flight profile. The simulation results are shown in Figure 56, Figure 57 and Figure 58.

Table 39. Features of Hunter flight simulation using KTG

Origin	KATL
Destination	KJFK
Flight time	372.7 min.
Flight distance	715.2 nmi.
Cruise speed	119 KTAS
Cruise altitude	18000 ft.
Takeoff weight	907.2 kg
Landing weight	792.28 kg
Duration of climb	21.2 min.
Duration of cruise	306.6 min.
Duration of descent	40 min.
Duration of landing	4.7 min.

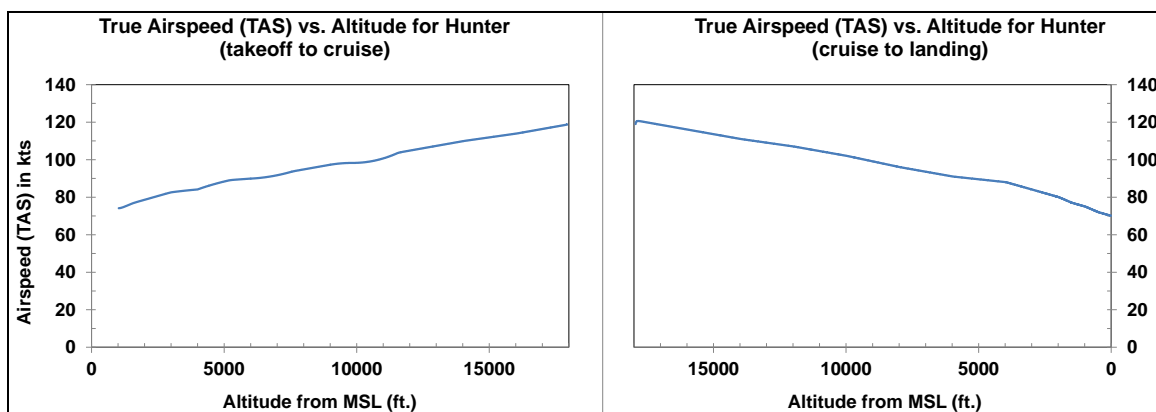


Figure 56. True airspeed (TAS) vs. altitude for Hunter flight from KATL to KJFK

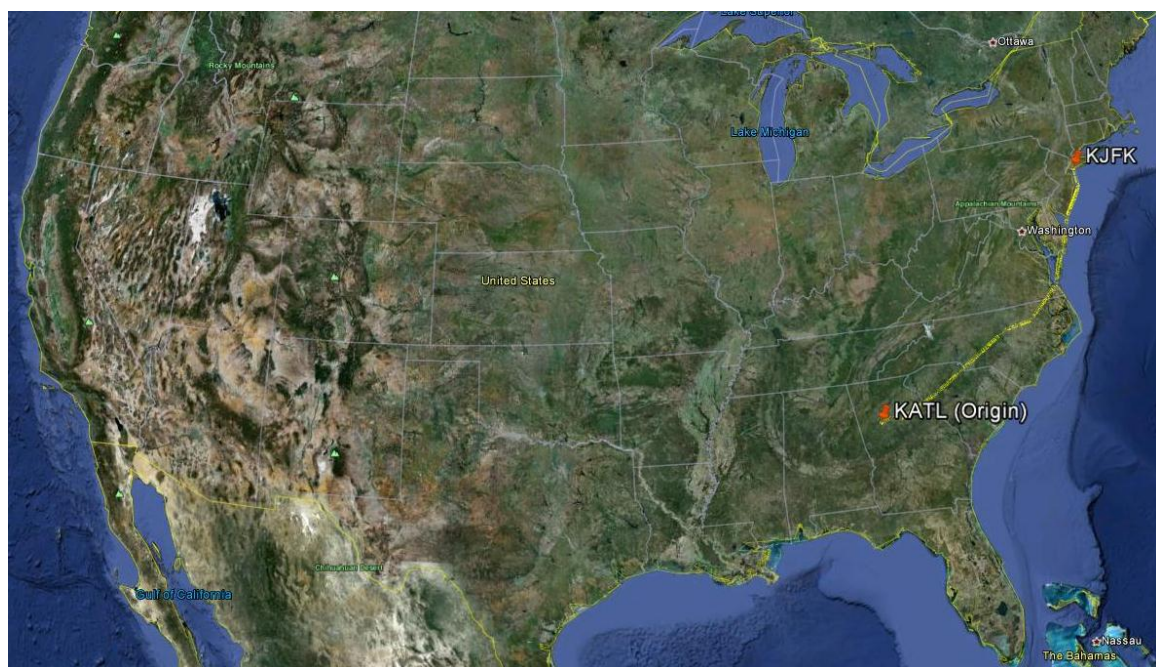


Figure 57. Plan-view of Hunter flight path from KATL to KJFK

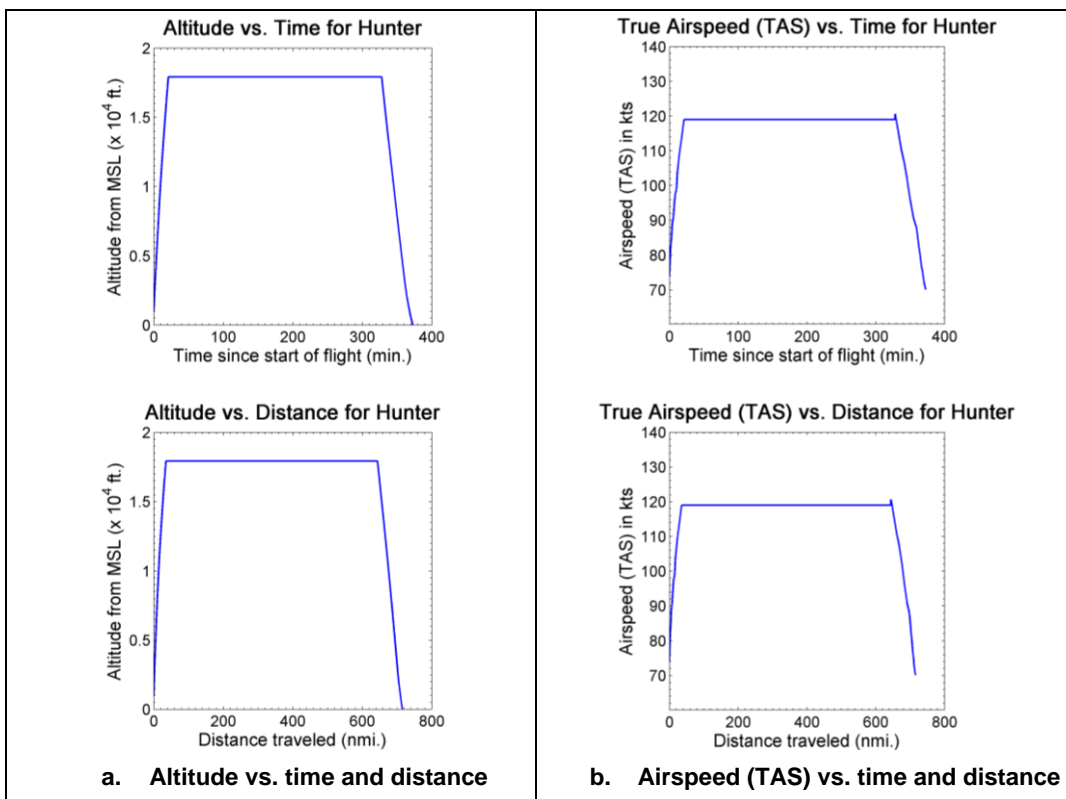


Figure 58. Variation in altitude and airspeed (TAS) with time and distance for Hunter flight from KATL to KJFK

9.10 Simulation of BADA Files for Cargo UAS (CUAS), Fire Scout (MQ8B) and NEO S-300 Mk II VTOL (S350) using KTG

Cargo UAS (CUAS), Fire Scout (MQ8B) and NEO S-300 Mk II VTOL (S350) are rotorcraft or a hybrid of rotorcraft and conventional aircraft. Therefore, they were not simulated using KTG, and the results from simulating and validating their flight profiles using these files are not presented here. On the other hand, the FAA's William J. Hughes Technical Center (FAA Tech Center) has been developing models to analyze and simulate rotorcraft. Consequently, they were approached to provide technical support in validating the BADA files for the four aforementioned aircraft. However, the timeline of this project was too short to take advantage of the Tech Center's expertise. A collaborative effort between NASA and the FAA Tech Center to develop adequate models for rotorcraft is strongly recommended to fill this gap in knowledge.

9.11 Summary of UAS Simulations in KTG

Results of UAS flight simulations using KTG are summarized in Table 40. Included in here are four main features of each flight to briefly distinguish the different aircraft: origin and destination airports, target cruise altitude and speed. Also indicated are whether the aircraft reached the target cruise altitude and speed in the simulation, and whether BADA files for each aircraft were validated by its manufacturer. As mentioned earlier, simulation results for each UAS flight were submitted to the corresponding aircraft manufacturer for validation. It should be noted that rotorcraft cannot be simulated in KTG. Hence, the BADA files of Cargo UAS, Fire Scout and NEO S-300 Mk II VTOL were not validated by this approach. As mentioned earlier, the Tech Center was approached to assist in validating BADA files for these aircraft, but the

process was not complete within the timeline of this project. Recommendations are made in the latter sections of this report on options to validate these files.

Table 40. Summary of nine UAS flights using KTG. Only origin, destination, cruise altitude and cruise speed are included here. Validation of BADA files implies the aircraft reached target cruise altitude in simulation.

UAS	Origin	Destination	Target Cruise Altitude (ft.)	Target Cruise Speed (KTAS)	Reached Target Cruise Altitude & Speed	BADA files validated by manufacturer
Shadow B (RQ7B)	KIAD	KJFK	8000	80	Yes	Yes
Global Hawk (RQ4A)	KMSP	KMCO	31000	343	Yes	Yes
Orbiter (ORBM)	KATL	KBHM	8000	39	Yes	Yes
Aerosonde (MK47)	KATL	KBHM	8000	49	Yes	Yes
Predator A (MQ1B)	KATL	KJFK	16000	111	Yes	Yes
Predator B (MQ-9)	KMSP	KMCO	31000	209	Yes	Yes
Gray Eagle (MQ1C)	KATL	KJFK	32000	203	Yes	Yes
Predator C (AVEN)	KMSP	KMCO	40000	331	Yes	Yes
Hunter (MQ5B)	KATL	KJFK	18000	119	Yes	Yes
Cargo UAS (CUAS)						
Fire Scout (MQ8B)						
NEO S-300 Mk II VTOL (S350)						

10 MACS File Validation

MACS files for the twelve UAS aircraft were validated by comparing the simulation results from MACS with those from KTG. The premise to this was that the validation of BADA files by the UAS manufacturer indirectly validated the KTG results.

10.1 Issues and Resolution

MACS was developed to simulate manned aircraft. Consequently, there were some issues to be resolved to modify the software and simulate UAS aircraft.

10.1.1 Issue 1: Speed vs. Altitude Constraints in MACS

During the simulation of Shadow B via MACS the aircraft could not reach its cruise altitude of 8000 ft. Investigation of MACS' software code indicated that an aircraft should have a minimum speed of 100 KCAS when flying between 3500 ft. and 10500 ft. to reach the cruise altitude. Since Shadow B's speed of 80 KCAS at 8000 ft. was less than this minimum speed, it had no vertical speed beyond the altitude of 3500 ft. causing it to not reach cruise altitude. **The following modifications were made to MACS' code to address this issue:**

MACS file modified: commonObjects/PerfDescr.java

Function: public int getMinimumSpeed(float altitude, boolean isMach)

Original code (starting line 634):

```
else {
    if (altitude < 3500.) {
        return (80);
    }
    else if (altitude <= 10500.) {
        return (100);
    }
    return (int) ((minCas) + 0.5f);
}
```

Modified code (commented out lines 635 through 640):

```
else {
    //    if (altitude < 3500.) {
    //        return (80);
    //    }
    //    else if (altitude <= 10500.) {
    //        return (100);
    //    }
    return (int) ((minCas) + 0.5f);
}
```

The method `getMinimumSpeed()` is invoked by the method `getVerticalSpeed()` in the file `calculators/AltChgCalculator.java` to determine the vertical speed at climb. The following is the logic which returns a value of zero for vertical speed:

```
public static float getVerticalSpeed(PerfDescr performance, float altitude, float ias, float initialWeight, float dragFactor, boolean up) {
    if (up && (ias < performance.getMinimumSpeed(altitude, false)) || altitude >= performance.getMaximumCruiseAltitude())) {
        return (0);
    }
}
```

10.1.2 Issue 2: Simulation of Slow Flying UAS Aircraft

It was found that simulation of slow flying UAS aircraft, such as Shadow B and Predator A, in MACS required large computer memory. For example, during the simulation of Predator A from KMSP to KMCO (about 1160 nmi.) at a cruise speed of 93 KCAS and cruise altitude of 16000 ft., resulted in the software's memory usage exceeding 4 GB and crashed the Java Virtual Machine (JVM) since the MACS JVM's maximum memory was set to 4 GB. As a result, the flight was modified to fly from Nashville International Airport (KBNA) to KATL, which are much closer to each other (about 190 nmi.). Even with this short distance, MACS required about 2.5 GB of memory. This issue was also observed when simulating Global Hawk. However, Global Hawk has a higher cruise speed (225 KCAS) compared to Predator A, and MACS was able to complete the simulation before exceeding its memory limits. It is not known as to why MACS cannot successfully simulate a slow flying aircraft, or what modifications are necessary to solve this issue. Therefore, **no immediate solution was found to address this issue.**

10.1.3 Issue 3: Simulation of Rotorcraft and Electric Aircraft

No provision was found to configure and simulate rotorcraft flights in MACS. Further, the aircraft model data files for UAS rotorcraft and electric aircraft could not be developed due to the absence of relevant data fields in the files. Consequently, the files for Orbiter (electric aircraft), Cargo UAS, Fire Scout and NEO S-300 Mk II VTOL were incomplete, and hence were not simulated in MACS. **No immediate solution was found to address this issue.**

10.2 Simulation of Shadow B (RQ7B) using MACS

Important features of Shadow B's flight simulation using MACS are shown in Table 41. Unlike KTG, aircraft weight at takeoff and landing are not recorded in MACS and indicated as such. The flight was simulated from KBNA to KATL to prevent MACS from exceeding its memory usage limits and thereby successfully complete the simulation due to the slow speed of Shadow B. The plots in Figure 59 show the variation in true airspeed (TAS) of shadow B with altitude. The plot on the left hand side is from takeoff to cruise altitude and that on the right is from cruise to landing. It is not known what caused the rapid increase in speed during the climb phase, and the jaggedness and the associated increases in speed beyond the cruise speed in the right hand plot. The spikes in airspeed in Figure 60 are a different representation of the jaggedness in Figure 59, and hence could not be explained. Since it is not yet known as to how MACS interprets the files for UAS aircraft, no hypothesis was formed to explain the simulation results.

Table 41. Features of Shadow B flight simulation using MACS

Origin	KBNA
Destination	KATL
Flight time	149.4 min.
Flight distance	191.5 nmi.
Cruise speed	86 KTAS
Cruise altitude	8000 ft.
Takeoff weight	Not available
Landing weight	Not available
Duration of climb	3.6 min.
Duration of cruise	127.2 min.
Duration of descent	12 min.
Duration of landing	6 min.

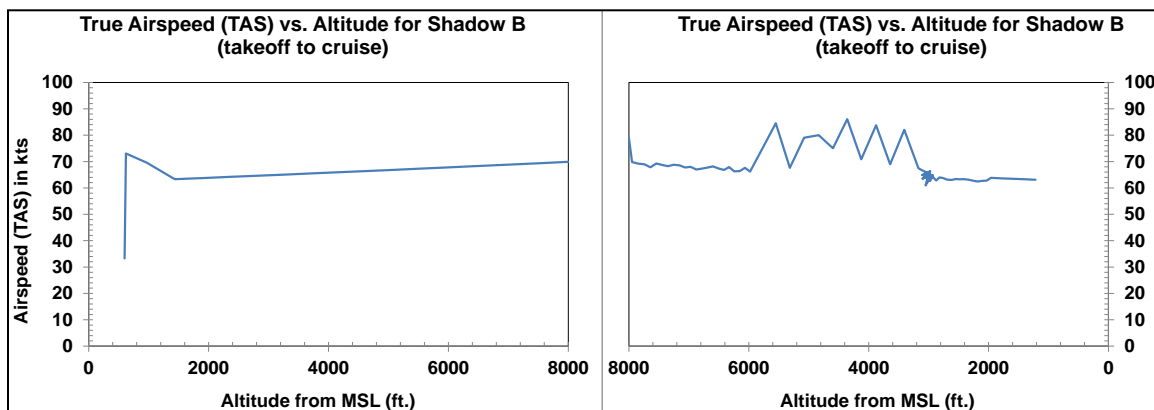


Figure 59. True airspeed (TAS) vs. altitude for Shadow B flight simulation using MACS from KMSP to KMCO

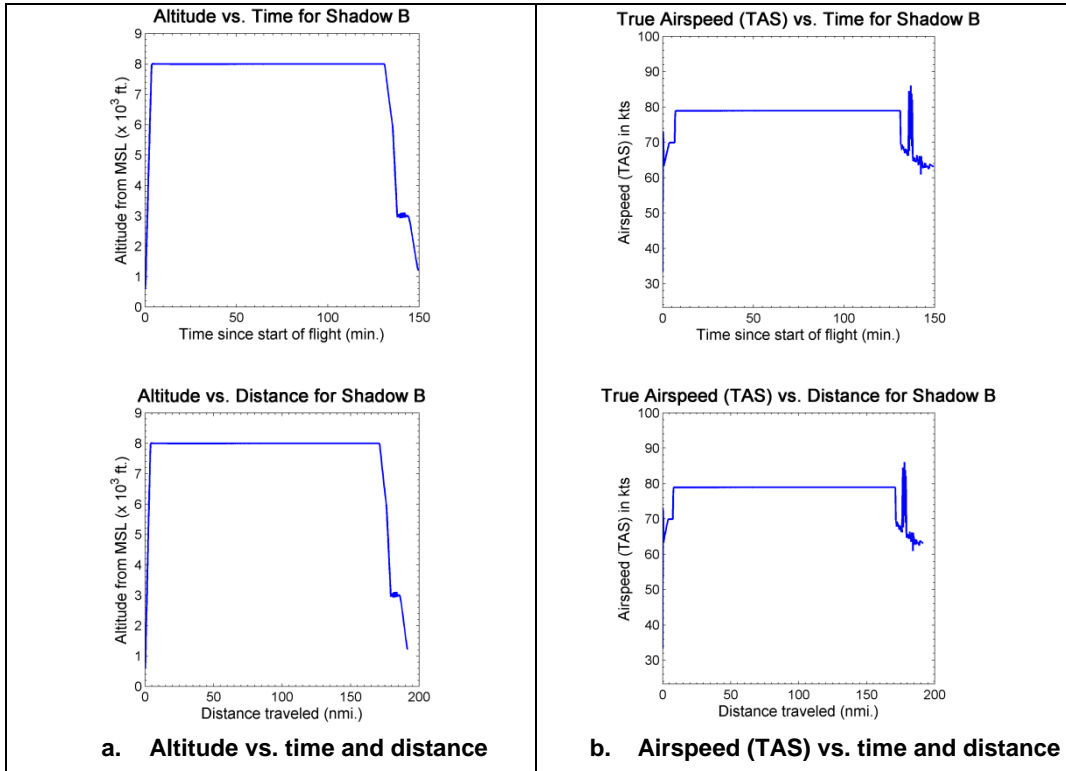


Figure 60. Variation in altitude and airspeed (TAS) with time and distance for Shadow B flight simulation using MACS

10.3 Simulation of Global Hawk (RQ4A) using MACS

Results of Global Hawk's flight simulation using MACS are shown in Figure 61 and Figure 62, with the important features shown in Table 42. The reason for the decrease in speed during descent from 363 KTAS to 197 KTAS, within a span of 96 sec. and for a 246 ft. drop in altitude (right hand plot in Figure 61, and Figure 62b), is not known. The reasons for this behavior are not known but they are suspected to be the same as for Shadow B.

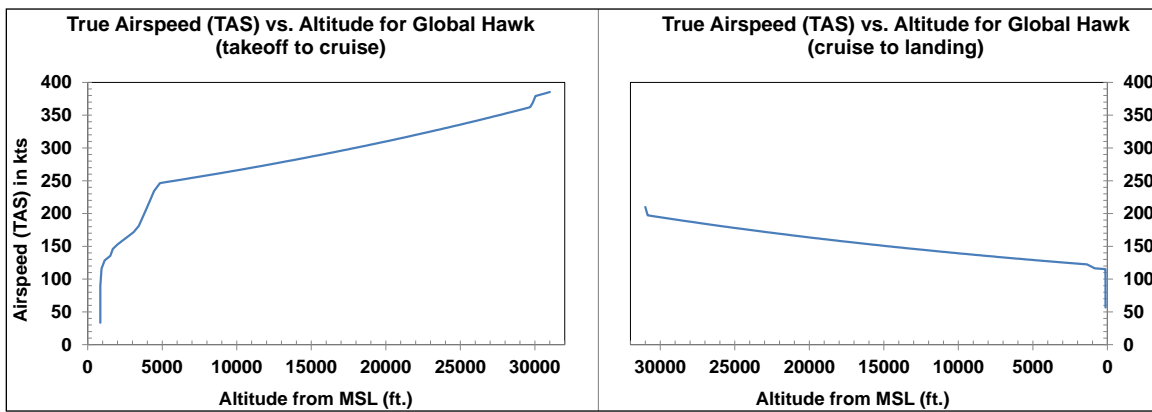


Figure 61. True airspeed (TAS) vs. altitude for Global Hawk flight simulation using MACS from KMSP to KMCO

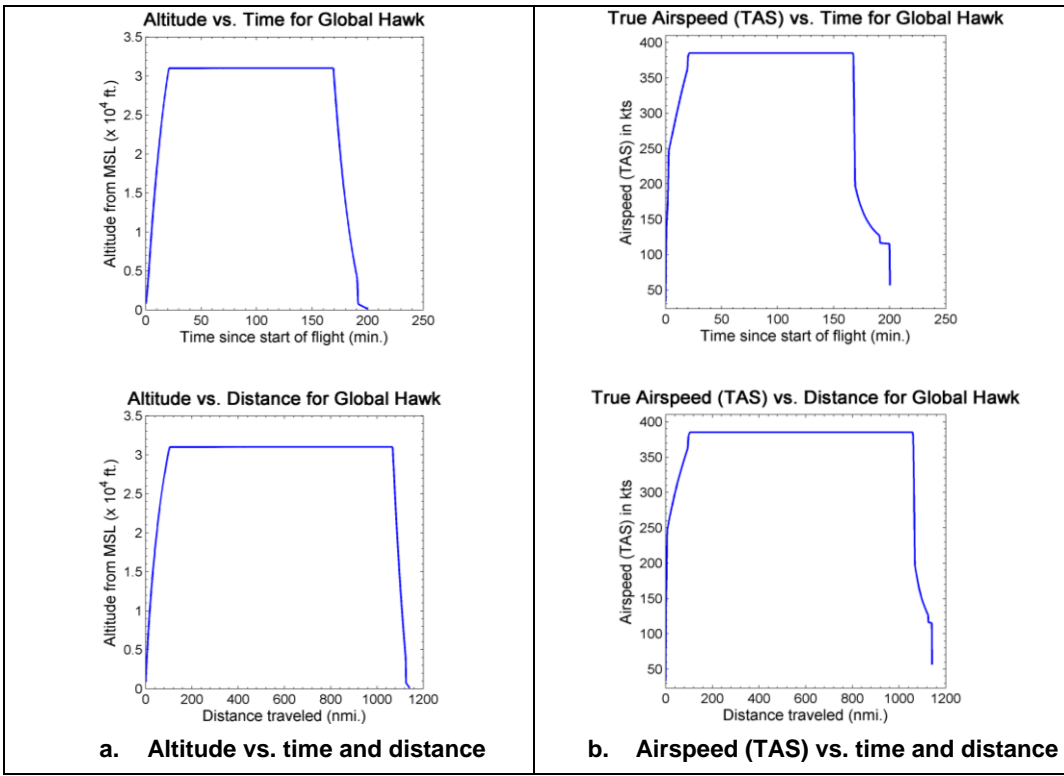


Figure 62. Variation in altitude and airspeed (TAS) with time and distance for Global Hawk flight simulation using MACS

Table 42. Features of Global Hawk flight simulation using MACS

Origin	KMSP
Destination	KMCO
Flight time	200.1 min.
Flight distance	1140.7 nmi.
Cruise speed	385 KTAS
Cruise altitude	31000 ft.
Takeoff weight	Not available
Landing weight	Not available
Duration of climb	20.9 min.
Duration of cruise	147.9 min.
Duration of descent	22 min.
Duration of landing	8.8 min.

10.4 Simulation of Aerosonde (MK47) using MACS

Table 43. Features of Aerosonde flight simulation using MACS

Origin	KBNA
Destination	KATL
Flight time	177.8 min.
Flight distance	180.8 nmi.
Cruise speed	49 KTAS
Cruise altitude	8000 ft.
Takeoff weight	Not available
Landing weight	Not available
Duration of climb	49 min.

Duration of cruise	Did not reach Cruise
Duration of descent	103.9 min.
Duration of landing	24.9 min.

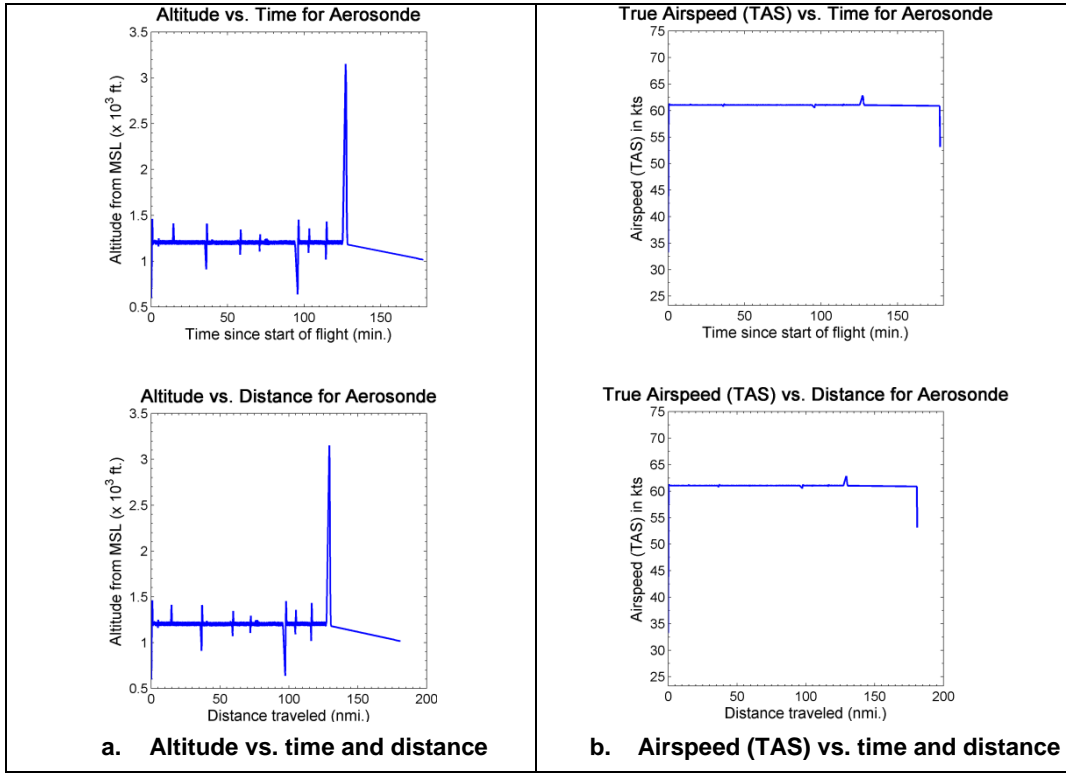


Figure 63. Variation in altitude and airspeed (TAS) with time and distance for Aerosonde flight simulation using MACS

10.5 Simulation of Predator A (MQ1B) using MACS

Important features of Predator A's flight simulation using MACS are shown in Table 44. It should be noted that, unlike Shadow B and Global Hawk, the flight did not reach cruise altitude and speed. The slow speed of Predator A is a possible reason. However, as mentioned earlier, it is not known as to why MACS cannot simulate a slow flying aircraft. Consequently, simulation results similar to Figure 61 were not compiled for Predator A. Other simulation results are shown in Figure 64. Similar to Shadow B and Global Hawk, the reason for the sharp fluctuations in speed (Figure 64b) is not known. The flight was simulated from KBNA to KATL to prevent MACS from exceeding its memory usage limits and thereby successfully complete the simulation due to the slow speed of Predator A.

Table 44. Features of Predator A flight simulation using MACS

Origin	KBNA
Destination	KATL
Flight time	100.8 min.
Flight distance	185.1 nmi.
Cruise speed	117 KTAS
Cruise altitude	16000 ft.
Takeoff weight	Not available
Landing weight	Not available
Duration of climb	69.4 min.

Duration of cruise	Did not reach Cruise
Duration of descent	80.7 min.
Duration of landing	17.9 min.

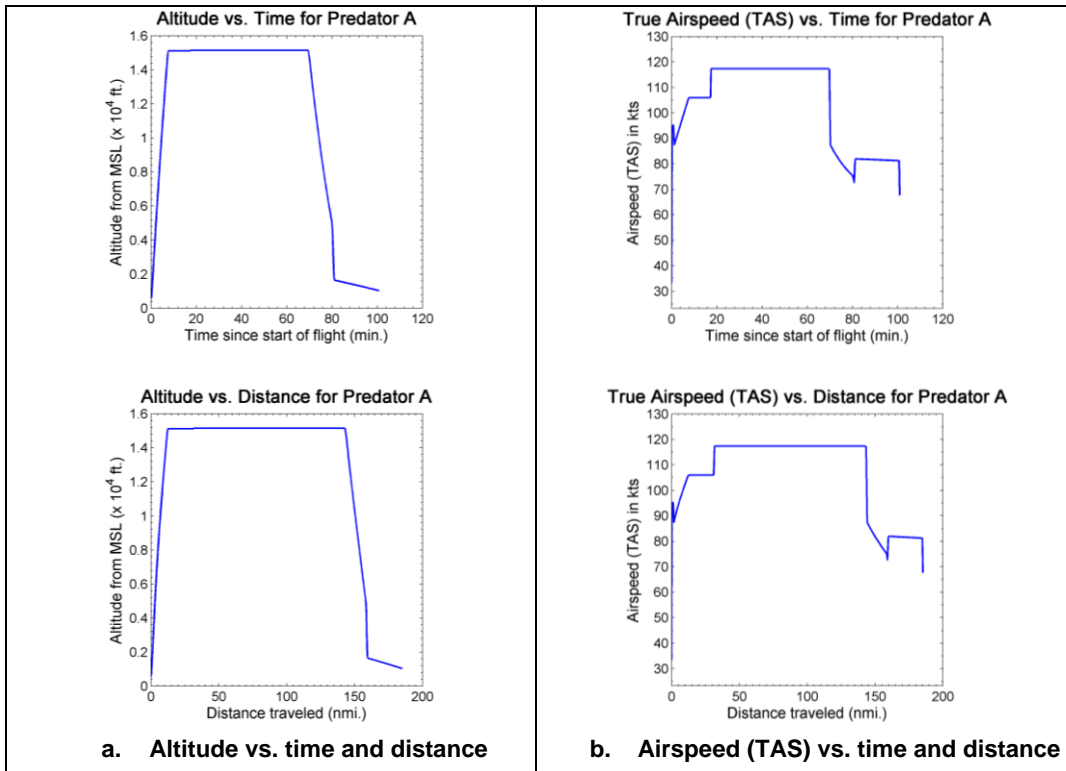


Figure 64. Variation in altitude and airspeed (TAS) with time and distance for Predator A flight simulation using MACS

10.6 Simulation of Predator B (MQ-9) using MACS

Important features of Predator B's flight simulation using MACS are shown in Table 45. It should be noted that, unlike Shadow B and Global Hawk, the flight did not reach cruise altitude and speed. While Predator B flies faster than Predator A, it is slower compared to Global Hawk, and this is a possible reason for the unsuccessful simulation. The flight was simulated from KBNA to KATL to prevent MACS from exceeding its memory usage limits and thereby successfully complete the simulation due to the slow speed of Predator B (relative to Global Hawk). However, as mentioned earlier, it is not known as to why MACS cannot simulate a slow flying aircraft. Consequently, simulation results similar to Figure 61 were not compiled for Predator B. Other simulation results are shown in Figure 65. Similar to Shadow B and Global Hawk, the reason for the sharp fluctuations in speed (Figure 65b) is not known.

Table 45. Features of Predator B flight simulation using MACS

Origin	KBNA
Destination	KATL
Flight time	87.7 min.
Flight distance	181.5 nmi.
Cruise speed	209 KTAS
Cruise altitude	31000 ft.
Takeoff weight	Not available
Landing weight	Not available
Duration of climb	31.12 min.

Duration of cruise	Did not reach Cruise
Duration of descent	20.85 min.
Duration of landing	15.08 min.

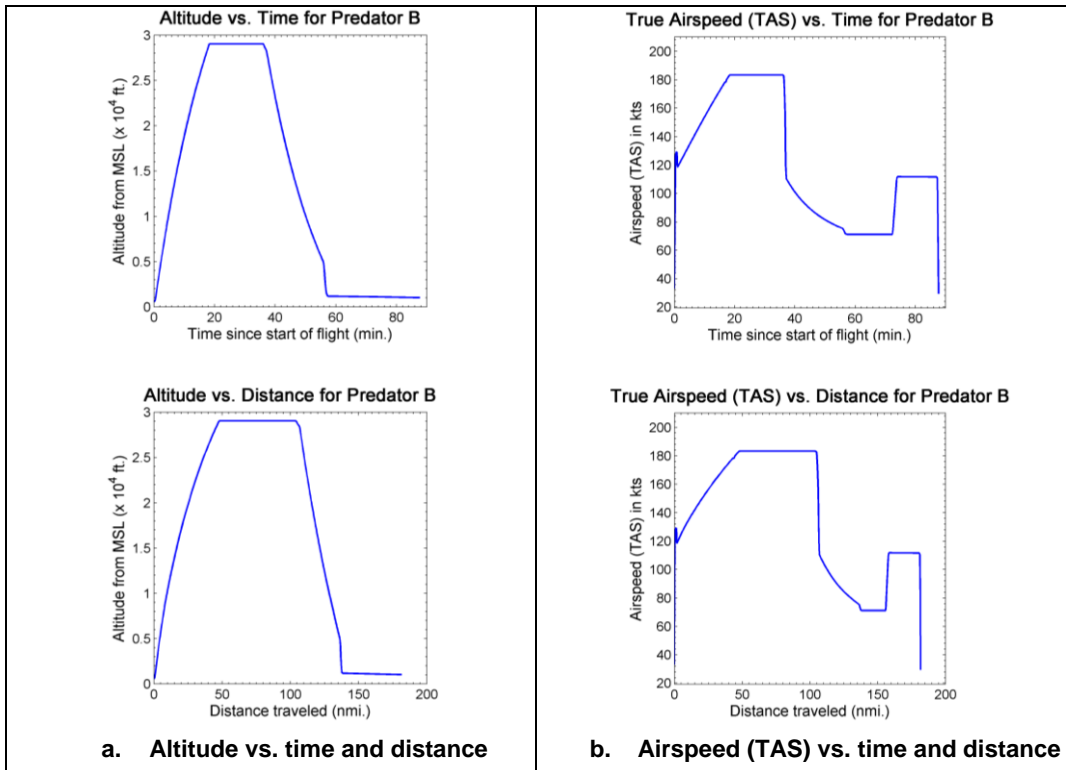


Figure 65. Variation in altitude and airspeed (TAS) with time and distance for Predator B flight simulation using MACS

10.7 Simulation of Gray Eagle (MQ1C) using MACS

Important features of Gray Eagle's flight simulation using MACS are shown in Table 46. It should be noted that, similar to Predator B, the flight did not reach cruise altitude and speed, possibly due to its slow speed compared to Global Hawk. The flight was simulated from KBNA to KATL to prevent MACS from exceeding its memory usage limits and thereby successfully complete the simulation due to the slow speed of Gray Eagle (relative to Global Hawk). However, as mentioned earlier, it is not known as to why MACS cannot simulate a slow flying aircraft. Consequently, simulation results similar to Figure 61 were not compiled for Gray Eagle. Other simulation results are shown in Figure 66. Similar to Shadow B and Global Hawk, the reason for the sharp fluctuations in speed (Figure 66b) is not known.

Table 46. Features of Predator A flight simulation using MACS

Origin	KBNA
Destination	KATL
Flight time	97.84 min.
Flight distance	181.9 nmi.
Cruise speed	203 KTAS
Cruise altitude	32000 ft.
Takeoff weight	Not available
Landing weight	Not available
Duration of climb	23.47 min.
Duration of cruise	Did not reach Cruise

Duration of descent	59 min.
Duration of landing	14.95 min.

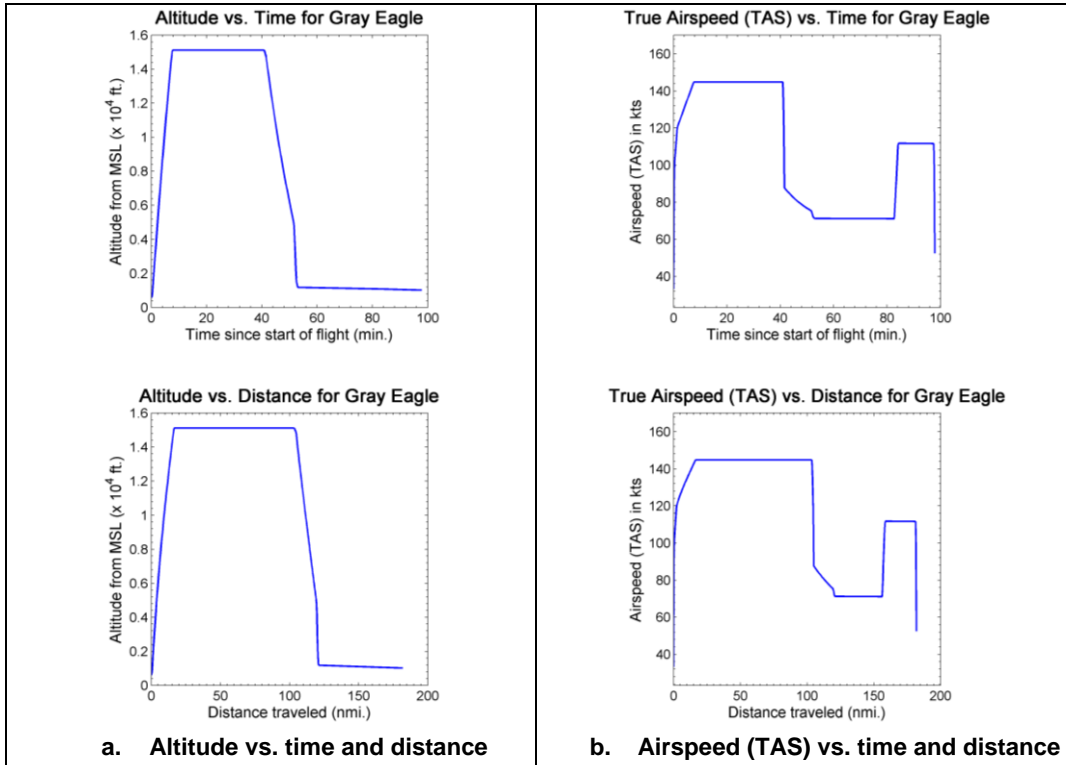


Figure 66. Variation in altitude and airspeed (TAS) with time and distance for Gray Eagle flight simulation using MACS

10.8 Simulation of Predator C (AVEN) using MACS

Important features of Predator C's flight simulation using MACS are shown in Table 47. It should be noted that, similar to Predator B, the flight did not reach cruise altitude and speed, possibly due to its slow speed compared to Global Hawk. The flight was simulated from KBNA to KATL to prevent MACS from exceeding its memory usage limits and thereby successfully complete the simulation due to the slow speed of Predator C (relative to Global Hawk). However, as mentioned earlier, it is not known as to why MACS cannot simulate a slow flying aircraft. Consequently, simulation results similar to Figure 61 were not compiled for Gray Eagle. Other simulation results are shown in Figure 67. Similar to Shadow B and Global Hawk, the reason for the sharp fluctuations in speed (Figure 67b) is not known.

Table 47. Features of Predator C flight simulation using MACS

Origin	KBNA
Destination	KATL
Flight time	75.8 min.
Flight distance	182.1 nmi.
Cruise speed	331 KTAS
Cruise altitude	40000 ft.
Takeoff weight	Not available
Landing weight	Not available
Duration of climb	33.1 min.
Duration of cruise	Did not reach Cruise
Duration of descent	29.7 min.
Duration of landing	12.6 min.

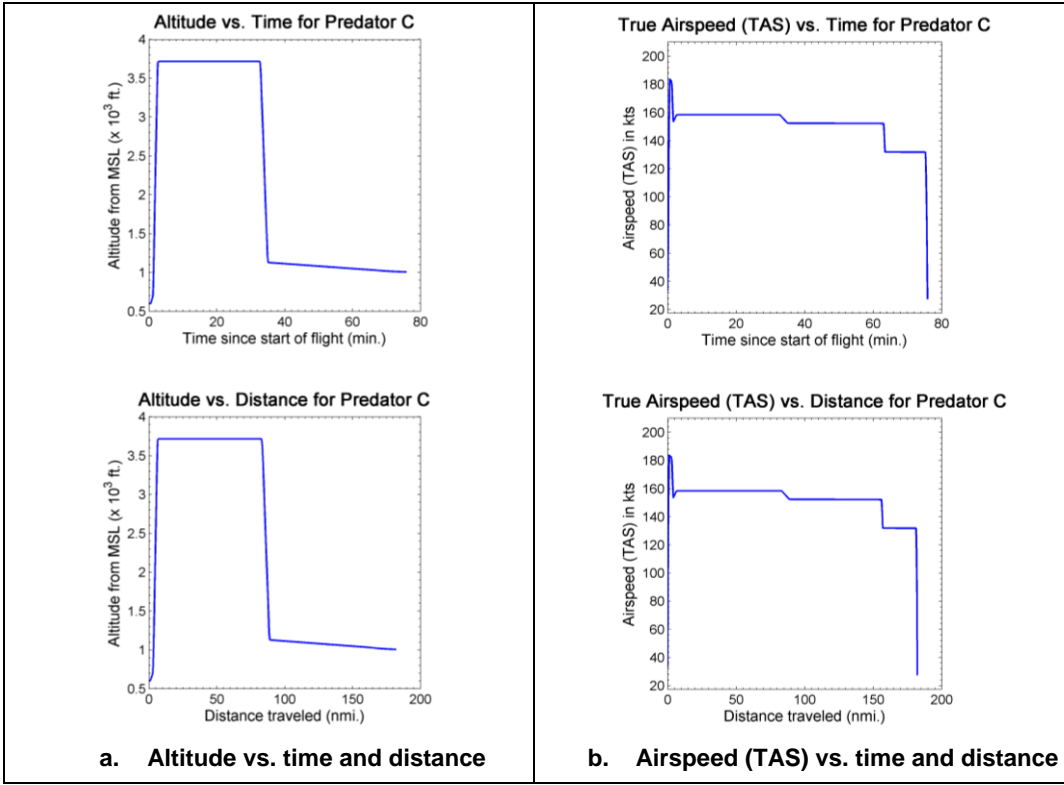


Figure 67. Variation in altitude and airspeed (TAS) with time and distance for Predator C flight simulation using MACS

10.9 Simulation of Hunter (MQ5B) using MACS

Important features of Hunter's flight simulation using MACS are shown in Table 48. It should be noted that, similar to Predator A, the flight did not reach cruise altitude and speed, possibly due to its slow speed compared to Global Hawk. The flight was simulated from KBNA to KATL to prevent MACS from exceeding its memory usage limits and thereby successfully complete the simulation due to the slow speed of Hunter (relative to Global Hawk). However, as mentioned earlier, it is not known as to why MACS cannot simulate a slow flying aircraft. Consequently, simulation results similar to Figure 61 were not compiled for Hunter. Other simulation results are shown in Figure 68. Similar to Shadow B and Global Hawk, the reason for the sharp fluctuations in speed (Figure 68b) is not known.

Table 48. Features of Hunter flight simulation using MACS

Origin	KBNA
Destination	KATL
Flight time	123.9 min.
Flight distance	191 nmi.
Cruise speed	119 KTAS
Cruise altitude	18000 ft.
Takeoff weight	Not available
Landing weight	Not available
Duration of climb	81.2 min.
Duration of cruise	Did not reach Cruise
Duration of descent	17.4 min.
Duration of landing	24.82 min.

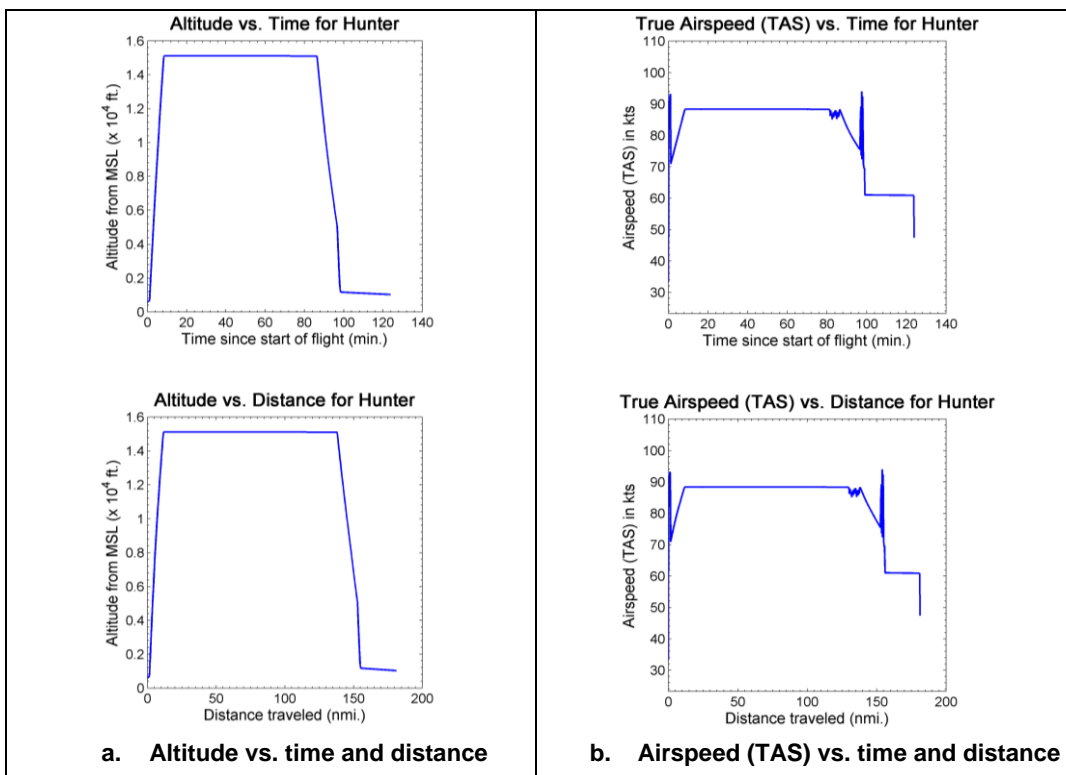


Figure 68. Variation in altitude and airspeed (TAS) with time and distance for Hunter flight simulation using MACS

10.10 Simulation of BADA Files for Orbiter (ORBM), Cargo UAS (CUAS), Fire Scout (MQ8B) and NEO S-300 Mk II VTOL (S350) using MACS

As mentioned earlier, the MACS files for Orbiter (ORBM), Cargo UAS (CUAS), Fire Scout (MQ8B) and NEO S-300 Mk II VTOL (S350) did not truthfully represent the aircraft because: 1) Orbiter is an electric aircraft and cannot be correctly represented within the schema of MACS, and 2) the other three aircraft are either rotorcraft or a hybrid of rotorcraft and conventional aircraft, which cannot be represented in MACS. Therefore, these aircraft were not simulated in MACS and the results from simulating and validating their MACS files are not presented here.

10.11 Summary of UAS Simulations in MACS

Results of UAS flight simulations using KTG are summarized in Table 49. Included in here are four main features of each flight to briefly distinguish the different aircraft: origin and destination airports, target cruise altitude, and cruise speed reached. Also indicated is the cruise altitude reached by the aircraft in simulation. As mentioned earlier, MACS simulation results for each UAS flight were compared to the corresponding results from KTG for validation, the premise being that the KTG results were validated by the UAS manufacturer. It should be noted that electric aircraft and rotorcraft cannot be simulated in MACS. Hence, the MCAS BADA files of Orbiter (electric aircraft), Cargo UAS, Fire Scout and NEO S-300 Mk II VTOL were not validated by this approach. The FAA's William J. Hughes Technical Center (FAA Tech Center) was contacted for assistance in validating MACS files for these aircraft. However, the process could not be completed during the current project's contract period. However, the issues and difficulties identified in developing these MACS files are discussed in the latter sections of this report, along with recommendations for validating the files.

Table 49. Summary of nine UAS flight simulations in MACS. Only origin, destination, cruise altitude and cruise speed are included here.

UAS	Origin	Destination	Target Cruise Altitude (ft.)	Target Cruise Speed (KTAS)	Target Cruise Altitude & Speed Reached?	Similar to KTG?
Shadow B (RQ7B)	KBNA	KATL	8000	80	Yes*	No
Global Hawk (RQ4A)	KMSP	KMCO	31000	343	No	No
Aerosonde (MK47)	KBNA	KATL	8000	49	No	No
Predator A (MQ1B)	KBNA	KATL	16000	119	No	No
Predator B (MQ-9)	KBNA	KATL	31000	209	No	No
Gray Eagle (MQ1C)	KBNA	KATL	32000	203	No	No
Predator C (AVEN)	KBNA	KATL	40000	331	No	No
Hunter (MQ5B)	KBNA	KATL	18000	119	No	No
Orbiter (ORBM)					Electric aircraft and rotorcraft cannot be simulated in MACS	
Cargo UAS (CUAS)						
Fire Scout (MQ8B)						
NEO S-300 Mk II VTOL (S350)						

*Many unexplained behaviors observed in simulation, requiring more in-depth analysis of MACS source code that is beyond the scope of this project. Hence, files were not validated.

11 ACES Simulations for CNS Capabilities

As user selectable options in ACES, several Communication system, Navigation system and Surveillance system models are available for use in airspace simulations for experimentation to determine the implications of these real world systems on aircraft operations and airspace concepts. For UAS aircraft, many of these same systems are integrated (or are being considered for integration and use) onboard these unmanned aircraft in varied capacity by the UAS community and are, or may become, integral components of the UAS systems as the future of UAS architectures to enable their use in the NAS progresses. For the UAS in the NAS, Modeling and Simulation effort, twelve UAS aircraft models have been introduced into ACES and have been tested for the ability to configure their systems to use the ACES CNS models.

This summary report describes the process for adding these UAS into the latest version of ACES with CNS models, and outlines the steps taken to configure ACES to fly these aircraft with the CNS models. Results of the simulations performed are provided in summary table and comments on the p, improvement.

11.1 UAS Aircraft/BADA Data Installation and Preparation for CNS Simulations

11.1.1 Installation of UAS Aircraft Models into ACES and KTG

Prior to testing the UAS aircraft with ACES CNS models, databases in ACES and KTG were configured for nine UAS aircraft. This configuration process is explained in detail in Appendix B.

11.1.2 Develop Flight Data Sets

Since this was a first-use experience with the UAS aircraft, new Flight Data Sets (FDSs) were defined that were both appropriate to the UAS aircraft characteristics, and also were adequate to exercise the capabilities of the CNS models, especially for communications. The process for defining the FDSs for the simulations used the following information and guidelines:

- Speed and cruise altitudes were identified for use in the FDSs from the aircraft .PTF BADA files.
- Flight route distances were selected (with some experimentation) based on UAS size, weight and aircraft speed characteristics.
- FDS Flight routes were derived from existing FDSs. The routes used were variations on routes used to represent UAS operations for Homeland Security applications within ZAU Sector in previous UAS work, and were tailored for route length appropriate to the class of UAS that would use the FDS.
- The FDSs that were created flew UAS flights for gate-to-gate operations between Towered airports to allow for full execution of all communication messages that are part of our communications message sets. (see Note 1)
- Airline names used on the FDSs were created to be appropriate to the UAS vendor to help identify the type of UAS flown in a simulation. Aircraft names that were used mapped directly to the designators for the UASs that had been defined in the BADA and ACES database files (i.e. RQ4A, RQ7B, etc...)
- FDSs were defined for a single UAS flight each.

Note 1: The current architecture defined in ACES has yet to be tailored for UAS operations. Use of UAS flights gate-to-gate is strictly the default scenario for any aircraft, and is planned to be modified for UAS operations.

Note 2: Information regarding origin/destination airports, route distances, altitude and speed defined in these FDSs is indicated in the simulation summary chart - Table 50. Summary of results for from ACES simulations to test CNS capabilities of UAS aircraft

Testing: Each FDS was tested in independent simulations to verify its applicability prior to applying the CNS equipage. In several instances, initial FDSs were discovered to be defective for the purpose of this testing, because the airports/flight routes that were chosen were all located within the same TRACON where the KTG would alter the flight path to a route that would not allow for the flight duration and airspace transitions that were desired to enable applicability of the full communications message set application for CNS capability modeling. Once this situation was understood, two of the initial FDSs were rebuilt to use separated airports.

11.1.3 Develop CNS Plugin Configuration Files

The CNS Plugin in ACES allows the user to define the systems that comprise the compliment CNS avionics that are operational in a simulation. The implementation for use of these systems is managed by defining aircraft CNS equipage configuration files for whichever Communication (Comm.), Navigation (Nav.) or Surveillance (Surv.) system the user wishes to have functioning onboard an aircraft during an ACES system. Next, ACES collects and stores those data for analysis and evaluation in an output database.

To date, six CNS models are available:

- Surveillance System Models: Secondary Surveillance Radar (SSR) and Automatic Dependent Surveillance Broadcast (ADS-B)
- Communication System Models: Voice over VHF and Controller Pilot Datalink Communication (CPDLC) over VDL2
- Navigation System Models: VHF Omnidirectional Radar/Distance Measuring Equipment (VOR/DME) and Global Positioning System (GPS)

Equipage files were created for each UAS aircraft to enable the flights to use each of the Comm., Nav. and Surv. models as onboard and integrated systems. The exceptions to this were: 1) since VOR/DME navigation system will most likely never be used for UAS (currently GPS is the standard due to its technology advantages) no equipage files were created, and therefore, no flights were simulated using VOR/DME model, and 2) it was decided that for the two smallest UAS aircraft (Orbiter and Aerosonde) the equipment size for use of VHF Radios would be restrictive to ever expect them to be operated onboard those aircraft, and therefore no equipage files were generated (nor flights flown) for these UAS with Voice VHF.

11.2 Simulations: Tabulated Results

Forty three simulations were conducted using each of the different Comm., Nav. and Surv. models (mentioned earlier) configured as onboard systems. The results of the simulations are shown in Table 51. Included are data in the FDSs for the simulations such as aircraft names, the cruise speed and altitude, the distance of the flight route, and the origin and destination airports. Also identified are the results of the simulation and a comment column that briefly defines the information that was checked in the output data to verify successful operation of the tested CNS model.

Table 51. Summary of results for from ACES simulations to test CNS capabilities of UAS aircraft

Sim. Type: Comm., Nav., or Surv.	UAS Aircraft (Code)	UAS in Equipage File	Origin	Destination	Flight Distance (miles)	Cruise Altitude (ft.)	Cruise Speed (KTAS)	C, N & S Equipage	Sim. Result	Results Comment
<hr/>										
Surv.	ORBM	ORBM	KATW	KMKE	365	8000	39	SSR	Success	SSR Data in output database
Surv.	MK47	MK47	KATW	KMKE	365	8000	60	SSR	Success	SSR Data in output database
Surv.	MQ5B	MQ5B	KMSN	KGRR	775	18000	120	SSR	Success	SSR Data in output database
Surv.	RQ7B	RQ7B	KMSN	KGRR	775	15000	100	SSR	Success	SSR Data in output database
Surv.	MQ1B	MQ1B	KMSN	KGRR	775	15000	100	SSR	Success	SSR Data in output database
Surv.	MQ1C	MQ1C	KMSN	KGRR	775	15000	100	SSR	Success	SSR Data in output database
Surv.	MQ-9	MQ-9	KCMI	KMLI	989	20000	172	SSR	Success	SSR Data in output database
Surv.	AVEN	AVEN	KCMI	KMLI	989	31000	273	SSR	Success	SSR Data in output database
Surv.	RQ4A	RQ4A	KCMI	KMLI	989	28000	323	SSR	Success	SSR Data in output database
Surv.	ORBM	ORBM	KATW	KMKE	365	8000	39	ADSB	Success	ADSB Data in output database
Surv.	MK47	MK47	KATW	KMKE	365	8000	60	ADSB	Success	ADSB Data in output database
Surv.	MQ5B	MQ5B	KMSN	KGRR	775	18000	120	ADSB	Success	ADSB Data in output database
Surv.	RQ7B	RQ7B	KMSN	KGRR	775	15000	100	ADSB	Success	ADSB Data in output database
Surv.	MQ1B	MQ1B	KMSN	KGRR	775	15000	100	ADSB	Success	ADSB Data in output database
Surv.	MQ1C	MQ1C	KMSN	KGRR	775	15000	100	ADSB	Success	ADSB Data in output database
Surv.	MQ-9	MQ-9	KCMI	KMLI	989	20000	172	ADSB	Success	ADSB Data in output database
Surv.	AVEN	AVEN	KCMI	KMLI	989	31000	273	ADSB	Success	ADSB Data in output database
Surv.	RQ4A	RQ4A	KCMI	KMLI	989	28000	323	ADSB	Success	ADSB Data in output database
<hr/>										
Nav.	ORBM	ORBM	KATW	KMKE	365	8000	39	GPS	Success*	No GPS Data in output database
Nav.	MK47	MK47	KATW	KMKE	365	8000	60	GPS	Success*	No GPS Data in output database
Nav.	MQ5B	MQ5B	KMSN	KGRR	775	18000	120	GPS	Success*	No GPS Data in output database
Nav.	RQ7B	RQ7B	KMSN	KGRR	775	15000	100	GPS	Success*	No GPS Data in output database
Nav.	MQ1B	MQ1B	KMSN	KGRR	775	15000	100	GPS	Success*	No GPS Data in output database

Nav.	MQ1C	MQ1C	KMSN	KGRR	775	15000	100	GPS	Success*	No GPS Data in output database
Nav.	MQ-9	MQ-9	KCMI	KMLI	989	20000	172	GPS	Success*	No GPS Data in output database
Nav.	AVEN	AVEN	KCMI	KMLI	989	31000	273	GPS	Success*	No GPS Data in output database
Nav.	RQ4A	RQ4A	KCMI	KMLI	989	28000	323	GPS	Success*	No GPS Data in output database
<hr/>										
Comm.	UAVMQ5B	UAVMQ5B	KMSN	KGRR	775	18000	120	VoiceVHF	Success	G-A Msg VHF / A-G Msg VHF
Comm.	UAVRQ7B	UAVRQ7B	KMSN	KGRR	775	15000	100	VoiceVHF	Success	G-A Msg VHF / A-G Msg VHF
Comm.	UAVMQ1B	UAVMQ1B	KMSN	KGRR	775	15000	100	VoiceVHF	Success	G-A Msg VHF / A-G Msg VHF
Comm.	UAVMQ1C	UAVMQ1C	KMSN	KGRR	775	15000	100	VoiceVHF	Success	G-A Msg VHF / A-G Msg VHF
Comm.	UAVMQ-9	UAVMQ-9	KCMI	KMLI	989	20000	172	VoiceVHF	Success	G-A Msg VHF / A-G Msg VHF
Comm.	UAVAVEN	UAVAVEN	KCMI	KMLI	989	31000	273	VoiceVHF	Success	G-A Msg VHF / A-G Msg VHF
Comm.	UAVRQ4A	UAVRQ4A	KCMI	KMLI	989	28000	323	VoiceVHF	Success	G-A Msg VHF / A-G Msg VHF
Comm.	ORBM	ORBM	KATW	KMKE	365	8000	39	VDL2	Success	G-A Msg VDL2 / A-G Msg VDL2
Comm.	UAVMK47	UAVMK47	KATW	KMKE	365	8000	60	VDL2	Success	G-A Msg VDL2 / A-G Msg VDL2
Comm.	UAVMQ5B	UAVMQ5B	KMSN	KGRR	775	18000	120	VDL2	Success	G-A Msg VDL2 / A-G Msg VDL2
Comm.	UAVRQ7B	UAVRQ7B	KMSN	KGRR	775	15000	100	VDL2	Success	G-A Msg VDL2 / A-G Msg VDL2
Comm.	UAVMQ1B	UAVMQ1B	KMSN	KGRR	775	15000	100	VDL2	Success	G-A Msg VDL2 / A-G Msg VDL2
Comm.	UAVMQ1C	UAVMQ1C	KMSN	KGRR	775	15000	100	VDL2	Success	G-A Msg VDL2 / A-G Msg VDL2
Comm.	UAVMQ-9	UAVMQ-9	KCMI	KMLI	989	20000	172	VDL2	Success	G-A Msg VDL2 / A-G Msg VDL2
Comm.	UAVAVEN	UAVAVEN	KCMI	KMLI	989	31000	273	VDL2	Success	G-A Msg VDL2 / A-G Msg VDL2
Comm.	UAVRQ4A	UAVRQ4A	KCMI	KMLI	989	28000	323	VDL2	Success	G-A Msg VDL2 / A-G Msg VDL2
<hr/>										
* Simulation was successful for UASs equipped with GPS Navigation Model. Problem with KTG integration for navigation prevented model from being applied during the flight.										

11.3 Test Results

Results from the simulations were very positive, with all of the Comm. and Surv. model simulations completing as expected and generating correct output data.

The exception to this was for the use of the Nav. GPS system models, where the simulations would run and indicate a successful completion, but no navigation data was stored, indicating that the Nav. GPS model had not been applied for the flight. Investigating this further it was found that this was also the case for the VOR/DME Nav. model and for simulations that used a standard aircraft with the same results indicating that it had nothing to do with the UAS model. On final investigation, a simulation with the same standard aircraft was run using the MPAST trajectory generator, and the Nav. GPS model performed as expected.

The problem has been identified to Intelligent Automation and a fix to correct the KTG interoperability with the Navigation models has been defined but was not able to be implemented for the completion of this testing.

11.4 Problems Encountered and Precautions for use of CNS models with UAS

- Comm. model simulations: FDSs that define flights departing from and arriving at airports located within the same TRACON airspace appear to have their flight path altered to what appears to be a shorter route. This needs to be investigated further to determine just what does happen to the flight path, but this would be problematic for UAS simulations especially for smaller UAS where flight routes are typically of shorter duration and distance.
- Comm., Nav. or Surv. model simulations: There was one instance where in an airline name was used that did not correlate with an AOC that ACES uses in its AOC XRef file. In this case, communications was set up to use VDL2, however the simulation ran with the Comm. model defaulting to Voice VHF. This is a known problem with the ACES models use, but the remedy to this problem is simply that the user makes sure that all airlines defined in the FDS are common airline names that have an associated AOC. For our further UAS CNS modeling work, we are considering implementing an UAS AOC, where we would use and add as needed, UAS manufacturer airline designators and associate them to this AOC to ensure proper equipage of UAS aircraft, especially for larger simulations.

12 Conclusions

The purpose of this project was to provide performance data for twelve UAS aircraft, in formats usable by standard aviation models: BADA and MACS. BADA files for fixed-wing UAS aircraft were developed by modifying a NASA-developed aircraft sizing software called FLOPS. Separate aircraft models were developed to size rotorcraft, hybrid aircraft and electric aircraft. However, the fidelity of the output from these models is limited by the fact that the aircraft data from the UAS manufacturers were not complete and accurate due to proprietary restrictions.

Simulations were conducted using KTG for the BADA files, and the MACS software for MACS files. Simulation output from KTG were examined and validated by the UAS manufacturers. However, simulations were not conducted for two rotorcraft and one hybrid aircraft, due to limitations on KTG. Hence, their BADA files were not validated. Similarly, these

aircraft cannot be simulated in MACS, and hence, their MACS files were not validated. Furthermore, a number of difficulties and challenges were encountered in simulating the other UAS aircraft in MACS, either due to the lack of format support to represent UAS aircraft data as MACS files or due to limitations on MACS software. Therefore, MACS files of all twelve aircraft were not validated. Recommendations were made to resolve these issues to successfully represent all twelve UAS aircraft in BADA and MACS format. The FAA Tech Center was approached to assist in validating the BADA and MACS files for rotorcraft and hybrid aircraft. However, the effort needed was beyond the scope and timeline of this project and is included as one of the recommendations to extend the scope and benefits of this project.

The project also involved simulations to simulate the communication, navigation and surveillance (CNS) capabilities of UAS aircraft. CNS equipage files provided by the UAS manufacturers were used to configure and conduct the simulations in the Airspace Concept Evaluation System (ACES). KTG was the trajectory generator employed in these simulations. The communication and surveillance simulations were successful, whereas the navigation simulations require some modifications to ACES and KTG.

This project was focused on producing and validating only BADA and MACS data files for UAS aircraft. However, it is speculated that the challenges encountered in this process and the recommendations to be discussed in the following sections are applicable to almost all other data formats. Therefore, efforts to address these issues will be beneficial to the entire aviation community.

13 Recommendations for Future Work

13.1 Recommendations to Modify BADA Format for UAS Simulations

As described earlier, the EUROCONTROL developed the format of BADA files primarily for manned-aircraft. Consequently, many areas and topics were identified that either require modification or new definitions to accommodate UAS aircraft design and operations (Section 4). This section presents some of the important areas in BADA format to be modified for successful simulation of UAS aircraft.

Design-based modifications

Since the current BADA format does not have specific provisions, UAS aircraft have to be represented using the templates of existing manned-aircraft. However, this restricts the number of UAS aircraft that can be represented in the BADA format. In particular, there are no provisions to represent very light aircraft (e.g., Shadow B and Aerosonde), rotorcraft and hybrid aircraft (e.g., Cargo UAS and Hunter), and electric engines (e.g., Orbiter). Furthermore, there are no airline operations for UAS aircraft to compile the .APF BADA file. Since a wide variety of UAS aircraft are being currently developed and operated, the need to update BADA format is not only critical to conducting large-scale simulations of NAS, but also time-sensitive if the FAA has to meet the Congressional mandate of creating necessary framework to operate UAS aircraft in the NAS [12].

Operations-based changes

Current BADA format imposes certain restrictions on aircraft operations (e.g., stall speed criteria). These restrictions were formulated based on passenger safety and comfort for manned-aircraft. However, UAS aircraft operate outside the envelope of passenger flights, and hence, should not be subjected to these restrictions. Furthermore, there are no provisions to faithfully represent the flight profiles of UAS rotorcraft and hybrid UAS aircraft in BADA. During

discussions with the FAA Tech Center, their experts have voiced similar concerns regarding the current format of BADA in modeling rotorcraft and hybrid aircraft, and expressed interest in future efforts to update the format [13].

13.2 Recommendations to Modify MACS for UAS Simulations

The challenges and difficulties were encountered in developing MACS files were described in Section 5. Though these initially appear to be different from those encountered for BADA, there are many commonalties between them. For example, 1) both MACS and BADA were not able to represent and simulate rotorcraft and hybrid aircraft, and 2) data and operational rules for existing manned-aircraft were used to model fixed-wing UAS aircraft, leading to similar discrepancies between simulation output and expected aircraft performance. This section presents some of the important areas in MACS to be modified for successful simulation of UAS aircraft.

Aircraft Data

For majority of the twelve UAS aircraft studied in this project, detailed airframe drag data was not available due to the propriety nature of the information. Consequently, data from similarly sized manned-aircraft were substituted for or mapped to UAS aircraft, resulting in many discrepancies between simulation output and expected aircraft performance. Furthermore, electric aircraft, rotorcraft and hybrid aircraft cannot be represented and simulated in MACS (e.g., Orbiter, Cargo UAS, Fire Scout and NEO S-300 Mk II VTOL). The FAA Tech Center was approached to assist in the validation of MACS files for the rotorcraft, but this was beyond the scope and timeline of this project.

Modifications to MACS Software

MACS software was found to be consuming large computer memory to simulate slow flying UAS aircraft such as Shadow B. Furthermore, modifications were made to force the software into simulating the cruise segments of flight, which were not successful. Some of these issues might have been resolved by NASA experts but they were not readily available during the period of this project.

13.3 Validation of BADA and MACS Files for Rotorcraft and Hybrid Aircraft

As mentioned earlier, KTG was used to simulate UAS aircraft based on BADA files, the results from which were validated by the aircraft manufacturers. However, since, KTG cannot simulate rotorcraft and hybrid aircraft, the BADA files for Cargo UAS, Fire Scout and NEO S-300 Mk II VTOL were not validated. Similarly, since MACS cannot simulate these aircraft, the corresponding input files were also not validated. As mentioned earlier, a joint research effort between NASA and the FAA Tech Center to developing rotorcraft models is strongly needed and recommended to leverage the expertise of the two agencies in filling this gap in knowledge.

13.4 Other Recommendations

Kinematic Trajectory Generator (KTG)

KTG has been extensively verified and validated for simulations involving manned aircraft. However, key areas were identified that require modifications to simulate UAS aircraft in KTG.

- Different types of data are used as input to simulation an aircraft in KTG. These involve the four BADA files described earlier and a file defining the aircraft's control parameters (Appendix B). Therefore, the accuracy of simulation results from KTG is dependent on

the accuracy of BADA files and the control parameters file. However, all UAS aircraft simulations presented in this report were conducted using default setting for aircraft control parameters, due to lack of appropriate data. Effort required to compute specific control parameters for each UAS aircraft was beyond the scope of this project, and can be a valuable extension to improve the fidelity of the simulations.

- The present framework of KTG does not support the simulation of rotorcraft and hybrid aircraft due to lack of appropriate BADA and aircraft control parameters files. Modifications to BADA format based on aforementioned recommendations should be able to address this issue.
- Another important element currently not available in KTG is the ability to estimate an aircraft's engine thrust, which is essential to simulating rotorcraft and hybrid aircraft.

Airspace Concept Evaluation System (ACES)

ACES was used to conduct simulations to evaluate the CNS capabilities, requirements and limitations of UAS aircraft operations. However, similar to KTG, ACES is currently best suited to simulate manned-aircraft, requiring changes to ACES' configuration to conduct these simulations (Appendix B). While these changes addressed a number of difficulties in simulating UAS aircraft, many more remain:

- Very small UAS aircraft such as Aerosonde and Orbiter were also simulated using the separation rules for small aircraft category, which may lead to larger separation distances than otherwise necessary. On the other hand, separation criteria for such very small aircraft are non-existent, making this a very important operational issue that needs to be addressed immediately for successful real-world operations of such UAS aircraft.
- UAS aircraft can have a short range (less than 40 nmi.) due to limitations on actual aircraft range (small fuel tank) or the range of its ground control station imposing line-of-sight restrictions. However, current airspace definitions in ACES did not allow the simulation of such aircraft.

Fleet-level Simulations of UAS Aircraft

UAS aircraft were simulated in this project only to validate aircraft data (BADA, MACS and CNS equipage), limiting their scope. However, large-scale simulations involving fleets of UAS aircraft in multiple operational regimes are required to thoroughly understand their impact on current-day and future operations in the NAS. Further, such simulations also provide insights into challenges associated with HITL processes such piloting, controlling and managing the UAS traffic.

14 References

- [1] EUROCONTROL Experimental Centre, "Base of Aircraft Database (BADA) version 3.9," April 2011. [Online]. Available: http://www.eurocontrol.int/eec/gallery/content/public/document/eec/other_document/2011/EC-Technical-Report-110308-08.pdf.
- [2] Airspace Operations Laboratory (AOL), "The Multi Aircraft Control System (MACS)," NASA, [Online]. Available: <http://hspace.arc.nasa.gov/groups/AOL/technologies/macss.php>. [Accessed June 2011].
- [3] Y. Zhang, G. Satapathy, V. Manikonda and N. Nigam, "KTG: A Fast-time Kinematic Trajectory Generator for Modeling and Simulation of ATM Automation Concepts and NAS-wide System Level Analysis," in *AIAA Modeling and Simulation Technologies Conference*,

Toronto, Canada, 2010.

- [4] J. Mercer, T. Prevot, R. Jacoby, A. Globus and J. Homola, "Studying Nextgen Concepts with Multi Aircraft Control System," in *Modeling and Simulation Technologies Conference*, Honolulu, HI, 2008.
- [5] McDonnell Douglas Astronautics Company, "The USAF Stability and Control DATCOM," 1979. [Online]. Available: <http://www.holycows.net/datcom/media/e9d0267197b8160bffff8ab6ffffe415.zip>.
- [6] J. Berndt, "JSBSim Reference Manual," [Online]. Available: <http://jsbsim.sourceforge.net/JSBSimReferenceManual.pdf>. [Accessed 28 August 2012].
- [7] Blender Foundation, "Blender Website," [Online]. Available: <http://www.blender.org/>. [Accessed 28 August 2012].
- [8] "Aeromatic 2 Website," JSBSim, [Online]. Available: <http://jsbsim.sourceforge.net/aeromatic2.html>. [Accessed 28 August 2012].
- [9] FlightGear, "FlightGear Website," [Online]. Available: <http://www.flightgear.org/>. [Accessed 28 August 2012].
- [10] R. W. Prouty, *Helicopter Performance, Stability, and Control*, Boston, MA: PWS Engineering, 1986.
- [11] O. Rand and V. Khromov, "Helicopter Sizing by Statistics," *Journal of the American Helicopter Society*, vol. 49, no. 3, pp. 300-317, 2004.
- [12] U. S. Congress, February 2012. [Online]. Available: <http://www.gpo.gov/fdsys/pkg/CRPT-112hrpt381/pdf/CRPT-112hrpt381.pdf>. [Accessed 15 May 2012].
- [13] Konyak, M., *Private Communication with FAA William J. Hughes Technical Center*, Atlantic City, NJ, August 16, 2012.
- [14] A. Nuic, P. Damir and V. Mouillet, "BADA: An Advanced Aircraft Performance Model for Present and Future ATM Systems," *International Journal of Adaptive Control and Signal Processing*, pp. 850-866, 2010.

15 Appendix A: Industry Data of UAS Aircraft

15.1 Shadow B (RQ7B)

Table 52. Industry data for Shadow B (RQ7B). Provided by AAI.

Operations Performance Files (OPF)	
Design Range	685 nmi.
Design Endurance	9 hr.
Basic Geometry	
	

Wing Aspect Ratio	11.1
Wing span	19.8 ft.
Wing taper	0.7
Fuselage length	63.1 in.
Fuselage fineness	0.181
Tail size	
Tail Volume Coefficient	0.65% (horizontal volume coefficient)
Drag Polars	
Equation or Graph	$C_D = 0.0497 + C_L^2 / (\pi * 0.9 * AR) \rightarrow \text{Wing drag polar}$
Mass	
Max. mass of aircraft (Empty Weight)	333 lb. (Aircraft without fuel. Pop 300 installed)
Max. mass of aircraft (Gross Weight)	467 lb., max. (TGOW)
Max. payload	60 lb.
Flight envelope	
V_{MO} (in CAS or TAS)	136 KCAS
M_{MO} (Mach Max. Operating)	0.197
H_{max}	18000 ft., MSL
Aerodynamics	
S_{wet}	16.3 ft. ² (Fuselage)
	99.3 ft. ² (Total Surface Area)
S_{ref}	35.36 ft. ² (Wing)
$C_{lb,o}$ (Buffet Onset Lift Coeff.)	1.04
Stall speed (Initial Climb)	54 KIAS
Stall speed (Cruise)	54 KIAS
Stall speed (Take Off)	56 KIAS
Stall speed (Landing)	52 KIAS
Stall speed (Approach)	52 KIAS
Engine Thrust	
Max. thrust at Climb	
Max. thrust at Cruise	
Max. thrust at Descent	
Propulsion	
Engine	UEL 741AR74-1102
Brake engine power	38bhp @ 7800rpm
No. of cylinders	1 rotor (tri-tip)

Baseline engine power	38 bhp
Critical turbocharger altitude	N/A
Fuel consumption	BASFC _{min} = 2.2–2.3 L/hr.
	BSFC _{max} = 13.2–13.4 L/hr.
	BSFC _{cruise} = 0.56 lb./hp-hr.
Max. engine crankshaft speed	8000 rpm
Max. propeller shaft speed	8000 rpm
Engine displacement	208 cc/chamber (6188 cc piston engine equivalent)
Engine compression ratio	9.5:1
Engine envelope	X = 15.5 in.
	Y = 16.5 in.
	Z = 16.5 in.
Propeller type	Fixed pitch
Blade angle	22°
Propeller diameter	29 in.
Activity factor	(Proprietary)
Integrated design lift coefficient (for blade)	0.8
Fuel Consumption	
Thrust Specific Fuel Consumption	Do not currently have for this AV. Mostly used for jet aircraft performance
Brake Specific Fuel Consumption	0.54 lb./hp-hr. at 70 KIAS Cruise
Ground Movement	
Landing length	400 ft. (assumes length from touch down point to arresting net)
Takeoff length	AV is launched from ground aircraft
Width of runway	50 ft. (minimum)
Aircraft length	143 in.
Airline Procedures Files (APF)	
Climb Operating Speed	62 KCAS
Cruise Operating Speed	70 KCAS
Descent Operating Speed	65 KCAS

15.2 Global Hawk (RQ4A)

Table 53. Industry data for Global Hawk (RQ4A). Provided by AAI.

Operations Performance Files (OPF)	
Design Range	12000 nmi.
Design Endurance	35 hr.

Basic Geometry	
Wing Aspect Ratio	24.49
Wing Span	116.2 ft.
M.A.C (main span)	61.1 in.
Wing Taper	0.37
Fuselage Length	44.4 ft.
Fuselage Fineness	0.146
Tail Size	Effective horizontal span = 220 in. Effective horizontal area = 12046 in. ² Effective vertical area = 10396 in. ²
Horizontal Tail Volume Coefficient	0.51
Vertical Tail Volume Coefficient	0.019
Drag Polars	
Equation or Graph	$0.02118+0.0132*C_L^2$
Mass	
Max. Mass of AV (Empty Weight)	9200 lb.
Max. Mass of AV (Gross Weight)	26700 lb.
Max. Payload	2000 lb.
Max. Fuel Weight	14500 lb.
Flight Envelope	
Loiter Speed	343 KTAS
V _{MO} (in CAS or TAS)	400 KTAS (estimated)
H _{max}	65000 ft.
Aerodynamics	
S _{wet}	338180 in. ² (estimated)
S _{ref}	79386 in. ²
C _{lb,o} (Buffet Onset Lift Coeff.)	2.7
Stall Speed (Initial Climb)	95 KCAS
Stall Speed (Cruise)	108 KCAS
Stall Speed (Take Off)	83 KCAS
Stall Speed (Landing)	76 KCAS
Stall Speed (Approach)	80 KCAS
Propulsion	
Engine	Rolls-Royce F137-AD-100 dry weight: 1581 lb.

Thrust (take-off, SL STD, uninstalled)	36.9 kN (8295 lb.f)
No. of cylinders	Turbine
Critical Turbocharger Altitude	N/A
Fuel Consumption	$BSFC_{min}$
	$BSFC_{max}$
	$TSFC_{to} = 0.33 \text{ lb./lb.f-hr. (SL, STD, uninstalled)}$
Max. Engine Crankshaft Speed	N/A
Max. propeller shaft speed	N/A
Engine displacement	N/A
Engine compression ratio	N/A
Engine Envelope	X = 43.5 in. (estimated) Y = 115 in. (estimated) Z = 43.5 in. (estimated)
Propeller Type	N/A
Blade Angle	N/A
Propeller diameter	N/A
Activity factor	N/A
Integrated design lift coefficient (for blade)	N/A
Engine Thrust	
Max. Thrust at Cruise	7059 lb.f
Ground Movement	
Landing Length	8,000 ft. (ground roll)
Take Off Length	3,500 ft. (ground roll)
Width of Runway	N/A
Aircraft Length	44.4 ft.
Turn radius	133 ft. (ground)
Airline Procedures Files (APF)	
Cruise Operating Speed	343 KTAS

15.3 Orbiter (ORBM)

Table 54. Industry data for Orbiter. Provided by AAI.

Operations Performance File (OPF)	
Design Range	8.1 nmi. (omni antenna); 16.2 nmi. (small auto-tracking antenna); 43.2 nmi. (auto-tracking antenna)
Design Endurance	180 min.

Basic Geometry	
Wing Aspect Ratio	6 (estimated)
Wing Span	86.6 in.
M.A.C (Wing)	10.79 in.
Wing Taper Ratio	0.5
Fuselage Length	42.0 in. (estimated)
Fuselage Fineness Ratio	0.113
Tail Size (Winglet)	Effective horizontal span = N/A
	Effective horizontal area = N/A
	Effective vertical area = 134 in. ²
Horizontal Tail Volume Coefficient	N/A
Vertical Tail Volume Coefficient	0.027
Ultimate Structural Load Factor	12.5 G (estimated)
Drag Polars	
Equation or Graph	N/A
Mass	
Max. mass of aircraft (Empty Weight)	12.1 lb. (without payload)
Max. mass of aircraft (Gross Weight)	16.5 lb. (GTOW)
Max. payload	2.9 lb.
Max. fuel weight	N/A
Flight Envelope	
Loiter Speed	33 kts (estimated)
V _{MO} (in CAS or TAS)	70 kts
M _{MO} (Mach Max. Operating)	N/A
H _{max}	18000 ft.
Aerodynamics	
S _{wet}	3217 in. ² (estimated)
S _{ref}	1266 in. ² (estimated)

Clb. _o (Buffet Onset Lift Coeff.)	
Stall Speed (Initial Climb)	26 KIAS (estimated)
Stall Speed (Cruise)	26 KIAS (estimated)
Stall Speed (Take Off)	26 KIAS (estimated)
Stall Speed (Landing)	26 KIAS (estimated)
Stall Speed (Approach)	26 KIAS (estimated)
Engine Thrust	
Max. Thrust at Climb vs. Height	20 A 1.5 kgf at 20m/s
Max. Thrust at Cruise	7 A 0.5 kgf at 20m/s
Max. Thrust at Descent	0
Batteries	
Main Battery	Voltage = 25.9 V Capacity = 18 A-hr.
Propulsion	
Engine	N/A
Thrust (take-off, SL STD, uninstalled)	N/A
No. of cylinders	0
Baseline Engine Power	2072 W max at 80 A and 25.9 V (estimated)
Critical Turbocharger Altitude	N/A
Fuel Consumption	Max. efficiency = 84% (estimated)
	Max. efficiency current (>82%) = 15–40 A (estimated)
	Max. loading = 55 A per 30 sec. (estimated)
Maximum Engine Crankshaft Speed	10731 rpm
Engine displacement	N/A
Engine compression ratio	N/A
Engine Envelope	X = 2.2 in.
	Y = 4.84 in.
	Z = 2.2 in.
Propeller Type	Aeronaut Cam 14/10 two blade folding, fixed pitch
Pitch	10 in. (estimated)
Propeller diameter	14 in.
Ground Movement	
Landing Length	Parachute Landing
Take Off Length	Bungee launcher
Width of Runway	N/A
Aircraft Length	39.4 in.

Airline Procedures File (APF)	
Climb Operating Speed	31 kts (estimated)
Cruise Operating Speed	38 kts (estimated)
Descent Operating Speed	52 kts (estimated)

15.4 Aerosonde (MK47)

Table 55. Industry data for Aerosonde. Provided by AAI.

Operations Performance File (OPF)	
Design Range	50 nmi. (RF Line-of-Sight)
Design Endurance	12 hr.
Basic Geometry	
Wing Aspect Ratio	10.7
Wing Span	11.08 ft. 
M.A.C (Wing)	
Wing Taper Ratio	0.45 (Elliptical wing)
Fuselage Length	4.25 ft.
Fuselage Fineness Ratio	0.227
Tail Size (Winglet)	Effective horizontal span = 45.8 in.
	Effective horizontal area = 238 in. ²
	Effective vertical area = 172.4 in. ²
Horizontal Tail Volume Coefficient	0.62
Vertical Tail Volume Coefficient	0.039
Ultimate Structural Load Factor	3.8 (estimated)
Drag Polars	
Equation or Graph	N/A
Mass	
Max. mass of aircraft (Empty Weight)	48.9 lb. (without payload or fuel)
Max. mass of aircraft (Gross Weight)	75 lb.

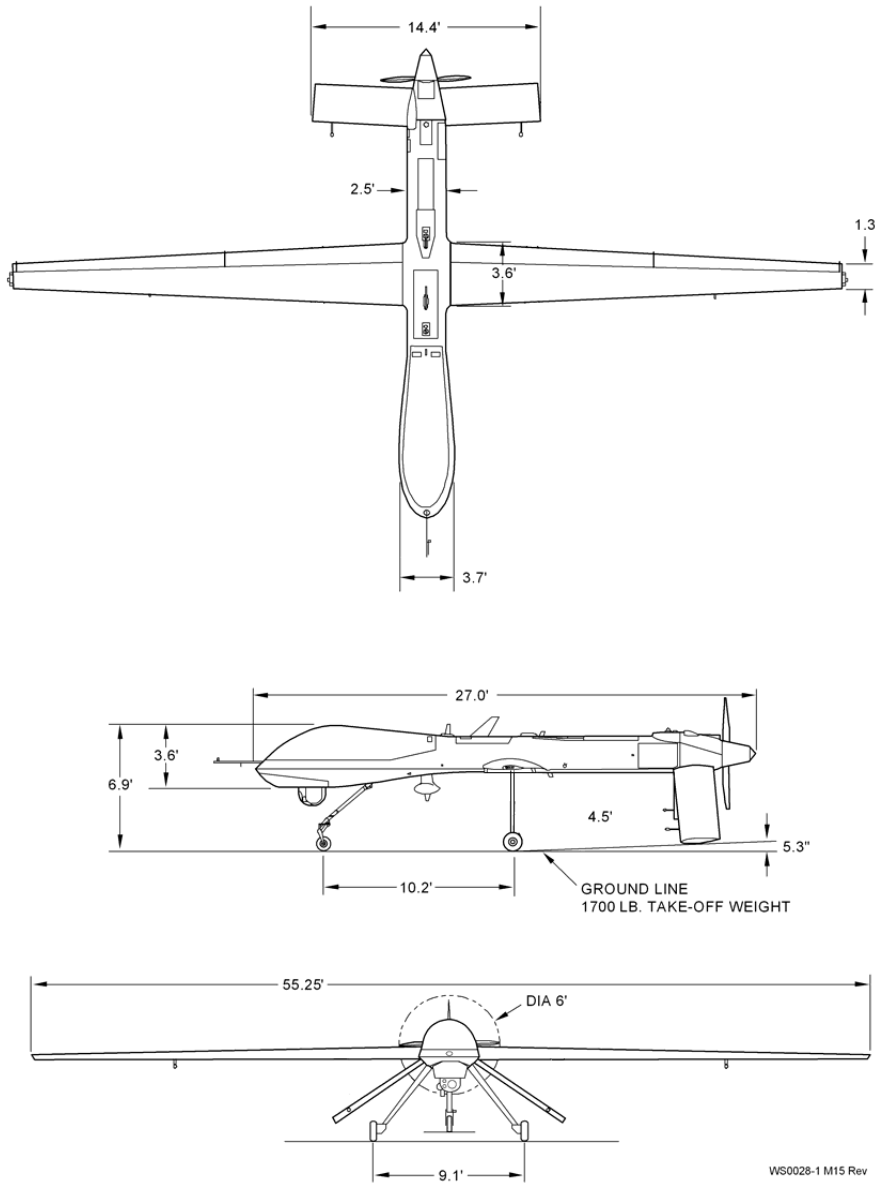
Max. payload	13.3 lb.
Max. fuel weight	
Flight Envelope	
Loiter Speed	45 KIAS
V _{MO} (in CAS or TAS)	65 KTAS
M _{MO} (Mach Max. Operating)	N/A
H _{max}	15423 ft. DA (Service ceiling)
Aerodynamics	
S _{wet} (Total)	5718 in. ²
S _{wet} (Fuselage)	1642 in. ²
S _{ref}	1392 in. ²
Clb. _o (Buffet Onset Lift Coeff.)	1.6
Stall Speed (Initial Climb)	35 KIAS
Stall Speed (Cruise)	35 KIAS
Stall Speed (Take Off)	35 KIAS
Stall Speed (Landing)	35 KIAS
Stall Speed (Approach)	35 KIAS
Engine Thrust	
Max. Thrust at Climb vs. Height	N/A
Max. Thrust at Cruise	4.9 lb. (estimated)
Max. Thrust at Descent	N/A
Propulsion	
Engine	75 HFDI Engine (heavy fuel direct inject JP5/Jp8)
Brake Engine Power	4 hp
No. of cylinders	1
Baseline Engine Power	6 (derated to 4) hp
Critical Turbocharger Altitude	N/A
Fuel Consumption	BSFC _{min} = 0.05247 gal./hr. (estimated)
	BSFC _{max} = 0.8767 lb./hp-hr. (estimated)
	BSFC _{cruise} = 0.5973 lb./hp-hr. (estimated)
Maximum Engine Crankshaft Speed	ECU Limited to 5750 RPM
Maximum Propeller Shaft Speed	ECU Limited to 5750 RPM
Engine displacement	75 cc
Engine compression ratio	8.9:1
Engine Envelope	X = 222 mm
	Y = 336 mm

	Z = 372 mm
Propeller Type	Fixed pitch
Pitch	14 in.
Propeller diameter	24 in.
Activity Factor	N/A
Integrated design lift coefficient (for blade)	N/A
Ground Movement	
Landing Length	Net recovery
Take Off Length	Catapult launch
Width of Runway	323 ft. X 323 ft. ground footprint
Aircraft Length	80 in.
Airline Procedures File (APF)	
Climb Operating Speed	40–50 KIAS
Cruise Operating Speed	40–50 KIAS
Descent Operating Speed	50–55 KIAS

15.5 Predator A (MQ1B)

Table 56. Industry data for Predator A. Provided by General Atomics.

Operations Performance File (OPF)	
Design Range	2115 nmi. (500 lb. of fuel and cruise at 15000 ft.)
Design Endurance	28 hr. (500 lb. of fuel and cruise at 15000 ft.)
Basic Geometry	



Wing Aspect Ratio	
Wing Span	55.25 ft.
M.A.C (Wing)	
Wing Taper Ratio	0.36
Fuselage Length	27.0 ft.
Fuselage Fineness Ratio	
Tail Size (Winglet)	Effective horizontal span = 14.4 ft.
	Effective horizontal area = 31.44 ft. ²
	Effective vertical area = 5.79 ft. ²
Horizontal Tail Volume Coefficient	
Vertical Tail Volume Coefficient	1.04
Ultimate Structural Load	1.5

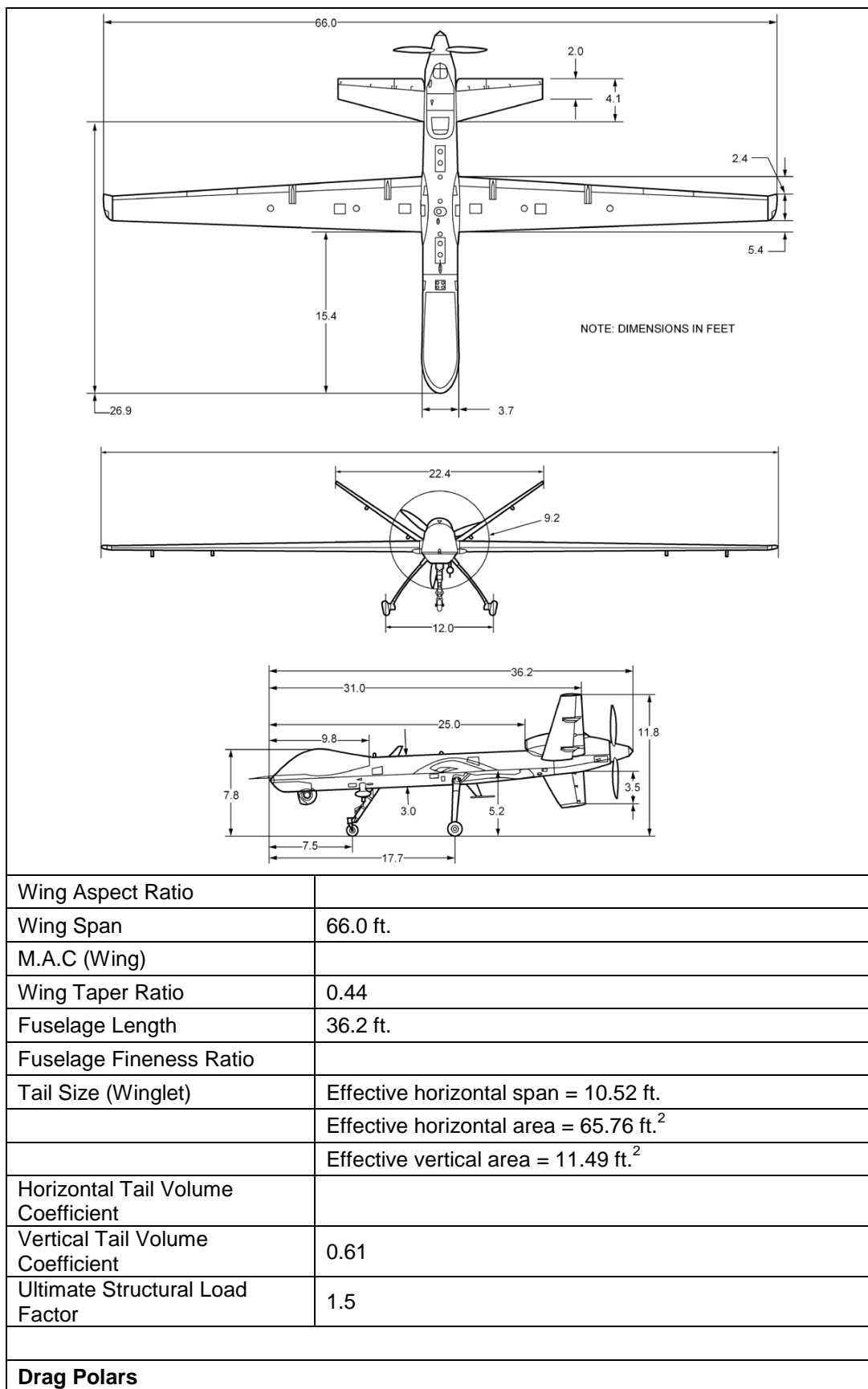
Factor	
Drag Polars	
Equation or Graph	
Mass	
Max. mass of aircraft (Empty Weight)	1665 lb.
Max. mass of aircraft (Gross Weight)	2250 lb.
Max. payload	450 lb.
Max. fuel weight	640 lb.
Flight Envelope	
Loiter Speed	
V _{MO} (in CAS or TAS)	120 KTAS
M _{MO} (Mach Max. Operating)	N/A
H _{max}	25000 ft. at MTOW under ISA conditions
Aerodynamics	
S _{wet} (Total)	272 ft. ²
S _{wet} (Fuselage)	
S _{ref}	132 ft. ²
Clb. _o (Buffet Onset Lift Coeff.)	1.6
Stall Speed (Initial Climb)	55 KIAS (2250 lb.)
Stall Speed (Cruise)	52 KIAS (2000 lb.)
Stall Speed (Take Off)	55 KIAS (2250 lb.)
Stall Speed (Landing)	49 KIAS (1750 lb.)
Stall Speed (Approach)	49 KIAS (1750 lb.)
Engine Thrust	
Max. Thrust at Climb vs. Height	Takeoff (ISA SLS): 400 lb. Climb, 0 ft. MSL: 260 lb. Climb, 1000 ft. MSL: 260 lb. Climb, 5000 ft. MSL: 260 lb. Climb, 10000 ft. MSL: 260 lb. Climb, 15000 ft. MSL: 260 lb. Climb, 20000 ft. MSL: 260 lb.
Max. Thrust at Cruise	140 lb.
Max. Thrust at Descent	0 lb.
Propulsion	
Engine	
Brake Engine Power	109 hp @ 5500 RPM

No. of cylinders	4
Baseline Engine Power	101 hp @ 550 RPM
Critical Turbocharger Altitude	15000 ft.
Fuel Consumption	$BSFC_{min} = 0.43 \text{ lb./hp-hr.}$
	$BSFC_{max} = 0.5 \text{ lb./hp-hr.}$
	$BSFC_{cruise} =$
Maximum Engine Crankshaft Speed	5800 RPM
Maximum Propeller Shaft Speed	2125 RPM
Engine displacement	1211 cc
Engine compression ratio	9.0:1
Engine Envelope	X = 2.05 ft.
	Y = 2.00 ft.
	Z = 1.8 ft.
Propeller Type	Variable Pitch
Number of Blades	2
Pitch	
Propeller diameter	73 in.
Activity Factor	115
Integrated design lift coefficient (for blade)	N/A
Ground Movement	
Landing Length	1000 ft. (Sea Level, Standard Day, No Wind, 1750 lb.)
Take Off Length	1800 ft. (Sea Level, Standard Day, No Wind, MGTOW)
Width of Runway	
Aircraft Length	27 ft.
Airline Procedures File (APF)	
Climb Operating Speed	
Cruise Operating Speed	
Descent Operating Speed	

15.6 Predator B (MQ-9)

Table 57. Industry data for Predator B. Provided by General Atomics.

Operations Performance File (OPF)	
Design Range	4370 nmi. (cruise at 30000 ft.)
Design Endurance	26 hr. (3900 lb. of fuel and cruise at 30000 ft.)
Basic Geometry	



Equation or Graph	
Mass	
Max. mass of aircraft (Empty Weight)	4900 lb.
Max. mass of aircraft (Gross Weight)	10500 lb.
Max. payload	4800 lb.
Max. fuel weight	3764 lb.
Flight Envelope	
Loiter Speed	
V _{MO} (in CAS or TAS)	230 KIAS or 249 KTAS
M _{MO} (Mach Max. Operating)	0.38
H _{max}	30000 ft. at MTOW under ISA conditions
Aerodynamics	
S _{wet} (Total)	529.41 ft. ²
S _{wet} (Fuselage)	
S _{ref}	256 ft. ²
Clb. _o (Buffet Onset Lift Coeff.)	1.23 (no flaps); 1.51 (30° flaps)
Stall Speed (Initial Climb)	100 KTAS @ 5000 ft. (MGTOW)
Stall Speed (Cruise)	110 KTAS @ 20000 ft. (8000 lb.)
Stall Speed (Take Off)	93 KTAS @ Sea Level (MGTOW)
Stall Speed (Landing)	70 KTAS @ sea Level (6000 lb.)
Stall Speed (Approach)	75 KTAS @ 5000 ft. (6000 lb.)
Engine Thrust	
Max. Thrust at Climb vs. Height	Proprietary
Max. Thrust at Cruise	Proprietary
Max. Thrust at Descent	Proprietary
Propulsion	
Engine	
Brake Engine Power	N/A
No. of cylinders	N/A
Baseline Engine Power	900 hp @ 100% RPM
Critical Turbocharger Altitude	N/A
Fuel Consumption	BSFC _{min} = 0.55 lb./hp-hr. at Sea Level; Static @ 100% RPM
	BSFC _{max} = 0.55 lb./hp-hr. at Sea Level; Static @ 100% RPM
	BSFC _{cruise} = 0.55 lb./hp-hr. at Sea Level; Static @ 100% RPM

Maximum Engine Crankshaft Speed	41730 RPM (Max. Continuous)
Maximum Propeller Shaft Speed	1591 RPM (Max. Continuous)
Engine displacement	N/A
Engine compression ratio	N/A
Engine Envelope	X = 42.82 in. (Before Modification)
	Y = 20.98 in. (Before Modification)
	Z = 26.62 in. (Before Modification)
Propeller Type	Variable Pitch
Number of Blades	3
Pitch	
Propeller diameter	110 in.
Activity Factor	Proprietary
Integrated design lift coefficient (for blade)	
Ground Movement	
Landing Length	1800 ft. (Sea Level, Standard Day, No Wind, 6000 lb.)
Take Off Length	3200 ft. (Sea Level, Standard Day, Dry Wings, MGTOW)
Width of Runway	
Aircraft Length	36.2 ft.
Airline Procedures File (APF)	
Climb Operating Speed	
Cruise Operating Speed	
Descent Operating Speed	

15.7 Gray Eagle (MQ1C)

Table 58. Industry data for Gray Eagle. Provided by General Atomics.

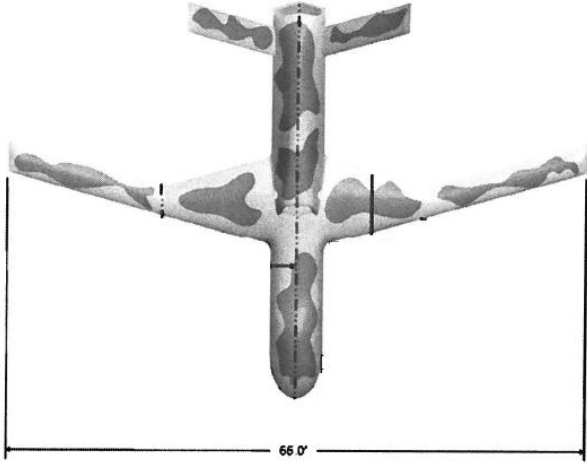
Operations Performance File (OPF)											
Design Range	2080 nmi. (cruise at 10000 ft.)										
Design Endurance	24 hr. (575 lb. of fuel and loiter at 10000 ft.)										
Basic Geometry											
<table border="1"> <tr> <td>Wing Aspect Ratio</td><td></td></tr> <tr> <td>Wing Span</td><td>56.3 ft.</td></tr> <tr> <td>M.A.C (Wing)</td><td></td></tr> <tr> <td>Wing Taper Ratio</td><td></td></tr> <tr> <td>Fuselage Length</td><td>27.5 ft.</td></tr> </table>		Wing Aspect Ratio		Wing Span	56.3 ft.	M.A.C (Wing)		Wing Taper Ratio		Fuselage Length	27.5 ft.
Wing Aspect Ratio											
Wing Span	56.3 ft.										
M.A.C (Wing)											
Wing Taper Ratio											
Fuselage Length	27.5 ft.										

Fuselage Fineness Ratio	
Tail Size (Winglet)	Effective horizontal span = 5.83 ft.
	Effective horizontal area = 32.3 ft. ²
	Effective vertical area = 6.56 ft. ²
Horizontal Tail Volume Coefficient	
Vertical Tail Volume Coefficient	0.028
Ultimate Structural Load Factor	1.5
Drag Polars	
Equation or Graph	
Mass	
Max. mass of aircraft (Empty Weight)	2600 lb.
Max. mass of aircraft (Gross Weight)	3600 lb.
Max. payload	1500 lb.
Max. fuel weight	590 lb.
Flight Envelope	
Loiter Speed	
V _{MO} (in CAS or TAS)	130 KIAS or 180 KTAS
M _{MO} (Mach Max. Operating)	N/A
H _{max}	32000 ft. at MTOW under ISA conditions
Aerodynamics	
S _{wet} (Total)	291.51 ft. ²
S _{wet} (Fuselage)	
S _{ref}	150 ft. ²
C _{lb,o} (Buffet Onset Lift Coeff.)	1.77 (20° flaps; C _{l,max})
Stall Speed (Initial Climb)	60 KIAS (20° flaps, 3200 lb.)
Stall Speed (Cruise)	92 KIAS (flaps scheduled, 3200 lb.)
Stall Speed (Take Off)	60 KIAS (20° flaps, 3200 lb.)
Stall Speed (Landing)	60 KIAS (20° flaps, 3200 lb.)
Stall Speed (Approach)	74 KIAS (20° flaps, 3200 lb.)
Engine Thrust	
Max. Thrust at Climb vs. Height	Takeoff (ISA SLS): 533 lb. Climb, 0 ft. MSL: 478 lb. Climb, 1000 ft. MSL: 473 lb. Climb, 5000 ft. MSL: 453 lb. Climb, 10000 ft. MSL: 420 lb. Climb, 15000 ft. MSL: 364 lb.

	Climb, 20000 ft. MSL: 312 lb.
Max. Thrust at Cruise	N/A
Max. Thrust at Descent	0 lb.
Propulsion	
Engine	
Brake Engine Power	
No. of cylinders	4
Baseline Engine Power	160 hp @ 3900 RPM
Critical Turbocharger Altitude	N/A
Fuel Consumption	$BSFC_{min} = 0.37 \text{ lb./hp-hr.}$
	$BSFC_{max} = 0.39 \text{ lb./hp-hr.}$
	$BSFC_{cruise} =$
Maximum Engine Crankshaft Speed	3990 RPM
Maximum Propeller Shaft Speed	2300 RPM
Engine displacement	1991 cc.
Engine compression ratio	18.0:1
Engine Envelope	X = 32.12 in.
	Y = 30.63 in.
	Z = 25.04 in.
Propeller Type	Variable Pitch
Number of Blades	3
Pitch	
Propeller diameter	80 in.
Activity Factor	
Integrated design lift coefficient (for blade)	
Ground Movement	
Landing Length	1800 ft. (Sea Level, Standard Day, No Wind, MGTOW)
Take Off Length	2300 ft. (Sea Level, Standard Day, Dry Wings, MGTOW)
Width of Runway	
Aircraft Length	27.5 ft.
Airline Procedures File (APF)	
Climb Operating Speed	
Cruise Operating Speed	
Descent Operating Speed	

15.8 Predator C (AVEN)

Table 59. Industry data for Predator C. Provided by AAI.

Operations Performance File (OPF)	
Design Range	5100 nmi. (cruise at 40000 ft.)
Design Endurance	14 hr. (6000 lb. of fuel and cruise at 40000 ft.)
Basic Geometry	
	
	
Wing Aspect Ratio	
Wing Span	66 ft.
M.A.C (Wing)	
Wing Taper Ratio	
Fuselage Length	44 ft.
Fuselage Fineness Ratio	
Tail Size (Winglet)	Effective horizontal span = 13 ft. Effective horizontal area = 89.92 ft. ² Effective vertical area = ft. ²
Horizontal Tail Volume Coefficient	
Vertical Tail Volume Coefficient	0.067
Ultimate Structural Load Factor	1.5
Drag Polars	
Equation or Graph	

Mass	
Max. mass of aircraft (Empty Weight)	8650 lb.
Max. mass of aircraft (Gross Weight)	15800 lb.
Max. payload	3500 lb. (external); 3000 lb. (internal)
Max. fuel weight	9000 lb.
Flight Envelope	
Loiter Speed	
V _{MO} (in CAS or TAS)	400 KTAS
M _{MO} (Mach Max. Operating)	0.62
H _{max}	40000 ft. at MTOW under ISA conditions
Aerodynamics	
S _{wet} (Total)	555.4 ft. ²
S _{wet} (Fuselage)	
S _{ref}	267 ft. ²
C _{Lb} . _o (Buffet Onset Lift Coeff.)	1.26 (Maximum CL with no flaps)
Stall Speed (Initial Climb)	105 KIAS
Stall Speed (Cruise)	112 KIAS
Stall Speed (Take Off)	105 KIAS
Stall Speed (Landing)	98 KIAS
Stall Speed (Approach)	98 KIAS
Engine Thrust	
Max. Thrust at Climb vs. Height	Proprietary
Max. Thrust at Cruise	1000 lb.
Max. Thrust at Descent	Proprietary
Propulsion	
Engine	
Brake Engine Power	
No. of cylinders	N/A
Baseline Engine Power	N/A
Critical Turbocharger Altitude	N/A
Fuel Consumption	BSFC _{min} = Proprietary
	BSFC _{max} = Proprietary
	BSFC _{cruise} = Proprietary
Maximum Engine Crankshaft Speed	N/A
Maximum Propeller Shaft Speed	N/A

Engine displacement	N/A
Engine compression ratio	N/A
Engine Envelope	X = 68 in.
	Y = 32 in.
	Z = 47 in.
Propeller Type	N/A
Number of Blades	N/A
Pitch	N/A
Propeller diameter	80 in.
Activity Factor	
Integrated design lift coefficient (for blade)	N/A
Ground Movement	
Landing Length	2700 ft. @ 14000 lb.; 2200 ft. @ 11000 lb. (Sea Level, Standard Day, No Wind)
Take Off Length	4000 ft. (Sea Level, Standard Day, Dry Wings, MGTOW)
Width of Runway	
Aircraft Length	44 ft.
Airline Procedures File (APF)	
Climb Operating Speed	
Cruise Operating Speed	
Descent Operating Speed	

15.9 Hunter (MQ5B)

Table 60. Industry data for Cargo UAS. Provided by AAI.

Operations Performance File (OPF)	
Design Range	108 nmi. (radius of operation)
Design Endurance	21 hr.
Basic Geometry	



Wing Aspect Ratio	11.0
Wing Span	34.25 ft.
M.A.C (Wing)	
Wing Taper Ratio	0.64
Fuselage Length	14.6 ft.
Fuselage Fineness Ratio	0.177
Tail Size (Winglet)	Effective horizontal span = 9.8 ft. Effective horizontal area = 21 ft. ² Effective vertical area = 12 ft. ²
Horizontal Tail Volume Coefficient	0.74
Vertical Tail Volume Coefficient	0.04
Ultimate Structural Load Factor	+3.8 / -1.5

Drag Polars

Equation or Graph	$C_D = 0.0596 + 0.034C_L^2$
-------------------	-----------------------------

Mass

Max. mass of aircraft (Empty Weight)	1450 lb.
Max. mass of aircraft (Gross Weight)	1950 lb.
Max. payload	500 lb. (fuel + payload)
Max. fuel weight	

Flight Envelope

Loiter Speed	60 kts
V _{MO} (in CAS or TAS)	120 KTAS

M_{MO} (Mach Max. Operating)	N/A
H_{max}	18000 ft.
Aerodynamics	
S_{wet} (Total)	435 ft. ²
S_{wet} (Fuselage)	131 ft. ²
S_{ref}	106 ft. ²
Clb_o (Buffet Onset Lift Coeff.)	
Stall Speed (Initial Climb)	53 KIAS
Stall Speed (Cruise)	53 KIAS
Stall Speed (Take Off)	53 KIAS
Stall Speed (Landing)	53 KIAS
Stall Speed (Approach)	53 KIAS
Engine Thrust	
Max. Thrust at Climb vs. Height	761 ft./min. (max. SL rate of climb)
Max. Thrust at Cruise	
Max. Thrust at Descent	
Propulsion	
Engine	Two APL Heavy Fuel Engines (one as tractor and one as pusher)
Brake Engine Power	57 hp
No. of cylinders	3
Baseline Engine Power	57 hp
Critical Turbocharger Altitude	11500 ft. MSL
Fuel Consumption	$BSFC_{min} =$
	$BSFC_{max} =$
	$BSFC_{cruise} =$
Maximum Engine Crankshaft Speed	4200 RPM
Maximum Propeller Shaft Speed	3590 RPM
Engine displacement	800 cc.
Engine compression ratio	18.5
Engine Envelope	X = 15.75 in.
	Y = 19.75 in.
	Z = 29.74 in.
Propeller Type	Two bladed, Fixed Pitch, Wooden
Number of Blades	2
Pitch	42 in. (forward engine); 47 in. (aft engine)
Propeller diameter	4.4 ft.
Activity Factor	

Integrated design lift coefficient (for blade)	
Ground Movement	
Landing Length	
Landing Length	2200 ft.
Take Off Length	1275 ft.
Width of Runway	100 ft.
Aircraft Length	23 ft.
Airline Procedures File (APF)	
Climb Operating Speed	60–80 KIAS
Cruise Operating Speed	80 KIAS
Descent Operating Speed	60–80 KIAS

15.10 Cargo UAS (CUAS)

Table 61. Industry data for Cargo UAS. Provided by AAI.

Operations Performance File (OPF)	
Design Range	600 nmi. (with 20 min. reserve)
Design Endurance	2.16 hr. (with full cargo load)
Basic Geometry	
Wing Aspect Ratio	10.2
Wing Span	45.2 ft.

M.A.C (Wing)	
Wing Taper Ratio	1
Fuselage Length	35 ft.
Fuselage Fineness Ratio	0.174
Tail Size (Winglet)	Effective horizontal span = 13 ft. Effective horizontal area = 41.4 ft. ² Effective vertical area = 51.7 ft. ²
Horizontal Tail Volume Coefficient	0.9196
Vertical Tail Volume Coefficient	0.1025
Ultimate Structural Load Factor	+4.5 / -1.5
Drag Polars	
Equation or Graph	N/A
Mass	
Max. mass of aircraft (Empty Weight)	12050 lb.
Max. mass of aircraft (Gross Weight)	22750 lb.
Max. payload	8000 lb.
Max. fuel weight	2700 lb.
Flight Envelope	
Loiter Speed	N/A
V _{MO} (in CAS or TAS)	250 KTAS (max. cruise at 15000 ft. ISA)
M _{MO} (Mach Max. Operating)	N/A
H _{max}	30000 ft. (ISA)
Aerodynamics	
S _{wet} (Total)	1307 ft. ² (estimated, not including rotor)
S _{wet} (Fuselage)	647 ft. ² (estimated)
S _{ref}	200 ft. ²
Clb. _o (Buffet Onset Lift Coeff.)	N/A
Stall Speed (Initial Climb)	N/A
Stall Speed (Cruise)	N/A
Stall Speed (Take Off)	N/A
Stall Speed (Landing)	N/A
Stall Speed (Approach)	N/A
Engine Thrust	
Max. Thrust at Climb vs. Height	
Max. Thrust at Cruise	11350 lb.

Max. Thrust at Descent	
Propulsion	
Engine	
Brake Engine Power	
No. of cylinders	0
Baseline Engine Power	1890 SHP _{max} SL (each)
Critical Turbocharger Altitude	N/A
Fuel Consumption	BSFC _{min} =
	BSFC _{max} = 0.462 lb./SHP-hr. (each)
	BSFC _{cruise} =
Maximum Engine Crankshaft Speed	N/A
Maximum Propeller Shaft Speed	2100 RPM
Engine displacement	
Engine compression ratio	17:1
Engine Envelope	X = 15.6 in. (nominal diameter)
	Y = 46 in. (length)
	Z = 15.6 in. (nominal diameter)
Propeller Type	Two Variable Pitch Pusher Propellers
Number of Blades	5
Pitch	Variable
Propeller diameter	92 in.
Activity Factor	N/A
Integrated design lift coefficient (for blade)	N/A
Ground Movement	
Landing Length	VTOL
Take Off Length	VTOL
Width of Runway	8.7 ft. (wheelbase)
Aircraft Length	55 ft. (rotor)
Airline Procedures File (APF)	
Climb Operating Speed	N/A
Cruise Operating Speed	225 KIAS
Descent Operating Speed	N/A

15.11 Fire Scout (MQ8B)

Table 62. Industry data for Fire Scout. Provided by AAI.

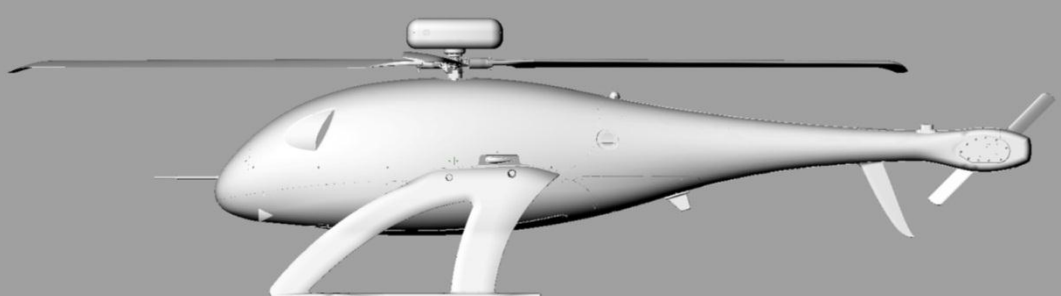
Operations Performance File (OPF)	
Design Range	110 nmi. (mission radius)
Design Endurance	5 hr. (maximum); 8 hr. (baseline payload)
Basic Geometry	
	
Main Rotor	Rotor Diameter: 27.5 ft.
	Number of blades: 4
	Chord (avg.): 7.6 in.
Tail Rotor	Rotor Diameter: 4.25 ft.
	Number of blades: 2
	Chord: 4.5 in.
Horizontal distance between tail and main rotor axes	16 ft.
Fuselage Length	23.95 ft. (with dual payload nose)
Fuselage Fineness	0.167
Tail Size	Effective horizontal span = 2.5 ft.
	Effective horizontal area = 3.1 ft. ²
	Effective vertical area = 4.7 ft. ²
Ultimate Structural Load Factor	+3.5 / -1.0
Drag Polars	
Equation or Graph	$0.28*s*q$
Mass	
Max. mass of aircraft (Empty Weight)	1457 lb.

Max. mass of aircraft (Gross Weight)	3150 lb.
Max. payload	600 lb.
Max. fuel weight	
Flight Envelope	
Loiter Speed	N/A
V _{MO} (in CAS or TAS)	125 KIAS
M _{MO} (Mach Max. Operating)	N/A
H _{max}	20000 ft.
Aerodynamics	
S _{wet} (Total)	422 ft. ² (fuselage, landing gear, tail rotor, main rotor)
S _{wet} (Fuselage)	286 ft. ²
S _{ref}	
Clb. _o (Buffet Onset Lift Coeff.)	N/A
Stall Speed (Initial Climb)	N/A
Stall Speed (Cruise)	N/A
Stall Speed (Take Off)	N/A
Stall Speed (Landing)	N/A
Stall Speed (Approach)	N/A
Engine Thrust	
Max. Thrust at Climb vs. Height	
Max. Thrust at Cruise	11350 lb.
Max. Thrust at Descent	
Propulsion	
Engine	Rolls-Royce 250-C20W (turboshaft)
Brake Engine Power	420 derated to 320 SHP
No. of cylinders	0
Baseline Engine Power	420 derated to 320 SHP
Critical Turbocharger Altitude	N/A
Fuel Consumption	BSFC _{min} = N/A
	BSFC _{max} = N/A
	BSFC _{cruise} = 0.709 lb./SHP-hr. (@ 75% cruise)
Maximum Engine Crankshaft Speed	6016 RPM (usual output speed)
Maximum Propeller Shaft Speed	420 RPM
Engine displacement	N/A
Engine compression ratio	7.2:1
Engine Envelope	X = 23 in.

	Y = 39 in.
	Z = 23 in.
Ground Movement	
Landing Length	VTOL
Take Off Length	VTOL
Width of Runway	27.5 ft. (rotor diameter)
Aircraft Length	30.03 ft. (with blades folded forward)
Airline Procedures File (APF)	
Climb Operating Speed	1380 ft./min. (rate of climb)
Cruise Operating Speed	110 KIAS
Descent Operating Speed	500 ft./min. (estimated normal rate of descent); 1500 ft./min. (estimated max. rate of descent)

15.12 NEO S-300 Mk II VTOL (S350)

Table 63. Industry data for NEO S-300 Mk II VTOL. Provided by AAI.

Operations Performance File (OPF)	
Design Range	67.5 nmi.
Design Endurance	4–5 hr.
Basic Geometry	
	
Main Rotor	Rotor Diameter: 11.5 ft.
	Number of blades: 3
	Chord (avg.): 5.5 in.
Tail Rotor	Rotor Diameter: 27.6 ft.
	Number of blades: 2
	Chord: 1.97 in.
Horizontal distance between tail and main rotor axes	6 ft.
Fuselage Length	10.33 ft.
Fuselage Fineness	0.187
Tail Size	Effective horizontal span = N/A

	Effective horizontal area = N/A
	Effective vertical area = 0.22 ft. ²
Ultimate Structural Load Factor	3.75
Drag Polars	
Equation or Graph	$D = 0.2*s*q$
Mass	
Max. mass of aircraft (Empty Weight)	187.4 lb.
Max. mass of aircraft (Gross Weight)	329.6 lb.
Max. payload	99.2 lb.
Max. fuel weight	
Flight Envelope	
Loiter Speed	N/A
V _{MO} (in CAS or TAS)	116.6 KIAS
M _{MO} (Mach Max. Operating)	N/A
H _{max}	13123.4 ft.
Aerodynamics	
S _{wet} (Total)	77.93 ft. ²
S _{wet} (Fuselage)	44.78 ft. ²
S _{ref}	
Clb. _o (Buffet Onset Lift Coeff.)	N/A
Stall Speed (Initial Climb)	N/A
Stall Speed (Cruise)	N/A
Stall Speed (Take Off)	N/A
Stall Speed (Landing)	N/A
Stall Speed (Approach)	N/A
Engine Thrust	
Max. Thrust at Climb vs. Height	
Max. Thrust at Cruise	
Max. Thrust at Descent	
Propulsion	
Engine	JetA1 Powered Single Turbine 9can also use electric motor)
Brake Engine Power	28 KW
No. of cylinders	0
Baseline Engine Power	28 KW

Critical Turbocharger Altitude	N/A
Fuel Consumption	$BSFC_{min} = 120 \text{ ml/min.}$
	$BSFC_{max} = 380 \text{ ml/min.}$
	$BSFC_{cruise} = 280 \text{ ml/min.}$
Maximum Engine Crankshaft Speed	N/A
Maximum Propeller Shaft Speed	900 RPM
Engine displacement	N/A
Engine compression ratio	7.5:1
Engine Envelope	X = 19.69 in.
	Y = 11.81 in.
	Z = 11.81 in.
Ground Movement	
Landing Length	VTOL
Take Off Length	VTOL
Width of Runway	11.5 ft. (rotor diameter)
Aircraft Length	10.34 ft. (rotor folded back)
Airline Procedures File (APF)	
Climb Operating Speed	1377.95 ft./min. (max. rate of climb)
Cruise Operating Speed	70 KIAS (estimated)
Descent Operating Speed	492.13 ft./min. (estimated max. rate of descent)

16 Appendix B: Configuration of ACES and KTG to Simulate UAS Aircraft

16.1 Introduction

The UAS aircraft studied in this project were simulated in KTG. Further, their communication, navigation and surveillance capabilities were simulated in ACES using KTG as the trajectory generator. As mentioned earlier, Cargo UAS, Fire Scout and NEO S-300 Mk II VTOL could not be simulated using ACES and KTG, and hence were excluded from these simulations. This section describes the procedure used to configure KTG and ACES databases to simulate these nine UAS aircraft.

16.2 Configuration of KTG Database

The four BADA files described and presented earlier for each UAS aircraft were added to the KTG database folder in ACES: `TrajectoryGenerators\ktg\core\data`.

In addition, the following KTG files were configured to support UAS simulations:

- `aircraft_control_gain.csv`
- `MPAS_SYNONYM.LST`

- SYNONYM_ALL.LST
- SYNONYM_ACES_KTG.OLD

16.2.1 Configuration of “aircraft_control_gain.csv”

File location: TrajectoryGenerators\ktg\core\data

This file contains the flight control parameters for each aircraft type. Due to lack of accurate data for UAS aircraft, the default values specified for existing conventional aircraft were used. For example, to simulate Global Hawk’s flight, its control parameters were added to this file in seven separate lines, where “RQ4A” was the aircraft code used to identify Global Hawk. The entries indicated as <<Line x>> are only shown for clarity and should not be included in the file:

```

<<Line 1>>
RQ4A,500,2.25,0,0,0.004,0,0.32,0,0.08,0.000002,0,0.0000081,0.024,0,-0.00000015,0,0
<<Line 2>>
RQ4A,1000,2.25,0,0,0.004,0,0.32,0,0.08,0.000002,0,0.0000081,0.024,0,-0.00000015,0,0
<<Line 3>>
RQ4A,2000,2.25,0,0,0.004,0,0.32,0,0.08,0.000002,0,0.0000081,0.024,0,-0.00000015,0,0
<<Line 4>>
RQ4A,5000,0.225,0,0,0.0004,0,0.032,0,0.008,0.000002,0,0.0000081,0.024,0,-0.00000015,0,0
<<Line 5>>
RQ4A,10000,0.0225,0,0,0.0004,0,0.032,0,0.008,0.000002,0,0.0000081,0.024,0,-0.00000015,0,0
<<Line 6>>
RQ4A,20000,0.0225,0,0,0.0004,0,0.032,0,0.008,0.000002,0,0.0000081,0.024,0,-0.00000015,0,0
<<Line 7>>
RQ4A,30000,0.0225,0,0,0.0004,0,0.032,0,0.008,0.000002,0,0.0000081,0.024,0,-0.00000015,0,0

```

16.2.2 Configuration of “MPAS_SYNONYM.LST,” “SYNONYM_ALL.LST” and “SYNONYM_ACES_KTG.OLD”

These files specify the names of the BADA files to be used for a particular aircraft. For example, to add Global Hawk, use “blank space” to separate entries in each file. Do not use “tabs” for “space.” Following the template for the entries of existing aircraft in each file is strongly advised to avoid any errors or misinterpretation of the files by KTG.

MPAS_SYNONYM.LST: No changes are necessary

SYNONYM_ALL.LST (a single continuous line):

CD - RQ4A	Global Hawk UAV	Northrop Grumman	RQ4A__	RQ4A	RQ4A	RQ4A
RQ4A	RQ4A	RQ4A	RQ4A	RQ4A	RQ4A	RQ4A

SYNONYM_ACES_KTG.OLD (a single continuous line):

CD * RQ4A	NORTHROP	GLOBAL HAWK UAV	RQ4A__	RQ4A /
-----------	----------	-----------------	--------	--------

16.3 Configuration of ACES Database

The UAS aircraft should be added to the table “aircraft_characteristics_ds” in the ACES file “aces_model_input_nodal_model.sql”. This file is shown here only as an example. The analyst should use the appropriate ACES database file being used in her/his simulations. This table specifies the aircraft’s speed (KCAS) during different phases of flight.

Location of table: Build\modules\acesutilities\data\database

The different entries in this table are:

- AIRCRAFT_CHARACTERISTICS_DS_ID: This is unique number assigned to each aircraft. The simplest way to assign this number would be to continue the sequence in the table.
- AIRCRAFT_TYPE_CATEGORY: It specifies the number of engines and type, and the aircraft weight category. J = Jet, T = Turboprop, P = Piston. S (small) = up to 12,500 lb.; M (medium) = 12,500 to 41,000 lb.; L (large jet) = 41,000 to 255,000 lb.; H (heavy) = more than 255,000 lb. For example, the Global Hawk has one turbofan engine and belongs to the “M (medium)” weight category. Since ACES does not support the “turbofan” engine type, turboprop (T) was used for Global Hawk. Hence, its entry in this field is “1T/M”.
- AIRCRAFT_TYPE: Aircraft code; RQ4A for Global Hawk.
- ENGINE_TYPE: J = Jet, T = Turboprop, P = Piston.
- SEPARATION_CATEGORY: S (small) = up to 12,500 lb.; M (medium) = 12,500 to 41,000 lb.; L (large jet) = 41,000 to 255,000 lb.; H (heavy) = more than 255,000 lb.
- FINAL_APPROACH_FIX: Speed at final approach fix in KCAS. The values for conventional aircraft are obtained from Table 64 and , based on engine type, number of engines and aircraft weight class. However, due to the large variation in the actual weight of UAS aircraft for the same weight and engine categories, speed corresponding to final-approach-fix’s altitude from the .PTF BADA file was used. For example, the Global Hawk belongs to the weight category M and has engine type T, resulting in an altitude of 1500 ft. for its final-approach-fix. From the .PTF file, this altitude corresponds to 125 KTAS during descent (green-box in Figure 69), since final-approach corresponds to the descent phase of flight. It should be noted that the speeds in .PTF file are in KTAS. Therefore, these were converted to KCAS.
- DEPARTURE_FIX: Same procedure as above, but using the speed corresponding to departure-fix altitude for a given weight category and engine type in Table 64. For Global Hawk, this is 161 KTAS at 8000 ft. during the climb phase (blue-box in Figure 69).
- ARRIVAL_FIX: Same procedure as DEPARTURE_FIX. For Global Hawk, this is 174 KTAS at 8000 ft. during the descent phase (blue-dotted-box in Figure 69).
- CRUISE_FIX: Same value as ARRIVAL_FIX.
- RUNWAY_LANDING_THRESHOLD: Same procedure as above but corresponding to descent speed at FL0 (Flight Level 0) in the .PTF BADA file. For Global Hawk, this is 115 KCAS (orange-box in Figure 69). It should be noted that at FL0, KTAS and KCAS are equivalent.
- RUNWAY_TAKEOFF_THRESHOLD: Same procedure as above, but using climb speed at FL0. For Global Hawk, this is 115 KCAS (orange-dotted-box in Figure 69).
- TAKEOFF_STALL_SPEED: This is indicated in the .OPF BADA file. For Global Hawk, this is 83 KCAS (highlighted with red-box in Figure 70).
- LANDING_STALL_SPEED: Same procedure as above. For Global Hawk, this is 76.7 KCAS (highlighted with orange-box in Figure 70).

Table 64. Flight crossing altitudes in TRACON airspace by aircraft weight and engine type

No. of Engines	Engine Type	Aircraft Weight Category	Rwy Takeoff Threshold (ft.)	Rwy Landing Threshold (ft.)	Final Approach Fix (ft.)	Cruise Fix (ft.)	Arrival Fix (ft.)	Departure Fix (ft.)
1	J	S	0	0	2000	2000	10000	10000
1	J	L	0	0	2000	2000	10000	10000
1	J	H	0	0	2000	2000	10000	10000
2	J	S	0	0	2000	2000	10000	10000
2	J	L	0	0	2000	2000	10000	10000
2	J	H	0	0	2000	2000	10000	10000
3	J	S	0	0	2000	2000	10000	10000
3	J	L	0	0	2000	2000	10000	10000
3	J	H	0	0	2000	2000	10000	10000
4	J	S	0	0	2000	2000	10000	10000
4	J	L	0	0	2000	2000	10000	10000
4	J	H	0	0	2000	2000	10000	10000
1	T	S	0	0	1500	1500	8000	8000
1	T	L	0	0	1500	1500	8000	8000
1	T	H	0	0	1500	1500	8000	8000
2	T	S	0	0	1500	1500	8000	8000
2	T	L	0	0	1500	1500	8000	8000
2	T	H	0	0	1500	1500	8000	8000
3	T	S	0	0	1500	1500	8000	8000
3	T	L	0	0	1500	1500	8000	8000
3	T	H	0	0	1500	1500	8000	8000
4	T	S	0	0	1500	1500	8000	8000
4	T	L	0	0	1500	1500	8000	8000
1	P	S	0	0	1000	1000	6000	6000
1	P	L	0	0	1000	1000	6000	6000
1	P	H	0	0	1000	1000	6000	6000
2	P	S	0	0	1000	1000	6000	6000
2	P	L	0	0	1000	1000	6000	6000
2	P	H	0	0	1000	1000	6000	6000
3	P	S	0	0	1000	1000	6000	6000
3	P	L	0	0	1000	1000	6000	6000
3	P	H	0	0	1000	1000	6000	6000
4	P	S	0	0	1000	1000	6000	6000
4	P	L	0	0	1000	1000	6000	6000
4	P	H	0	0	1000	1000	6000	6000

Table 65. Flight Calibrated Airspeed (CAS) in TRACON airspace by aircraft weight and engine type

No. of Engines	Engine Type	Aircraft Weight Category	Rwy Takeoff Threshold (KCAS) ¹	Rwy Landing Threshold (KCAS) ¹	Final Approach Fix (KCAS) ¹	Cruise Fix (KCAS) ¹	Arrival Fix (KCAS) ¹	Departure Fix (KCAS) ¹
1	J	S	120 ²	110 ²	180 ²	180 ²	250 ²	250 ²
1	J	L	160 ³	140 ³	180 ³	180 ³	250 ³	250 ³
1	J	H						
2	J	S	120	110	180	180	250	250
2	J	L	160	140	180	180	250	250
2	J	H	180	140	180	180	250	250
3	J	S	160 ⁴	140 ⁴	180 ⁴	180 ⁴	250 ⁴	250 ⁴
3	J	L	160	140	180	180	250	250
3	J	H	180	140	180	180	250	250
4	J	S						

4	J	L	160	140	180	180	250	250
4	J	H	180	140	180	180	250	250
1	T	S	120 ^b	125 ^b	160 ^b	160 ^b	170 ^b	170 ^b
1	T	L						
1	T	H						
2	T	S	120	125	160	160	170	170
2	T	L	145	130	170	170	190	190
2	T	H						
3	T	S						
3	T	L						
3	T	H						
4	T	S						
4	T	L	145	130	170	170	190	190
4	T	H						
1	P	L						
1	P	H						
2	P	S	100	90	130	130	170	170
2	P	L	140	130	160	160	190	190
2	P	H						
3	P	S	100 ^b	906	130 ^b	130 ^b	170 ^b	170 ^b
3	P	L	140'	130'	160'	160'	190'	190'
3	P	H						
4	P	S	100 ⁸	908	130 ⁸	130 ⁸	170 ⁸	170 ⁸
4	P	L	140	130	160	160	190	190
4	P	H						

1. Nominal CAS data were derived from the following sources (except as otherwise footnoted):

Shen, M.M and Hunter, C.G. "Time to Fly in the DFW Tracon", Seagull TM 92120-03, November, 1992.

Shen, M.M., Hunter, C.G. and Sorensen, J.A., "Analysis of Final Approach Spacing Requirements Part II", Seagull TM 92120-02, February, 1992.

Hunter, C.G., "Aircraft Flight Dynamics in the Memphis TRACON", Seagull TM 92120-01, January, 1992.

Dorsky, S. and Hunter, C.G., "Time to Fly in the Boston TRACON", Seagull TM 91120-01, May, 1991.

2. Surrogate CAS data: Same as 2JS

3. Surrogate CAS data: Same as 2JL

4. Surrogate CAS data: Same as 3JL

5. Surrogate CAS data: Same as 2TS

6. Surrogate CAS data: Same as 1PS

7. Surrogate CAS data: Same as 4PL

8. Surrogate CAS data: Same as 2PS

Following the procedure described earlier, the different speeds of Global Hawk for inclusion in ACES aircraft database yields the values in Table 66.

**Table 66. Different speed settings of Global Hawk for inclusion in ACES aircraft database.
Speeds are Calibrated Airspeed in knots (KCAS).**

AIRC RAFT _CHA RACT ERIST ICS_D S_ID	AIRC RAF T_TY PE_ CAT EGO RY	AIRC RAFT _TYP E	EN GIN E_ TY PE	SEPA RATI ON_C ATEG ORY	FINA L_A PPR OAC H_FI X	DE PA RT UR E_ FIX	AR RIV AL_ FIX	CR UIS E_ FIX	RUNW AY_LA NDING _THRE SHOL D	RUNW AY_TA KEOF F_THR ESHO LD	TAK EOF F_ST ALL_ SPE ED	LAN DIN G_S TAL L_S PEE D
14073 74885 85931	1T/M	RQ4A	T	M	123	143	155	155	115	115	83	76.7

BADA PERFORMANCE FILE										Mar 07 2012		
AC/Type: RQ4A__										SOURCE OPF FILE:	Mar 07 2012	
										SOURCE APF FILE:	Mar 07 2012	
Speeds: CAS(LO/HI) Mach Mass Levels [kg]										Temperature:	ISA	
climb - 210/230 0.40 low - 6280										Max Alt. [ft]:	65000	
cruise - 220/240 0.40 nominal - 11512										descent - 230/230 0.40 high - 14203		
FL	CRUISE				CLIMB				DESCENT			
	TAS	fuel		TAS	ROCD		fuel	TAS	ROCD	fpm	[kg/min]	
	[kts]	[kg/min]		[kts]	[fpm]		[kg/min]	[kts]	[fpm]		[kg/min]	
	lo	nom	hi		lo	nom	hi	nom		nom	nom	
0				115	1826	2452	1795	19.3	115	1140	2.5	
5				119	1766	2399	1735	19.1	117	1140	2.5	
10				121	1743	2371	1713	18.4	120	1225	2.5	
15				123	1786	2420	1755	18.1	126	1214	2.5	
20				124	1760	2389	1730	18.1	131	1079	2.5	
30	135	7.4	7.9	8.1	127	2047	2669	2017	17.6	133	1100	2.5
40	140	8.4	8.9	9.1	131	2185	2837	2154	19.1	137	1080	2.5
60	151	9.4	9.9	10.2	142	2271	2881	2173	18.2	148	1080	2.4
80	176	10.1	10.6	10.8	161	2364	2917	2195	18.1	174	1080	2.4
100	196	11.0	11.6	11.8	172	2392	2987	2264	17.6	193	1080	2.4

Figure 69. Different speeds for Global Hawk (RQ4A) in the BADA file “RQ4A__.PTF”. The file shown here is a section of the complete file.

```

CCCCCCCCCCCCCCCCCCCCCCCCCCCCCCCCCCCC RQ4A__.OPF CCCCCCCCCCCCCC/
CC // 
CC AIRCRAFT PERFORMANCE OPERATIONAL FILE // 
CC // 
CC // 
CC File_name: RQ4A__.OPF // 
CC // 
CC Creation_date: Mar 07 2012 // 
CC // 
CC Modification_date: Mar 07 2012 // 
CC // 
CC // 
CC===== Actype =====// 
CD RQ4A__ 1 engines Jet M // 
CC Northrop Grumman RQ4A with 1 F137AD100 engines wake // 
CC // 
CC===== Mass (t) =====// 
CC reference minimum maximum max payload mass grad / 
CD .11512E+02 .52337E+01 .14203E+02 .00000E+00 .12868E+00 / 
CC===== Flight envelope =====// 
CC VMO(KCAS) MMO Max.Alt Hmax temp grad / 
CD .24100E+03 .66600E+00 .65000E+05 .28927E+05 .00000E+00 / 
CC===== Aerodynamics =====// 
CC Wing Area and Buffet coefficients (SIM) / 
CCndrst Surf(m2) Clbo(M=0) k CM16 / 
CD 5 .50168E+02 .27236E+01 .00000E+00 .00000E+00 / 
CC Configuration characteristics / 
CC n Phase Name Vstall(KCAS) CD0 CD2 unused / 
CD 1 CR Clean .10782E+03 .21180E-01 .77917E-02 .00000E+00 / 
CD 2 IC Clean .95406E+02 .21180E-01 .17508E-01 .00000E+00 / 
CD 3 TO Clean .82990E+02 .21180E-01 .14705E-01 .00000E+00 / 
CD 4 AP Clean .79831E+02 .21180E-01 .11454E-01 .00000E+00 / 
CD 5 LD Clean .76672E+02 .21180E-01 .77308E-02 .00000E+00 / 

```

Figure 70. Different stall speeds for Global Hawk (RQ4A) in the BADA file “RQ4A__.OPF”. The file shown here is a section of the complete file.